Alma Mater Studiorum – Università di Bologna

DOTTORATO DI RICERCA IN

TECNOLOGIE INNOVATIVE ED USO SOSTENIBILE DELLE RISORSE DI PESCA E BIOLOGICHE DEL MEDITERRANEO (FISHMED-PHD)

Ciclo 34

Settore Concorsuale: 03/D1

Settore Scientifico Disciplinare: CHIM/11

"Innovative microbiome-based system for the improvement of productivity, safety and sustainability of mussels farming"

Presentata da: Margherita Musella

Coordinatore Dottorato

Prof. Stefano Goffredo

Supervisore

Prof. Marco Candela

Co-Supervisori

Res. Sc. Gian Marco Luna
Res. Sc. Mauro Marini
Ass. Prof. Giulio Zanaroli

Esame finale anno 2023

1

Abstact

Northwestern Adriatic Sea Mediterranean mussels are exposed to fluctuating environmental parameters and to natural and anthropogenic stressors. Today is well known that mussels can be defined as holobiont, even if remains a lot to elucidate about how an organism and its microbial component response to environmental stress.

This PhD dissertation aims to investigate microbiome possible adaptive patters exploiting the organism physiology response to stress, using the NGS sequencing method.

The experimental approach consisted of two phases to first determine (i) the microbiome at a tissue scale level, (ii) the microbiome and physiological response to natural and anthropogenic stress environment and the chemical assessment of the microecosystem the Northwestern Adriatic Sea Mediterranean Mussel lives in.

Results revealed firstly a robust microbiome well differentiated from seawater microecosystem, with compositional variations at the organ level. Thanks to those findings, digestive gland, the organ in which digestive and detoxification processes allow animal to tolerate and accumulate xenobiotics of natural and anthropogenic origin, was the selected tissue for the second phase of the project.

The second phase of the project evaluated the putative physiological variations and the compositional changes in microbiome of digestive gland. I then manage to assess microbiome region trends across the north Adriatic, with each sampling site well differentiated from the others.

Finally, a chemical method able to a powerful tool for the analytical detection of the major pollutants in mussels were validated. These first results may provide baseline information for future studies approaches of seasonal and region trends of microbiota profiles and physiological responses in terms of metabolism.

28

INDEX

96

1. Introduction

Bivalve organisms, belonging to the phylum Mollusca, are the second largest phylum of the invertebrates. Most of the microbiological studies conducted on mussels in recent years were, concerned with the identification of pathogens with harmful effects on human health (Erol et al., 2016; Daczkowska-Kozon et al., 2010). Although until now we have focused on the identification of pathogenic microorganisms, there is only a small part of all the microorganisms present in the marine ecosystem. The ocean is in fact the largest habitat on our planet, and microorganisms are its main inhabitants. Although the mechanisms are not fully known, we do know that these microorganisms play a key role in the primary production and circulation of nutrients, positioning themselves at the base of the trophic chains, preserving their biodiversity. The microorganisms present in the marine ecosystem do not live exclusively in the water column or in marine sediments but, are often associated symbiotically with multicellular organisms such as animals, plants or algae (Egan et al., 2013). This makes it necessary to consider multicellular organisms no longer as autonomous entities, but rather in the complex formed by host organism and microbial community, which takes the name of "holobiont". The set of all microorganisms that define symbiotic relationships with the host organism is called microbiota. The microbiota, in general, also ensures greater protection for the host from those that are pathogenic microorganisms: this can happen through various mechanisms, direct and indirect, since, for example, the microorganisms can compete and exclude pathogenic microorganisms present in the environment (Pickard et al., 2017) or the microbiota itself can stimulate the host's immune system (Pan et al., 2012), increasing its resistance against pathogens and parasites. Microorganisms can also produce bioactive chemical compounds or precursors that can contribute to the activation of the immune system (Floréz et al., 2015).

The northen Adriatic Sea is characterized by a global cyclonic circulation with seawater inflow to the northwest along the Croatian coast (EAC) and outflow to the southeast along the Italian coast (WAC) (Poulain,1999). This pattern is greatly influenced by winds, mainly Bora and Scirocco (Davolio et al., 2012), and by freshwater inputs (Boldrin et al., 2005). The largest source of freshwater and sediments

123 is represented by the Po River (mean annual discharge of 1500 m3s−1), accounting for about one third
124 of the total riverine freshwater input into the Adriatic Sea (Cattaneo et al., 2003; Marini et al., 2010).

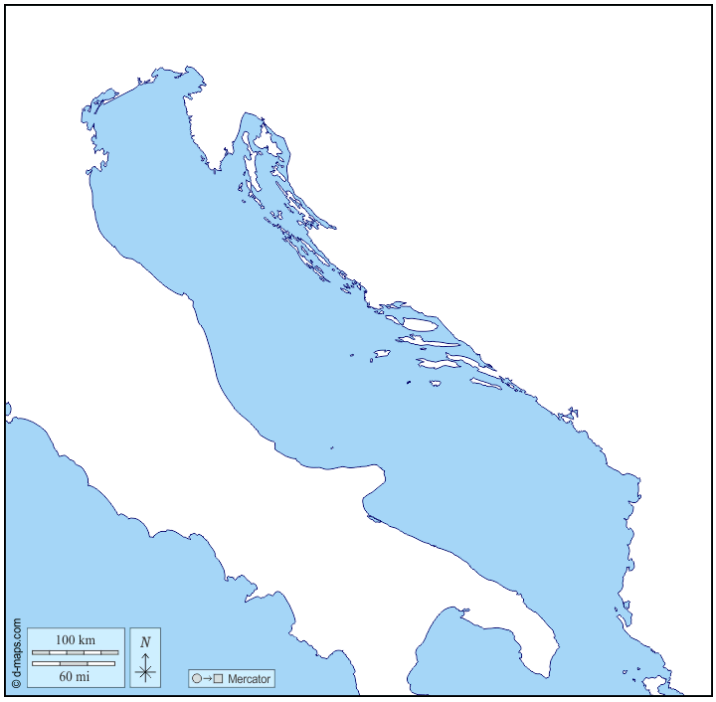

125

126 Fig.1 Adriatic Sea Area (https://d-maps.com/)

127

128 Po River discharges represent a remarkable load of pollution (Giani et al, 2012), receiving
129 wastewaters from the most industrialized and densely anthropized regions of northern Italy. Indeed,
130 this area is strongly affected by xenobiotics pollution, including a wide variety of compounds, i.e.
131 herbicide, antibiotics, personal care products. Those products impact severely the marine
132 environment due their high toxicity, persistence, and limited biodegradability. Surface water can be,
133 indeed, contaminated through direct or indirect emissions and groundwater can be contaminated by
134 pollutants that leach from the soil. Furthermore, the so-called emerging pollutants, i.e., personal care
135 products used by humans living in urban areas, are increasingly contributing to water pollution.
136 This area is not only affected by chemical and drugs pollution, but there are others anthropogenic
137 stressors that are a treat to the marine environment. The Adriatic Sea plays, indeed, an important role
138 in tourism recreation and economy growth of the coastal countries.

Therefore, it is of interest to be able to understand and quantify the impact of the environmental and human stressors on this area.

Since from north to south part of the Adriatic Sea display geographical, chemical and environmental gradients (Kraus et al., 2019), such conditions make mussel farms excellent field laboratories to explore the connection between the health and productivity of farmed mussels and the environmental quality.

1.1 The microbiota of the North-Adriatic Mytilus galloprovincialis

Mediterranean mussels like other bivalve mollusks, are key ecosystem engineers through their attachment to the substrate in dense mono- and multilayered beds. Alongside their ecological importance, mussels have a relevant economic value as a species of interest in aquaculture and, at the same time, have long been employed in the biomonitoring of environmental quality in coastal areas (Faggio et al., 2018; Capolupo et al., 2017; Carella et al., 2018; Moschino et al., 2016). Indeed, their powerful filter feeding activity links them to the surrounding environment, allowing to filter large volumes of water, while concentrating different types of waterborne or particulate pollutants as well as microorganisms (Gagné et al., 2019; Pagano et al., 2016; Neori et al., 2004).

Up to now, most of the microbiological studies on mussels focused on the identification of pathogenic bacteria with deleterious health effects (Erol et al., 2016; Richards et al., 2010; DaczkowskaKozon et al., 2010). However, marine organisms, including mussels, can be described as holobionts, given their life-long association with host-selected symbiont microbial communities known as microbiota (Pita et al., 2018; Glasl et al., 2016). These symbionts can endow the host with a set of probiotic functions (i.e. defense against pathogens, immunological regulation and improved nutritional efficiency), supporting homeostasis and health (O'Brien et al., 2019; Rausch et al., 2019; Simon et al., 2019). Consequently, the mussel microbiota should be considered as an integral component of the host physiology. However, to the best of our knowledge, only few and fragmentary studies aimed at the

description of the mussel microbiota have been performed (Li et al., 2019; Vezzulli et al., 2018; Cappello et al., 2015; Kamada et al., 2013) and the resulting knowledge is still fragmentary.

1.2 The holobiont Mytilus galloprovincialis response to natural and anthropic environment stress

The marine ecosystem is interconnected with the terrestrial ecosystem, hence changing any component in each system automatically affects another's functioning. In particular, coastal habitats are severely impacted by the contaminants receiving from the terrestrial surroundings that affect organism health, biodiversity, and consequently, ecosystem functioning (Islam and Tanaka, 2004; Lacroix et al., 2017). Besides chemical pollution, changes may also occur due to climate changes such as seawater warming, salinity variations, and ocean acidification (Landrigan et al., 2020). In this context, investigations of the regulatory mechanisms governing stress responses of marine organisms may elucidate the critical pathways setting the limits of animal acclimatization to anthropogenically modified marine environments.

Marine mussels dominate sessile fauna of many coastal areas and estuaries. These environments are characterized by wide fluctuations of abiotic and biotic parameters, which make mussels ideal model organisms for studying physiological alterations driven by environmental changes (Figueras et al., 2019; Franzellitti et al., 2020).

Environmental studies with mussels highlighted seasonal fluctuation of microbial indices, contaminant bioaccumulation, cellular biomarkers, and key physiological functions (Azizi et al., 2018; Caricato et al., 2010; Ivankovic et al., 2005; Rom´eo et al., 2003; Sheehan and Power, 1999; Shen et al., 2020; Vernocchi et al., 2007), and suggest the influence of abiotic factors (temperature, pH, salinity, food availability), and endogenous factors (i.e., gender bias and reproductive stage) for those biological responses (Blanco-Rayo´n et al., 2020; Grbin et al., 2019; Grenier et al., 2020). Molecular biomarkers based on expression analysis of stress responsive genes are pointing out crucial insights into mechanisms regulating animal ability to survive and thrive in dynamic and changing

marine environments (Evans and Hofmann, 2012; Gracey, 2007). Indeed, in environmentally relevant species as marine mussels, the modulation of mRNA levels is the earliest signal of an ongoing physiological alteration that can potentially forecast changes at higher levels of the biological organization (Gracey, 2007). There are several studies employing mussels as model organisms in field experiments to infer transcriptomic changes with environmental quality (Blalock et al., 2020; Franzellitti et al., 2010; Kerambrun et al., 2016; Rossi et al., 2016; Sforzini et al., 2018; Venier et al., 2006). Conversely, few studies emphasized that mussel gene transcription may be modulated by natural environmental parameters or by endogenous factors (Banni et al., 2011; Counihan et al., 2019; Schmidt et al., 2013b).

1.3 Assessment of water pollution impact on the Mediterranean mussel

The ongoing and significant release of hazardous chemical compounds, including the so-called emerging pollutants (https://www.sciencedirect.com/science/article/pii/S2095633915000039), into the aquatic environment is a problem that has long been known, but only in recent years, has become of increasing concern to regulators charged with environmental and health protection. While many studies exist on the fate and effects of such pollution in terrestrial organisms, such knowledge in the ones from marine and coastal aquatic ecosystems is more limited. Water contamination can be the result of a variety of human activities. Industrialization and urbanization along with intensification of agricultural activity and animal husbandry have led to a large-scale release of contaminants. Surface water can be contaminated through direct or indirect emissions and groundwater can be contaminated by pollutants that leach from the soil. Around the world, agriculture and farming are the leading cause of water pollution due to the extensive use of bioactive compound for crop protection and animal raising. Antibiotic use is common in the raising of animals worldwide, for growth promotion and disease prevention. Many antibiotic classes are currently utilized in the beef, dairy, swine, and poultry industries. In 2018, among the antibiotic sales for livestock, tetracyclines accounted for 66%, penicillins for 12%, macrolides for 8%, sulfonamides for 5%, aminoglycosides for 5%, lincosamides

for 2%, cephalosporins for 1%, and fluoroquinolones for less than 1%. The European Union banned the use of antibiotic growth-promoters in 2006, and new regulations set to begin in 2022 include a ban of antibiotic medicated feeds for prevention, as well as a ban on imported meat raised using growth promoters. About 95% of antibiotics administered to food-producing animals have been found unmetabolized or in the form of antibiotic residues in urine and feces, reaching manures and then contaminating water. This ubiquitous contamination has been proven worldwide, with over one hundred drug residues detected, all drug classes combined. The presence of antibiotics in the aquatic environment is a serious concern because it accelerates the proliferation of antibiotic-resistant microorganisms, with a high risk of resistance transfer to pathogenic microorganisms, thus lowering the therapeutic effect of antibiotics. Along with animal husbandry, agriculture is another major cause of pollution, due to the large-scale use of pesticides and herbicides to increase the quantity and quality of crops. The release of contaminants can reach many different environments even far from each other. Pesticides can leach through the soil into groundwater and thus consequently reach the marine ecosystem. The diffusion in the environment of individual pesticides depends on the water solubility and the chemical stability. In Europe, between 13% to 30% of all surface water is monitored by the EEA where one or more pesticides have been detected above effect threshold from 2013 to 2019, while exceedances of one or more pesticides were detected at between 3% and 7% of groundwater monitoring sites. Pesticides most often causing exceedance in surface waters are the insecticides imidacloprid and malathion, and the herbicides MCPA, metolachlor and metazachlor though some of these are no longer legally approved for use. In groundwater, the herbicide atrazine and its metabolites cause most exceedances. Despite restrictions on atrazine since 2007, it continues to be found in groundwater because of its high persistency.

Considering the potential effects of many pesticides and herbicides, their persistence and their large use, these compounds comprise a major risk to people and to the wider environment. For this reason, The European Green Deal aims to reduce the use of chemical pesticides by 50% within 2030 in the zero-pollution action plan, farm to fork strategy and biodiversity strategy.

Finally, many other drugs and personal care products used by humans living in urban areas are increasingly contributing to water pollution, being recently defined ad emerging pollutants and representing new and emerging pollutants and representing chemicals that are not commonly monitored but once in the environment cause adverse ecological and human health effects. For instance, psychotropic drugs and insect repellents have been found among the most common residues deriving from anthropic areas. In light of the above, the importance of monitoring contaminants in the various ecosystems using sensitive and reliable techniques is evident.

Assessment of aquatic pollution levels, however, cannot be based solely on the quantification of hazardous compounds in environmental samples (eg. water, sediments and soil), but the bioaccumulation of xenobiotics in organisms inhabiting the specific environment need to be accounted, allowing a system level vision of the chemical treat for the entire ecosystem, in complete accordance with the One Health approach. Among living organisms used in this frame, bivalves possess a critical role, not only for their involvement in the trophic chain as a key organism, but also as a useful sentinel organism for monitoring the effects of anthropogenic substances on the health status of the aquatic environment. Therefore, the determination of residues in these sentinel marine organisms, considered "proxies", is central for monitoring pollution of aquatic ecosystems. Furthermore, their consumption as food is very high all over the world (i.e. in the EU the yearly average mussel consumption is 1,28 kg per capita) therefore the presence of contaminant residues are clearly a critical public health concern, in mussels as well as in other edible marine species, to be monitored through specific analyzes. Developing analytical methods to detect pollution residues in various aquatic edible species is thus an important aspect, joining environmental monitoring with risk assessment of dietary intake.

In recent years a few multi-residue methods capable of quantifying different classes of organic pollutants have been developed. Despite the efforts made in the last decades for the optimization of analytical methods, given the wide variability in physicochemical properties and matrix complexity, their extraction and chromatographic separation remains a challenge.

In fact, bivalve matrices like mussels are very complex and contain various interferences, like lipids and proteins, that may interfere with detection and quantitation affecting selectivity and sensitivity. Because of the high content of fatty compounds, mussels result one of the most difficult matrices to be analyzed. Given the ample differences in the physicochemical properties of the molecules involved in the multi-residual analyzes, it is necessary to use extraction methods based on different strategies Several sample clean-up techniques are usually combined to increase the extraction capacity (the greater number of analytes) and the recovery rate. The common preprocessing techniques usually involve first liquid-solid extraction, often enhanced with microwave-assisted extraction (MAE) for antibiotics extraction, or pressurized liquid extraction (PLE), followed by a liquid–liquid extraction (LLE) using solvents with different polarity. The obtained fractions, if needed, can be further purified for example by solid phase extraction (SPE) with its ability to concentrate the analytes, Quick, easy, cheap, effective, rugged, and safe (QuEChERS) methods comprising both the extraction and clean-up steps have been widely adopted owing to their simplicity and reliability and have now become the standard approach for not excessively fatty matrices. Despite the great effort made in recent years, no single extraction methods or combinations of these were capable of obtaining high recoveries for analytes of different classes like pesticides and antibiotic at the same time.

2. Aim of this thesis

To date, some preliminary studies have attempted to characterize the microbiota associated with the organism Mytilus galloprovincialis and its variability as a function of stressful environmental conditions, such as the presence of glyphosate or in response to thermal stress (Iori et al., 2020; Li et al., 2019). However, the studies conducted so far have not taken into consideration the microbiota associated with Mytilus galloprovincialis in its complexity. Recent studies conducted on the clam and the Pacific oyster have highlighted the presence of a variability in the microbiota depending on the tissue-related: this variability seems to be related to the different physiological function that covers each organ and, consequently, the composition of the microbiota varies and, finally the functional relationships between microbiota and host change, in relation to the specific organ, tissue or district (Meisterhans., 2015). In consideration of what said above, the first aim (i) of this study is to characterize the microbiota of the Mediterranean mussel at the molecular level, investigating - for the first time – the tissue-specific differences, using a Next Generation Sequencing 16S marker gene approach. This study evaluates also the transcriptional profiles of genes related to metabolic, detoxification, antioxidant, and lysosomal responses in Mediterranean mussels (Mytilus galloprovincialis) under the influence of natural seasonal variations of environmental variables, gender bias, and gonadal cycle. We purposely addressed those environmental parameters and/or endogenous factors that literature review (Lindsay et al., 2020) shows that the composition of gut microbial community of a species can vary seasonally with host diet, metabolic demands, and life stage. These changes in microbial community composition seem to comprehensively contribute to the host flexibility to cope with environmental changes, enabling the host to live within different environments, adapt to seasonal changes and maintain its physiological performance. Therefore, considering this vital role of microbial communities in the maintenance of the host health (Rausch et al., 2019; Simon et al., 2019) also in response to environmental conditions (Vanwonterghem and Webster, 2020), this study also explores basal responses of the mussel digestive gland (DG) microbiome to seasonal changes (ii), allowing to figure out microbiome variations occurring

concomitantly with host physiological changes across seasonality and region trends. Finally, the ongoing and significant release of hazardous chemicals compounds, including the so-called emerging pollutants into the aquatic environment is a problem that has long been known, but only in recent years, has been of increasing concern to regulators charged with environmental and health protection. However, the assessment of these hazardous chemical compounds cannot be based solely on their quantification in environmental samples, rather their analysis in bioaccumulating marine organisms, specifically in edible species, represent a critical aspect. An optimized and validated method (iii) for the determination of pharmaceutical and pesticides residues in mussels (Mytilus Galloprovincialis) is presented herein.

3. Materials and Methods

3.1 Tissue-scale microbiota of the Mediterranean mussel (*Mytilus galloprovincialis*) and its relationship with the environment

3.1.1 Sampling and sample preparation

Mussel (*M. galloprovincialis* Lam.) sampling was carried out in April 2019 (spring season) in a farm located in Cesenatico, Italy (position: 44°09′04″N 12°32′60″E), by professional fishermen of the "Cooperativa Promoittica" (Cesenatico, Italy). The location is approved for direct commercialization of mussels (European legislation 91-492-EEC) and is sited within an area routinely monitored by the Regional Agency for Prevention, Environment and Energy of Emilia-Romagna, Italy (ARPA-ER) to assess the status of the marine ecosystem and seawater quality (https://www.arpae.it). Twenty-five mussels of commercial size (5-7 cm in length) were collected and immediately stored in coolers (+4°C) to be transferred within a few hours to the laboratory. In the laboratory, the mussels were cleaned and gently washed and then dissected under sterile conditions.

Specifically, for each animal, hemolymph was taken from the posterior adductor muscle using a sterile 1-ml syringe and transferred to a sterile tube. A 100-µl aliquot was employed to assess the health status of the animals through the evaluation of lysosomal membrane stability (LMS) on mussel hemocyte cells according to Buratti *et al.* (2013). LMS was employed in these preliminary assessments as it is a proven sensitive and reliable biomarker of general health status in bivalves (Viarengo *et al.*, 2007). The digestive gland, foot, gill and stomach were dissected from each individual as well, snap-frozen in liquid nitrogen, and stored at -80°C along with hemolymph until analysis.

Two liters of seawater were collected at a depth of 3 m near the mussel farm (position: 44°9′04″N 12°32′60″E), as well as 3 miles away from the collection site (44°5′53″N 12°35′28″E) (Figure S1). Seawater samples were stored in coolers (+4°C) during transport to the laboratory and then

immediately processed. A summary of the samples, sample size and handling methods is reported in Table S1.

3.1.2 Microbial DNA extraction

Total microbial DNA was extracted from approximately 20-30 mg of the digestive gland, foot, gill and stomach, and from 200 µl of hemolymph, using the DNeasy PowerSoil kit (Qiagen, Hilden, Germany) according to the manufacturer's instructions with only minor adjustments in the homogenization step. Specifically, all samples were homogenized using the FastPrep instrument (MP Biomedicals, Irvine, CA) at 6 movements per sec for 1 min. The elution step was repeated twice in 50 µl, incubating the columns for 5 min at 4°C before centrifugation. DNA samples were stored at −20°C for subsequent processing.

Seawater samples were filtered on 0.45-µm pore size MF-Millipore membrane filters using a vacuum pump. Total microbial DNA was extracted from membrane filters using the DNeasy PowerWater kit (Qiagen) according to the manufacturer's protocol.

3.1.3 PCR amplification and sequencing

The V3–V4 hypervariable region of the 16S rRNA gene was PCR-amplified using the 341F and 785R primers with added Illumina adapter overhang sequences, as previously described in Barone *et al.,* 2019. The PCR program used was as follows: 95°C for 3 min as initial denaturation, then 30 cycles of denaturation at 95°C for 30 sec, annealing at 55°C for 30 sec and elongation at 72°C for 30 sec, and 5 min at 72°C for the final elongation. PCR reactions were purified with Agencourt AMPure XP magnetic beads (Beckman Coulter, Brea, CA). Indexed libraries were prepared by limited-cycle PCR, using the Nextera technology (Illumina, San Diego, CA). After a further clean up step as described above, libraries were normalized to 4 nM and pooled. The sample pool was denatured with 0.2 N NaOH and diluted to a final concentration of 6 pM with a 20% PhiX control. Sequencing was performed on an Illumina MiSeq platform using a 2 × 250 bp paired-end protocol, according to the

manufacturer's instructions. Sequence reads were deposited in the National Center for Biotechnology Information Sequence Read Archive (NCBI SRA; BioProject ID PRJNA XXX).

3.1.4 Bioinformatics and statistics

Raw sequences were processed using a pipeline combining PANDAseq (Masella *et al.,* 2012) and QIIME 2 (Boylen *et al.,* 2019; https://qiime2.org). High-quality reads were clustered into amplicon sequence variants (ASVs) using DADA2 (Callahan *et al.*, 2016). Taxonomy was assigned using the VSEARCH classifier (Rognes *et al.*, 2016) and the SILVA database as a reference (Quast *et al.,* 2012). Unassigned sequences and those assigned to eukaryotes (i.e. chloroplasts and mitochondrial ones) were discarded.

Alpha rarefaction was performed using Faith's Phylogenetic Diversity (PD whole tree). A trade-off rarefaction value of 1,900 reads per sample was chosen to capture the extent of diversity in our data. Beta diversity was estimated by computing weighted and unweighted UniFrac distances.

All statistical analysis was performed using R version 3.5.1 (https://www.r-project.org/). Unweighted UniFrac distances were plotted using the vegan package, and the significance of data separation in the principal coordinates analysis (PCoA) was tested using a permutation test with pseudo-F ratios (function adonis in the vegan package). Alpha diversity was evaluated using two different metrics: Simpson Index (complement) and observed ASVs. Between-tissue differences for alpha diversity were assessed by Wilcoxon test. P-values were adjusted for multiple comparisons using the false discovery rate (FDR) (function p.adjust in the stats package), and a P-value ≤ 0.05 was considered as statistically significant. Representative sequences of taxa of interest were aligned to the 16S Microbial NCBI database (release September 2019) with BLASTn (version 2.9.0), considering at least 80% of sequences identity. Metagenome prediction of SILVA-picked ASVs was performed with PICRUSt2 (Barbera *et al.,* 2019; Czech *et al.,* 2019; Galvin *et al.,* 2019; Louca *et al.,* 2018; Ye *et al.,* 2009), using Metacyc (Caspi *et al.,* 2018) as reference for the pathways annotation and a NSTI threshold of 2. Over abundant pathways in the different mussel organs and seawater were obtained in pairwise

Wald tests, as implemented in DESeq2 package (Love *et al.,* 2014). Over abundant pathways with Bonferroni corrected p-value ≤ 0.05 and an absolute (log_2 fold change) ≥ 2 were retained. Clustering analysis was performed on the pathways abundances adopting Kendall's correlation coefficients as metric and Ward-linkage method.

3.2 Variability of metabolic, protective, antioxidant, and lysosomal gene transcriptional profiles and microbiota composition of *Mytilus galloprovincialis* farmed in the North Adriatic Sea (Italy)

3.2.1 Mussel sampling

Seven sampling campaigns were performed from a mussel farm located in the Northwestern Adriatic Sea by professional fishermen of the "Cooperativa Pro.mo.ittica" (Cesenatico, Italy) (Fig. 1A). This area is characterized by a combination of shallow waters and high riverine inputs (dominated by the Po river outflow) (Marini et al., 2008), that makes its coastal environments as one of the most eutrophic and most productive in the Mediterranean, promoting an intense mussel farming activity (Brigolin et al., 2017). The study area is generally characterized by sudden and anomalous rise/drop of temperature, salinities, or eutrophic level, mainly related to climatological events and riverine inputs from the Italian border (https://www.arpae.it). Furthermore, the area is characterized by the periodical rise of algal blooms and the occurrence of algal toxins which are accumulated by mussels (Buratti et al., 2013). These phenomena may elicit transitory stress conditions in mussels.

The selected sampling site is routinely monitored by the Regional Agency for Prevention, Environment and Energy of Emilia-Romagna, Italy (ARPA-ER) to evaluate seawater parameters, algal biomass and the occurrence of algal toxins (https://www.arpae.it). During the sampling period, no relevant events of algal blooms were recorded, although

449 in June a peak of chlorophyll-a > 10 μg/L indicates the onset of transitory eutrophic conditions.
450 No hypoxic conditions (dissolved oxygen <3 mg/L) were recorded; however, a relevant
451 reduction was recorded in July and August. Sea surface temperatures followed the monthly
452 profile and overall range of variability typical of a shallow- water ecosystem as the study area,
453 with winter temperatures < 10 ◦C, summer values > 27 ◦C (Fig. 1B). In March and in May, two
454 events of relatively low salinity were recorded (Fig. 1B). In March, climatological records
455 reported in the ARPA-ER database indicates the occurrence of heavy rains and snow melting as
456 well as high riverine inputs. The low salinity was paralleled by a reduction of transparency,
457 likely related to the input of sediments and debris along with freshwater inflow, while the low
458 chlorophyll-a values indicate a low algal biomass (Fig. 1B). In May, high riverine inputs were
459 recorded. These inputs determined an increase of eutrophic level with rise of algal biomass
460 (mainly diatoms of the genus Chaetoceros sp.).
461 Mussel samples were collected once a month, from February to August 2018. At each sampling
462 time point, 60 randomly selected mussels were collected directly in the field, immediately stored
463 in coolers (4 ◦C) and transferred to the laboratory, where they were cleaned and washed and
464 immediately processed for tissue (mantle/gonad complexes and digestive glands) dissection
465 under sterile conditions. Tissues were snap-frozen in liquid nitrogen and then stored at 80 ◦C.
466 Sex was determined in individual mussels using the sex-specific gene method (Fraser et al.,
467 2016). Specifically, the method consists in the quantification through real-time PCR (qPCR) of
468 expression of the mussel vitelline envelope receptor for lysine (VERL), and vitelline coat lysine
469 (VCL) mRNAs in the mantle/gonad complex. The transcripts are specifically expressed in
470 females and males, respectively, and serve as a proxy of gonadal cycle (Hines et al., 2007). This
471 method proved suitable differentiating males from females both during gametogenesis and sex-
472 ual resting stage, when histology does not allow the observation of gametes (Anantharaman and
473 Craft, 2012; Fraser et al., 2016). RNA extraction and cDNA preparation from mussel
474 mantle/gonad complexes was as reported below. qPCR reactions were performed in duplicate

for each sample using primer pairs and protocols reported previously (Anantharaman and Craft, 2012) (Table S2). Threshold cycle (CT) values were determined by setting a constant baseline. Sex was determined calculating the intra animal ΔCT as CT(VCL) CT(VERL) (Anantharaman and Craft, 2012). Negative values indicate males and positive values indicate females. Relative VCL or VERL expression values across season (Fig. 1C) were inferred by a comparative CT method (Schmittgen and Livak, 2008) using the normalization and statistical strategy re- ported below. As reported previously (Anantharaman and Craft, 2012), both VERL and VCL expression levels significantly decreased from winter to summer (Fig. 1C). Based on visual microscopic inspection of gonads (Hines et al., 2007), transcript levels of both sex specific genes was found to be associated to the presence and abundance of gametes. Mussel biometric parameters are reported in Table S1. A production metric, the condition factor, was calculated, with values being un- changed across seasons and similar between females and males (Fig. 1D; Table S1). The lysosomal membrane stability (LMS) was assessed in mussel living hemocytes through the neutral red retention assay according to (Buratti et al., 2013). LMS is a well-consolidated general stress biomarker and a prognostic indicator for putative pathologies. As such, it addressed to as an integrated pathophysiological indicator of general health status (Martínez-Go´mez et al., 2015). According to Martínez-Go´mez et al. (2015), neutral red retention time (NRRT) values recorded in this study fall within the range representing stressed but compensating organisms (Table S1). Furthermore, while males show almost constant NRRT values across season, females show a sig- nificant reduction of NRRT values from winter to summer, which indicate increased stress levels.

3.2.2 RNA extraction, cDNA preparation, and qPCR analyses

For each animal, 200 mg of mantle/gonad complex (sex identifica- tion and gonadal cycle) or digestive glands were independently ho- mogenized in a suitable volume of the TRI Reagent (Sigma Aldrich, Milan, Italy) and total RNA was extracted using the DirectZol kit (Zymo Research, Freiburg, Germany) following the manufacturer's in- structions. RNA concentration and quality were confirmed using the Qubit system with the Qubit RNA assay kit (Thermo Scientific, Milan, Italy) and electrophoresis using a 1.2% agarose gel under denaturing conditions. The analysis of UV absorbance spectra of the samples (λ = 200–340 nm) allowed the calculation of Absorbance (A) ratio A260/ A280 addressing the occurrence of protein contaminations (cut-off values > 1.8 and <2.0), and the ratio A260/A230 addressing the occurrence of contaminants that may be present in the samples, such as guanidine thiocyanate, which is a component of the TRI Reagent (cut-off value > 1.7). First strand cDNA for each sample was synthesized from 1 μg total RNA using the iScript supermix (BioRad Laboratories, Milan, Italy) following the manufacturer's instructions.

Expression profiles of selected transcripts in digestive glands were assessed by qPCR using primer pairs listed in Table S2 and protocols reported in previous studies (see references in Table S2). 18S and 28S were selected as reference gene products for qPCR data normalization by a preliminary stability analysis of 6 established candidate transcripts (Balbi et al., 2016). Relative expression values of target mRNAs were inferred by a comparative CT method (Schmittgen and Livak, 2008) using the StepOne and DataAssist softwares (Thermo Fisher, Milan, Italy). Data were reported as relative expression (fold change) with respect to a reference sample (Winter male).

3.2.3 Microbial DNA extraction and sequencing

Total microbial DNA was extracted from approximately 20–30 mg of digestive gland tissue using the DNeasy PowerSoil kit (Qiagen, Hilden, Germany) according to (Musella et al., 2020). The V3–V4 hypervariable region of the 16S rRNA gene was amplified using the 341F and 785R primers with added Illumina adapter overhang sequences, as previously described (Barone et al., 2019). The thermal cycle consisted of initial denaturation at 95 ◦C for 3 min, 30 cycles at 95 ◦C for 30 s, annealing at 55 ◦C for 30 s, extension at 72 ◦C for 30 s and 5 min at 72 ◦C for final extension. PCR reactions were then cleaned up with Agencourt AMPure XP magnetic beads (Beckman Coulter, Brea, CA). Indexed libraries were prepared by limited-cycle PCR, using the Nextera technology and then pooled after a further clean up step as described above and normalized to 4 nM. The sample pool was denatured with 0.2 N NaOH and diluted to a final concentration of 6 pM with a 20% PhiX control. Sequencing was performed on Illumina MiSeq platform using a 2 250 bp paired end protocol, according to the manufacturer's instructions (Illumina, San Diego, CA). Sequencing reads were deposited in SRA-NCBI.

3.2.4 Statistical and bioinformatic analyses

qPCR data were analyzed using the REST software (Pfaffl et al., 2002) to test for statistical differences in mRNA levels of the treatment groups vs the reference condition. Further pairwise comparisons were performed with the Mann-Whitney U test (GraphPad Prism v9). Data visualization, and graphics were obtained with the ggplot2 R package in R (R Development Core Team, 2018). In any case, statistical differences were accepted when $P < 0.05$.

The complete dataset was further analyzed by a 2-way permutation multivariate analysis of variance (PERMANOVA) using PRIMER v6 (Anderson et al., 2008) to test for variations of transcriptional profiles among sex and season groups. Log-transformed variations of the target transcripts were used to calculate similarity matrices based on the Euclidean distance (999 permutations). When the main tests revealed statistical differences ($P < 0.05$), PERMANOVA

pairwise comparisons were carried out. Distance-based redundancy linear modeling (DISTLM) with a test of marginality in PRIMER was also performed to account for the contribution of environmental parameters and gonad cycle in explaining the total observed variance in the transcriptional profiles. DISTLM used the BEST selection procedure and adjusted R2 selection criteria. BEST/BioEnV analysis in PRIMER 6 was also carried out using a Spearman rank correlation to identify the best correlated environmental variables that explained the observed patterns of gene transcriptions (999 permutations).

For DG microbiome analyses, raw sequences were processed using a pipeline combining PANDAseq (Masella et al., 2012) and QIIME 2 (https://qiime2.org) (Bolyen et al., 2019). High-quality reads were clustered into amplicon sequence variants (ASVs) using DADA2 (Call- ahan et al., 2016). A normalized ASV table has been used, so that for all samples the same number of reads have been considered. Taxonomy was assigned using the SILVA database as a reference (Quast et al., 2013). Unassigned sequences and those assigned to eukaryotes (i.e. chloro- plasts and mitochondrial ones) were discarded. Beta diversity was esti- mated by computing unweighted UniFrac distance. All statistical analyses were performed using R software version (R Development Core Team, 2018). ASVs were filtered for prevalence, retaining only ASV showing a relative abundance >1% in at least 10% of samples. UniFrac distances were plotted using the vegan package, and permutation test pseudo-F ratios (function adonis in the vegan package) was computed to test the significance of data separation in the principal coordinate's analysis (PCoA).

Kendall correlation test and a DISTLM analysis with a test of mar- ginality was used to determine associations between the PCoA co- ordinates (Kendall correlation) or relative abundances of microbic phyla (DISTLM) and expression profiles of selected transcripts. False discovery rate (FDR) (function p.adjust in the stats package) was used to adjust P-values, and a P-value 0.05 was considered as statistically significant. DISTLM used the BEST selection procedure and adjusted R2 selection criteria.

3.3 *Microbiome characterization of M. galloprovincialis along a spatial and temporal environmental stress gradient.*

3.3.1. Mussels collection

Total of 450 samples were collected, in particular 50 per site 150 per season, separated in digestive gland and gill tissues, were collected in autumn, spring and summer.

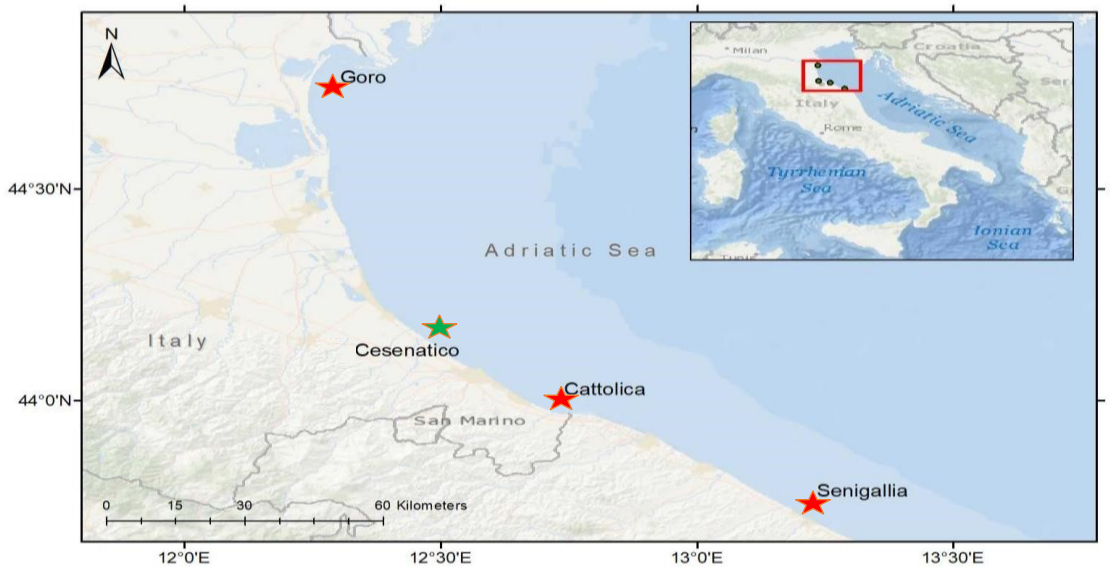

Fig 1. Study area, location of the mussel farms assessed in this study in the NorthWestern Adriatic Sea (Italy). Location and season effects. Mussels were collected from the three locations, namely: Goro, Cattolica, and Senigallia (figure 1). The farms at Goro, Cattolica, and Senigallia represent from the north to the south coastal part of the western Adriatic Sea. Those farms are generally well-established in the area. Other than the location factor, to stimulate the seasonal effects, sampling was carried out in consecutive three seasons, including autumn, spring, and summer in each location. Each sample consisted of twelve mussels of commercial size (5–7 cm in length) and immediately transferred to the laboratory for further analysis.

3.3.2 Microbial DNA extraction

Total microbial DNA was extracted from approximately 20–30 mg of the digestive gland, foot, gill and stomach, and from 200 µl of hemolymph, using the DNeasy PowerSoil kit (Qiagen, Hilden, Germany) according to the manufacturer's instructions with only minor adjustments in the homogenization step. Specifically, all samples were homogenized using the FastPrep instrument (MP Biomedicals, Irvine, CA) at 6 movements per s for 1 min. The elution step was repeated twice in 50 µl, incubating the columns for 5 min at 4 °C before centrifugation. DNA samples were stored at −20 °C for subsequent processing.

Seawater samples were filtered on 0.45-µm pore size MF-Millipore membrane filters using a vacuum pump. Total microbial DNA was extracted from membrane filters using the DNeasy PowerWater kit (Qiagen) according to the manufacturer's protocol. 2.3. PCR amplification and sequencing

The V3–V4 hypervariable region of the 16S rRNA gene was PCRamplified using the 341F and 785R primers with added Illumina adapter overhang sequences, as previously described in Barone et al., 2019. The PCR programused was as follows: 95 °C for 3 min as initial denaturation, then 30 cycles of denaturation at 95 °C for 30 s, annealing at 55 °C for 30 s and elongation at 72 °C for 30 s, and 5 min at 72 °C for the final elongation. PCR reactions were purified with Agencourt AMPure XP magnetic beads (Beckman Coulter, Brea, CA). Indexed libraries were prepared by limited-cycle PCR, using the Nextera technology (Illumina, San Diego, CA). After a further clean up step as described above, libraries were normalized to 4 nM and pooled. The sample pool was denatured with 0.2 N NaOH and diluted to a final concentration of 6 pM with a 20% PhiX control. Sequencing was performed on an Illumina MiSeq platform using a 2 × 250 bp paired-end protocol, according to the manufacturer's instructions.

3.3.3 Bioinformatics and statistics

Raw sequences were processed using a pipeline combining PANDAseq (Masella et al., 2012) and QIIME 2 (Bolyen et al., 2019; https://qiime2.org). High-quality reads were clustered into amplicon sequence variants (ASVs) using DADA2 (Callahan et al., 2016). Taxonomy was assigned using the VSEARCH classifier (Rognes et al., 2016) and the SILVA database as a reference (Quast et al., 2013). Unassigned sequences and those assigned to eukaryotes (i.e. chloroplasts and mitochondrial ones) were discarded.

Alpha rarefaction was performed using Faith's Phylogenetic Diversity (PD whole tree). A trade-off rarefaction value of 1900 reads per sample was chosen to capture the extent of diversity in our data. Beta diversity was estimated by computing weighted and unweighted UniFrac distances.

All statistical analysis was performed using R version 3.5.1 (https:// www.r-project.org/). Weighted UniFrac distances were plotted using the vegan package, and the significance of data separation in the principal coordinates analysis (PCoA) was tested using a permutation test with pseudo-F ratios (function adonis in the vegan package). Alpha diversity was evaluated using two different metrics: Simpson Index (complement) and observed ASVs. Pvalues were adjusted for multiple comparisons using the false discovery rate (FDR) (function p.adjust in the stats package), and a P-value $\leq .05$ was considered as statistically significant.

3.4 *Development and validation of a liquid chromatography – mass spectrometry method for multiresidue analysis in mussel of the Adriatic Sea*

3.4.1. Chemicals

Water of HPLC-MS grade (Millipore) was produced using the depurative system Milli-Q Synthesis A 10 (Molsheim, France). Methanol (MeOH), hexane, cyclohexane, dichloromethane (DCM), acetone and acetonitrile (ACN), all of HPLC-grade were purchased from Merck (Darmstadt, Germany). Acetic acid (98% pure), Magnesium sulfate monohydrate (MgSO4·H2O), Ethylenediaminetetraacetic acid (EDTA), and sodium hydroxide (98% pure) were purchased from Fluka (Buchs, Switzerland).

Metolachlor, Alachlor, Atrazine, Sulfamethoxazole, Erythromycin A dehydrate, Tetracycline, Doxycycline hyclate and Amoxicillin trihydrate standards were purchased from Merck Life Science BV (Overijse, Belgium). Carbamazepine, Atrazine-desethyl-desisopropyl, N,N-Diethyl-meta-toluamide standards and 3-((3-cholamidopropyl) dimethylammonio)-1-propanesulfonate (CHAPS) were purchased from Merck KGaA (Darmstadt, Germany). Isotopically labeled internal standards (ILISs) Metolachlor-(2-ethyl-6-methylphenyl-d11), Alachlor-d_{13}, Atrazine-d_5, Carbamazepine- $^{13}C_6$, Sulfamethoxazole-(phenyl-$^{13}C_6$) were from Merck Life Science BV (Overijse, Belgium).

Supel QuE Z-Sep+ Tube, Supel QuE PSA/C18 Tube, Supel QuE Citrate (EN) extraction tubes, Supel QuE Acetate (AC) extraction tubes and LiChrolut EN 200mg 6ml SPE materials were acquired from Merck KGaA (Darmstadt, Germany). C18 (500 mg, 6 mL) SPE columns were purchased from SiliCycle (Quebec, Canada).

3.4.2. Standard solutions

Single stock solutions (1 mg/mL) of Metolachlor, Alachlor, Atrazine, Sulfamethoxazole, Erythromycin A dehydrate, Carbamazepine, Tetracycline, Doxycycline hyclate, Amoxicillin

669 trihydrate standards and respective ILISs (Metolachlor-(2-ethyl-6-methylphenyl-d11), Alachlor-d_{13},
670 Atrazine-d_5 and Sulfamethoxazole-(phenyl-$^{13}C_6$) were prepared in methanol and stored until use at -
671 80° C.
672 Carbamazepine- $^{13}C_6$ was already available at a concentration of 100 µg/mL in methanol. Stock
673 solution of Atrazine-desethyl-desisopropyl was prepared in methanol at a concentration of 100 µg/mL
674 and stored until use at -80° C.
675 Standard solutions used for method validation were obtained diluting stock solutions in mobile phase.
676 Spiked sample solutions used for optimization of extraction procedure and calibration curve were
677 obtained diluting stock solution in methanol in the range 0.002-500 ng/mL and then treated as samples
678 (see section 2.5).
679

680 ### 3.4.3 Instrumentation conditions

681 Liquid chromatography was performed using a 2690 Alliance system (Waters, Milford, MA, USA)
682 coupled to a triple quadruple mass spectrometer (Quattro-LC, Micromass), equipped with an ESI
683 source, operating in the multiple reaction monitoring (MRM) acquisition mode. The optimal analytical
684 separation was achieved by using an Atlantis T3 Column (5 µm, 2.1 mm X 150 mm, Waters) in
685 gradient elution with a mobile phase composed of 0.01% acetic acid in water (A) and 0,01% acetic
686 acid in a solution of methanol and acetonitrile 65:35 (v/v) (B). The initial conditions, 10% of solvent
687 B, were held for 5 min, then solvent B was increased to 60% over 7 min followed by a further rise to
688 80% over 3 min and a successive further rise to 90% over 2 min. These conditions were held for 25
689 min. Finally, mobile phase B was returned to its initial conditions over 10 min. The separation was
690 completed within 37 minutes. The flow rate was 0.14 mL/min, the column temperature was
691 maintained at 20°C with an injection volume of 5 µL.
692 The MS/MS experimental conditions were tuned by direct infusion of the single analytes. The
693 detection was performed in positive mode (2500 V) and the spectra were acquired in multiple reaction
694 monitoring (MRM) mode. Argon gas was selected as collision gas and nitrogen as nebulizer and heater

gas. Nitrogen was used as nebulizer gas at 117 L/h flow rate and as desolvation gas at 622 L/h. Ion source block and desolvation temperatures were set at 120 °C and 180 °C, respectively. Capillary and cone voltages were 2,90 kV and 60 V, respectively. For optimization of MS parameters, individual standard solutions were prepared in methanol (10 mM) and introduced into ESI source by direct infusion at a flow rate of 20 mL/min.

3.4.4 Sample collection, pooling and storage

Mediterranean mussels (Mytilus galloprovincialis) of commercial size (4–6 cm in length), obtained from a government certified mussel farm (Cooperativa Copr.al.mo, Cesenatico, Italy) were transferred to the laboratory in seawater tanks and acclimated in aquaria containing 35-psu filtered seawater at 16 °C with continuous aeration (> 90 % oxygen saturation). During acclimatization, mussels were fed once a day with a commercial algal slurry (Koral, Xaqua). Mussels were immediately analyzed to assess their good initial health status employing the lysosomal membrane stability (neutral red retention assay) (Buratti et al., 2013) (data not shown). Whole mussel soft mass was dissected from 15 groups of animals (3 animal/group). Pooled samples were then homogenized using a UltraTurrax system (IKA), frozen at -20°C and finally lyophilized.

3.4.5 Sample extraction procedure

The optimized extraction procedure reported in Figure 1 offered the best compromise among recoveries, limit of detection and matrix effect. Aliquots of 250 mg dry weight (dw) of whole mussel powder were transferred into a centrifuge tube and stored at -20°C until sample clean-up. The extraction procedure was as follow: 1) Aliquot was thawed, 10 µL of IS 10 µM were added and the freezed-dried sample was extracted with 1 mL of cold ACN:MeOH (50:50 v/v) mixture, 10 µL of EDTA 25 mM and 0,25 g of $MgSO_4$ were added. The sample was vortexed for 2 min, cooled for 10 min at -20°C and centrifuged with a controlled temperature of 4°C at 3600 rpm for 2 min for protein precipitation, the supernatants, obtained from two identical replicated extractions were collected. 2)

721 The sample powder pellet underwent a second double extraction with 1 mL of a previously
722 refrigerated solution of Hexane:Acetone (50:50 v/v) and the addition of 10 µL of EDTA 25 mM. The
723 sample was vortexed for 2 min, cooled for 10 min at -20°C and centrifuged with a controlled
724 temperature of 4°C at 3600 rpm for 2 min. 3) The supernatants were collected and mixed with the
725 ones obtained with ACN:MeOH (50:50 v/v) mixture. The extracted solution was vacuum dried with
726 a UNIVAPO Vacuum Concentrator (UniEquip, Monaco). 4) The oily residue was re-dissolved in 200
727 µL of CHAPS 0,6% (m/v) aqueous solution. The sample was vortexed for 1 min and centrifuged at
728 3600 rpm for 10 min. The supernatant was collected and stocked separately. 5) 100 µL of MeOH were
729 added to the remaining residues, the sample was vortexed for 1 min and centrifuged at 3600 rpm for
730 7 min. 6) The supernatant was collected and stocked with the previously collected supernatant. 7) This
731 solution was centrifuged with a controlled temperature of 4°C at 13400 rpm for 10 min. 100 µL of the
732 filtered (0.45 µm syringe filter) supernatant were injected in the LC-MS system.

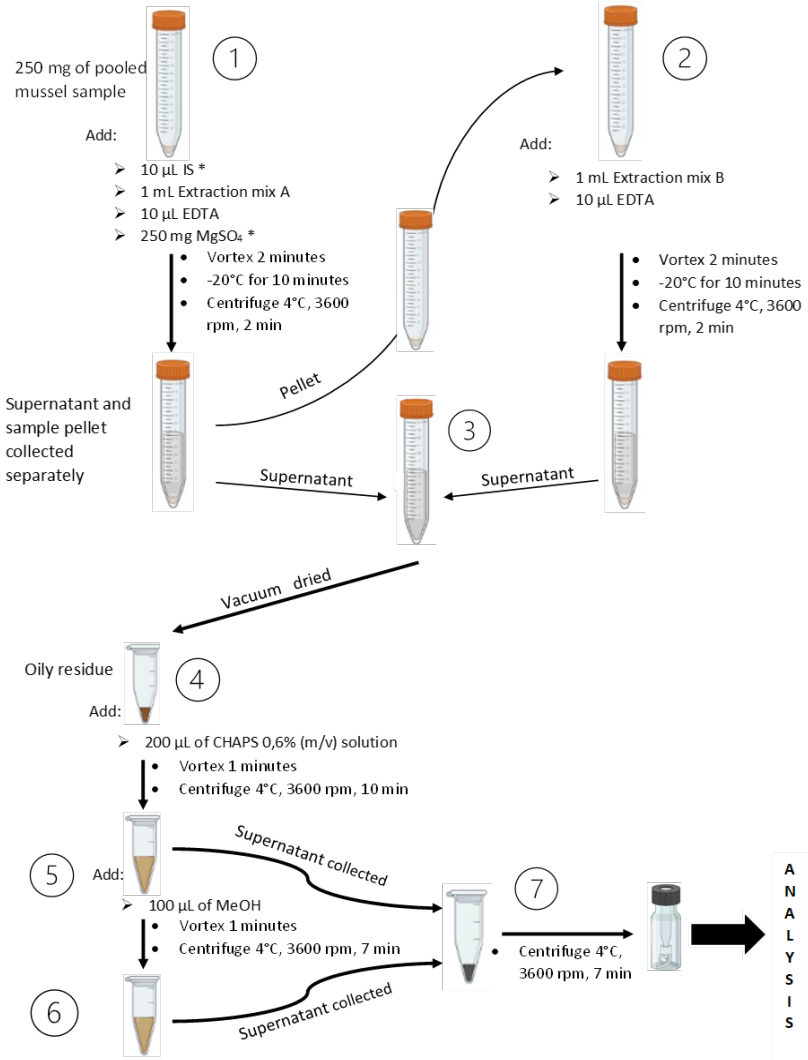

Fig. 2. Optimized extraction procedure

3.4.6 Optimization of extraction procedure

To determine the optimum extraction procedure, different organic solvents were tested: hexane, cyclohexane, dichloromethane, acetonitrile, methanol and acetone. The optimization on the solvents was conducted as to maximize recoveries for the analytes and when possible, to decrease matrix effect. Finally as described in section 2.5, we obtained the best compromise using two separated extraction mixtures: the first with CAN:MeOH (50:50) solution and the second with a hexane:acetone (50:50) solution.

To improve recoveries of analytes, micro volumes of a solution of EDTA (25mM) and 0,25 g of $MgSO_4$ were added to the mussel pellet during extraction.

745 Extraction temperature was also optimized. Different thermal sample treatments were evaluated, in
746 particular sample preparation as described in section 2.5 was conducted in parallel at room
747 temperature, or involving the use of refrigerated solvents and a rapid cooling cycle (-20°C for 20
748 minutes). Percentage agreement of target analytes from cold treated versus room temperature was
749 calculated.
750 Sample clean-up by means of solid phase extraction (SPE) was evaluated. After solvent extraction
751 with CAN/MeOH and hexane/acetone as reported in paragraph 2.5, the sample was dryed and
752 resuspended with 1ml of the mobile phase and SPE was tested. Two different SPE were tested
753 LiChrolut EN (200 mg, 6 mL) and Silicycle C18 (500 mg, 6 mL). SPE columns were activated with
754 5 mL of MeOH and 5 mL of H_2O. The resuspended sample was added to the SPE cartridge. The
755 cartridge was washed with 1ml of water and the analytes were eluted with MeOH. Aliquots of 1 ml
756 were collected, dried and quantified as per optimized procedure described in paragraph 2.3.
757 Recoveries and matrix effect were calculated.
758 Sample clean-up was also considered by the use of two alternative extraction procedures based on
759 dispersive SPE (d-SPE) such as QuECheERS method, including Supel QuE Citrate (EN) + Supel QuE
760 Z-Sep+ Extraction tubes and Supel QuE Acetate (AC) + Supel QuE PSA/C18 extraction Tube, this
761 specific powder mixes were employed because especially indicated for improving recoveries of
762 pesticides from fat matrixes. Prior extraction with CAN:MeOH salts were added and the standard
763 Quechers and d-SPE procedure was applied. The obtained solution was then evaporated, resuspended
764 in 200 µL of mobile phase, centrifugate and the supernatant was stocked separately. The remaining
765 residues was treated as described *in points 5), 6) and 7)* in section 2.5 (without using CHAPS solution).
766 The use of a surfactant was assayed. CHAPS is a zwitterionic surfactant typically used
767 to solubilize biological macromolecules. We employed it in our procedure to dissolve the oily residues
768 obtained after drying our extraction solvent and thus improve our recoveries. A side-by-side
769 comparison of the quantitation of CHAPS treated/untreated samples was conducted.
770

3.4.7 Method validation

For each analyte, the method performance was evaluated by the determination of retention time (RT), transition ion ratios, recovery, accuracy (trueness), precision (expressed as the intra- and inter-day repeatability), linearity, as well as method detection limits (MDL) and method quantification limits (MQLs)

Selectivity was evaluated by comparing the chromatograms obtained from standards, samples, and spiked sample solutions.

The instrumental linearity was also assessed through six-point calibration curves in matrix-matched curve containing a precise amount of each IS (10 MQL) obtained by dilution of the stock solution with methanol in the range 0.002-500 ng/mL and then spiked in mussel matrix without analytes.

MDL and MQL were determined in spiked samples before the extraction (n=3) considered as the minimum detectable amount of analyte with signal-to noise ratio (S/N) of 3 and 10, respectively.

Accuracy and precision of the whole method were calculated intra (n=3) and inter-day (n=9) from three repeated injections of spiked sample solution (QC) at 3 different concentrations (low to high) and extracted. Low concentration was coincident with the MQL, medium concentration was 10 MQL and high concentration was 100 MQL.

To evaluate potential matrix effects the following approach was adopted: a pooled mussel sample (mussel matrix without analytes) was extracted as per the protocol (section 2.5); the final supernatant was then spiked with analyte standard solutions at three concentration levels (low, medium and high) and analyzed. Quantitation on this sample was compared to results obtained on a mobile phase standard solution at the same analyte concentration levels. The percentage matrix effect (matrix ion suppression/enhancement) was calculated. If ME ≈ 0% there is no observed matrix effect, if ME > 0% then an ion-enhancement occurred, and if ME < 0% an ion-suppression occurred.

Recovery experiments were performed in triplicate at three concentration levels (low: MQL, medium: 10 MQL and high: 100 MQL) by comparing the area ratio of the analyte to the IS of sample fortified before and after extraction. In these conditions, both samples are subjected to the same matrix effect

797 contribute, making eventual differences dependent only to the efficiency of the extraction. The
798 different samples were analyzed, and percentage absolute recoveries were calculated.
799
800 ### 3.4.8 Short-term storage stability
801 To investigate the effects of different storage methods during daily operations, stability of mixed
802 standard solutions was assessed. Mixed standard solutions placed in a 2 mL amber glass LC vials,
803 were stored under three different conditions, room temperature, at 4°C in the autosampler, at -20°C,
804 for 8 hours to assess the possible loss of analytes during sample processing and analysis time. The t
805 = 0 and t = 8 h standard solutions at the same concentrations were a
806
807
808

4. Results

4.1 Tissue-scale microbiota of the Mediterranean mussel (*Mytilus galloprovincialis*) and its relationship with the environment

A total of 121 samples (25 digestive glands, 25 gills, 21 stomachs, 25 feet, 18 hemolymph samples and 7 seawater samples) were analyzed (Table S1). For each sample, the microbiota structure was profiled by NGS of the V3–V4 hypervariable region of the 16S rRNA gene. A total of 5 621 255 paired-end sequences passed quality filtering (mean per sample ± SD, 46 456 ± 68 116). High-quality reads were clustered into 18 787 ASVs (8 532 ± 4 634).

The overall composition of the M. galloprovincialis microbiota is reported in Figure 2A. The phyla Proteobacteria (mean relative abundance (r. a.) ± SD, 44.8% ± 27.2%), Firmicutes (18.5% ± 20.2%) and Bacteroidetes (14.8% ± 12.8%) dominated the ecosystem. Spirochaetes, Verrucomicrobia, Actinobacteria, Tenericutes, Planctomycetes, Cyanobacteria, Fusobacteria, Chloroflexi and Chlamydiae were subdominant components, with a mean r. a. of about 5%. At the family level, the most represented taxa were an unclassified family of the Alteromonadales order (10.7 ± 21.6%) and Flavobacteriaceae (8.8% ± 9.6%) (Figure 2B). Spirochaetaceae, Ruminococcaceae, Lachnospiraceae, Bacillaceae, Vibrionaceae, Verrucomicrobiaceae, Hahellaceae and Rhodobacteraceae were subdominant families, showing a mean r. a. ranging from 3% to 5%. Consistently, among the dominant genera we reported unclassified taxa of Alteromonadales (10.6% ± 21.4%) and Flavobacteriaceae (5.4% ± 6.3%). Spirochaeta 2, Bacillus, Vibrio, Endozoicomonas, an unclassified genus of Verrucomicrobiaceae and Mycoplasma were all subdominant

genera with mean r. a. between 3% and 5% (Figure 3C).

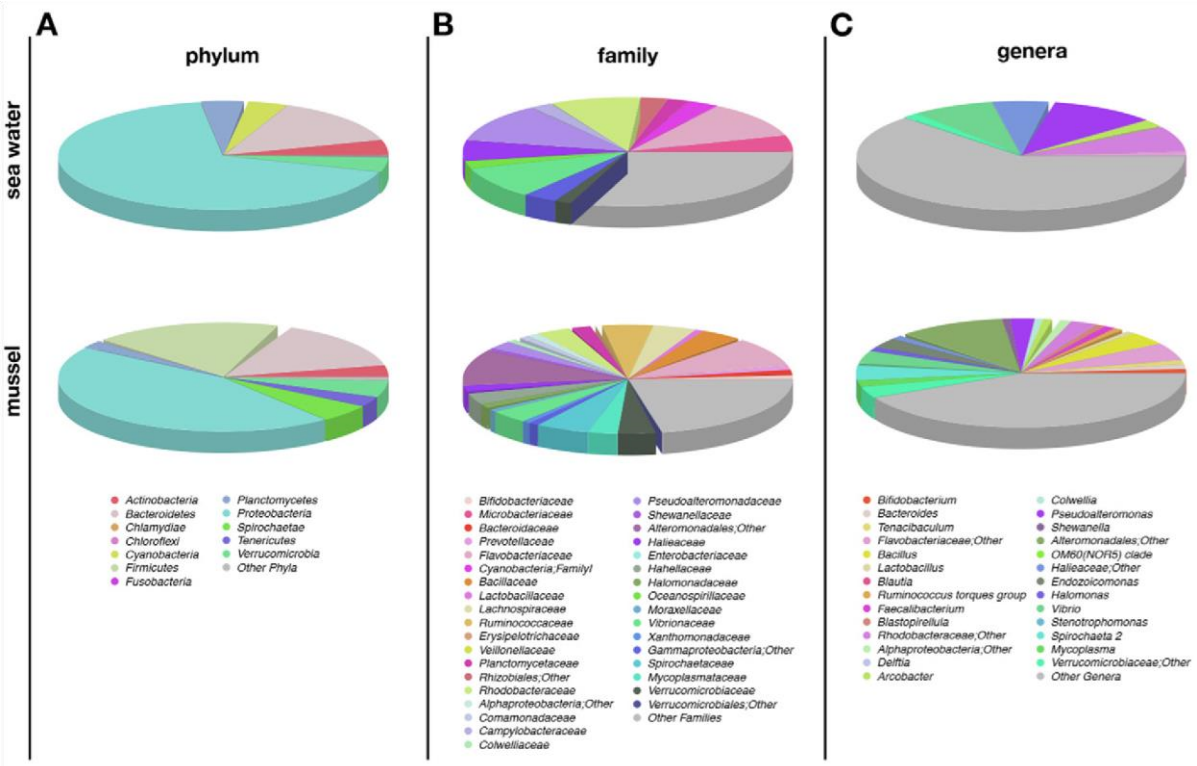

Fig 3. The whole Mytilus galloprovincialis and seawater microbiota. Pie charts summarizing the phylum- (A), family- (B) and genus-level (C) microbiota composition of Mediterranean mussels and seawater. Only phyla with relative abundance ≥1% in at least 10% of samples, families with relative abundance ≥1.5% in at least 10% of samples and genera with relative relative abundance ≥2% in at least 10% of samples are represented.

As for seawater, Proteobacteria (68.6 ± 8.4%) and Bacteroidetes (14.8% ± 3.2%) were the dominant phyla (Figure 3A), with Actinobacteria, Verrucomicrobia and Planctomycetes being subdominant components (mean r. a., 5%). The most represented families were Pseudoalteromonadaceae (11.6% ± 8.6%), Flavobacteriaceae (11.0% ± 4.3%) Vibrionaceae (9.3% ± 9.2%), Rhodobacteraceae (8.8% ± 4.0%) and Halieaceae (6.1% ± 5.9%). Microbacteriaceae, FamilyI of Cyanobacteria, Campylobacteraceae, Planctomycetaceae, and Verrucomicrobiaceae were subdominant components, with a mean r. a. ranging from 2% to 5% (Figure 3B). At the genus level, Pseudoalteromonas (11.7% ± 8.4%), Vibrio (9.0% ± 8.7%), and unknown genera belonging to the Rhodobacteraceae (7.5% ± 4.8%) and Halieaceae families (6% ± 6.6%) were the dominant taxa. Among the subdominant ones,

Synechococcus, Arcobacter and an unclassified genus of Verrucomicrobiaceae were present, all showing average r. a. between 2% and 3% (Figure 3C).

4.1.1 Tissue-specific composition of M. galloprovincialis microbial ecosystems

To explore peculiarities of microbiota composition in the different tissues of M. galloprovincialis, an unweighted UniFrac-based PCoA of the compositional profiles of mussel samples, as well as of seawater, was carried out. As expected, the seawater samples clustered apart from all mussel organs (Figure 3A) and the mussel samples significantly segregated according to the tissue type (permutation test with pseudo-F ratios, P-value ≤ 0.001). To assess the degree of microbiota variation between tissues, pairwise adonis permutation tests were performed (Table S2). Even if showing overall low R2 values, all between-tissue comparisons of the microbiota structure were found to be significant (P-value ≤ 0.03), highlighting the high level of organ specificity of mussel microbiota (Figure 4A).

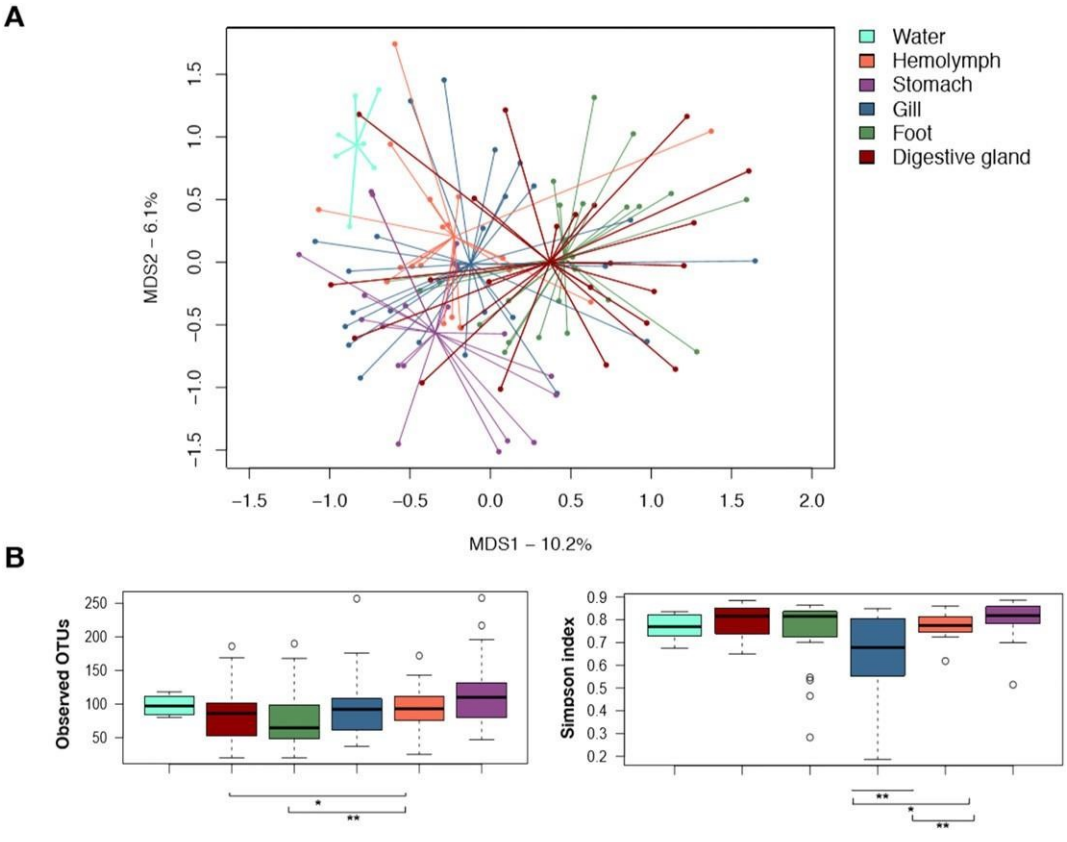

*Fig.4. Alpha and beta diversity of M. galloprovincialis tissue and seawater microbiota. (A) PCoA based on unweighted UniFrac distances between the microbiota structures of the samples taken from each organ of M. galloprovincialis and seawater. Samples are significantly separated (permutation test with pseudo-F ratios, P-value ≤.001). (B) Box and whiskers plots showing the alpha diversity values, measured as amplicon sequence variants (ASVs) and Simpson index- complement. *, P-value ≤.05, Wilcoxon test.*

With regard to alpha diversity, no significant differences in species richness were found among the seawater and mussel ecosystems. However, the gill microbiota showed lower evenness (calculated as Simpson index- complement) than that of the digestive gland and stomach (Wilcoxon test, P-value < 0.03).

For what concerns the compositional structure, the microbiota from each organ showed a specific layout of dominant families (Figure 5). In particular, Ruminococcaceae (mean r. a. ± SD, 14% ± 14%) and Lachnospiraceae (10% ± 13.2%) dominated the digestive gland microbial ecosystem. Spirochaetaceae were dominant in the foot (2% ± 26%), while an unclassified family of the Alteromonadales order (43% ± 25%) and Hahellaceae (11% ± 9.6%) dominated the gills, Mycoplasmataceae (15% ± 18%) the stomach and Flavobacteriaceae (19% ± 11.2%) the hemolymph (Figure 4). The relative abundance of the most represented families in all Mediterranean mussel organs and seawater is provided in Table S3.

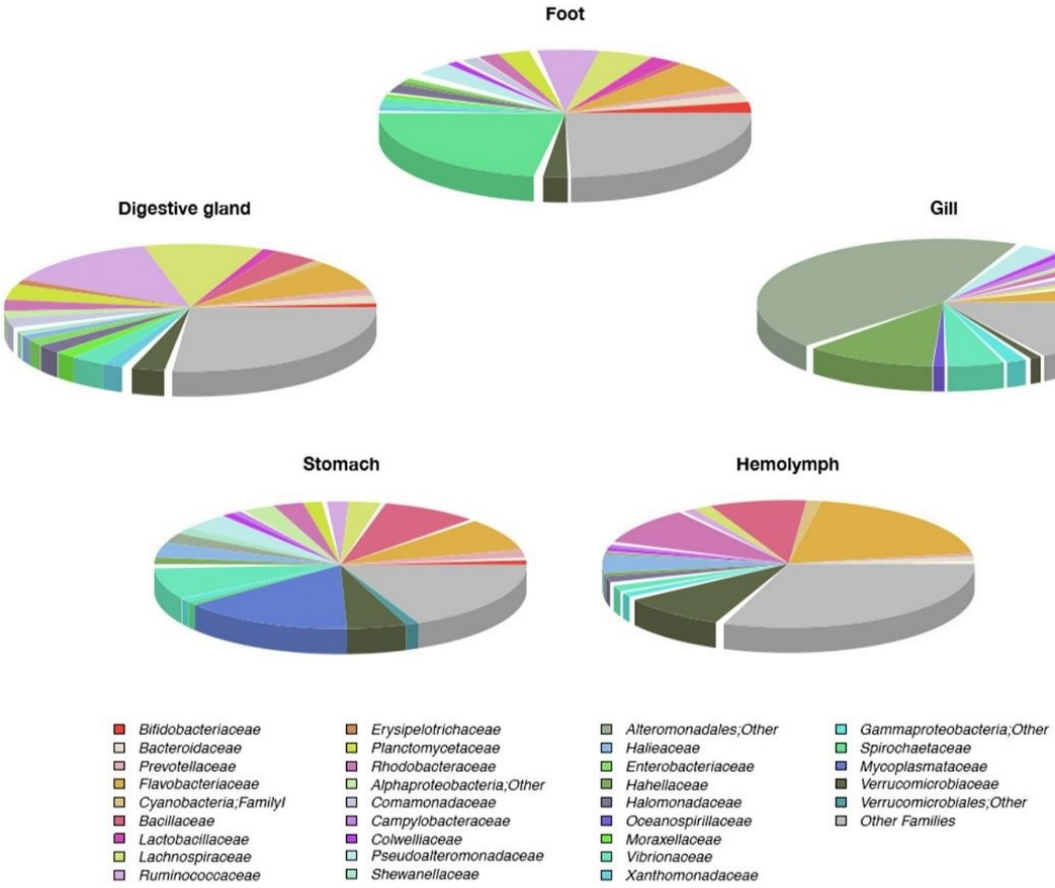

Fig.5. The tissue-specific M. galloprovincialis microbiota composition at the family level. Pie charts summarizing the family-level microbiota composition of the digestive gland, foot, gill, stomach and hemolymph of M. galloprovincialis. Only bacterial families with a relative abundance of ≥1.5% in at least 10% of samples are represented.

4.1.2 Impact of mussel farming on the microbiota composition of the surrounding seawater

With the aim of assessing the impact of mussel farming on the surrounding seawater, we compared the microbiota composition between 6 seawater samples collected close to the mussel farm and a sample collected 3 miles away from the farm as a control (Figure S1).

As shown in Figure S2, we noticed a variation in the family-level relative abundance profiles between the seawater surrounding the mussel farm and the control water. In particular, the families Pseudoalteromonadaceae and Verrucomicrobiaceae showed greater relative abundance in the seawater surrounding the mussel farm than in the control water (mean r. a. ± SD, 13.4% ± 7.9% vs.

1%, and 1.9% ± 1.7% vs. 0%, respectively), while Halieaceae was more represented in the control water (r. a., 10.9% vs. seawater near the farm, 5.3% ± 6.4%).

Interestingly, the family Vibrionaceae, which includes several species known as opportunistic and potential pathogens of marine organisms (Baker-Austin et al., 2018; Le Roux et al., 2015), was also more represented in the seawater surrounding the mussel farm (10.6% ± 9.3%) than in the control water (1.5%). In order to identify the Vibrionaceae-related ASVs down to species level, their sequences were mapped onto the 16S Microbial NCBI database. The best hit was Vibrio splendidus (>80% identity), a well-known potential pathogen.

4.1.3 Predicted *functional profiling of M. galloprovincialis and seawater microbiomes.*

To gain insight into the peculiar functional variations of the microbiota in the different M. galloprovincialis organs/tissues, as well as in the seawater, correspondent metagenomes were inferred from the phylogenetic profiles using PICRUSt2. A differential abundance analysis was carried out, resulting in 94 Metacyc pathways being significantly over-abundant in at least one mussel organ or seawater metagenome (Supplementary Table S4). Samples were than clustered according to the abundance profile of the 94 over-abundant pathways (Figure 6).

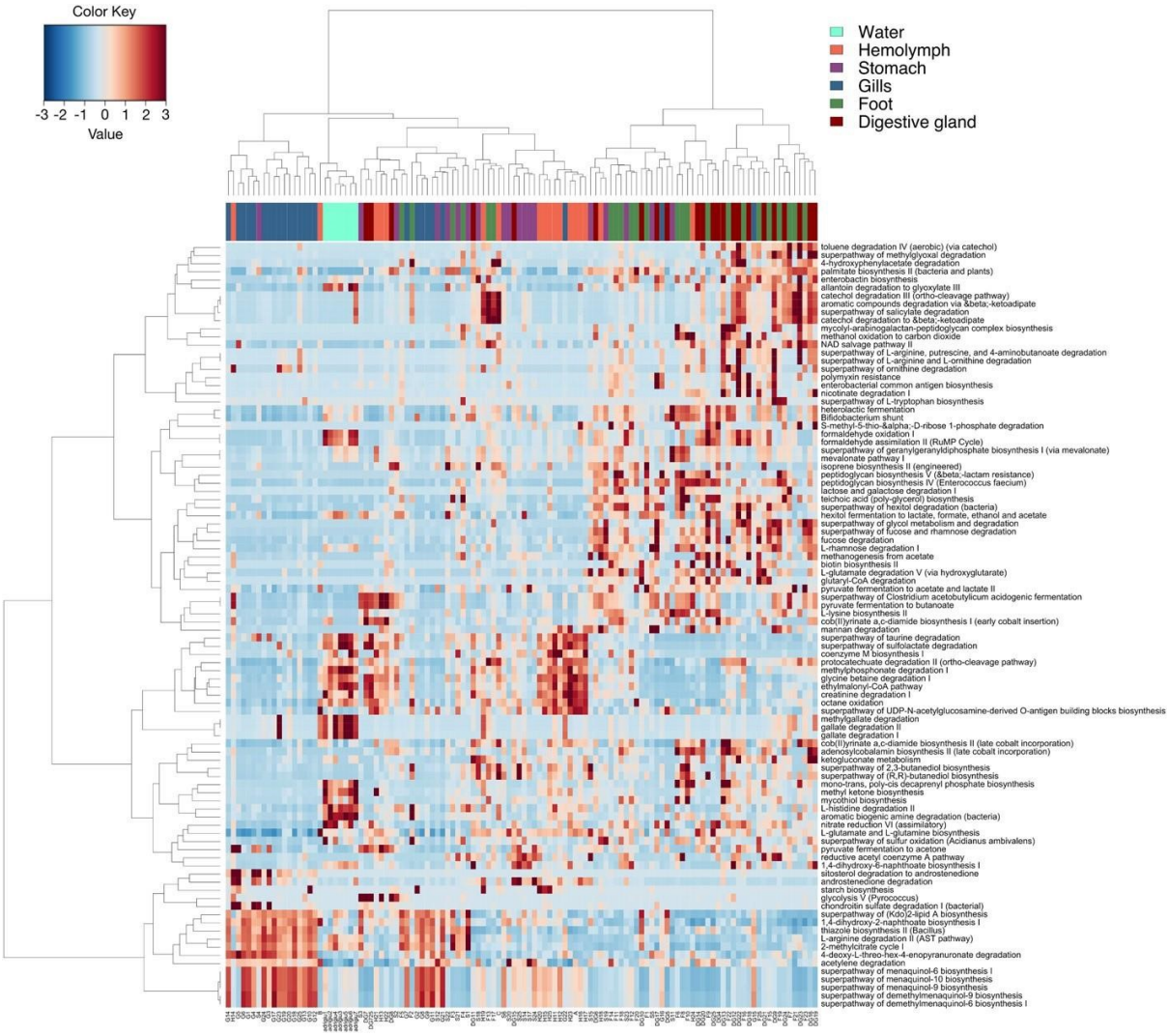

Fig. 6. Hierarchical clustering of the inferred metagenomes from the different tissue of M. galloprovincialis and seawater. The heatmap shows Ward-linkage clustering based on the Kendall correlation coefficients of the sample abundances profile of the 94 over-abundant pathways (Wald test logarithmic fold change of 2, P-value ≤.05). Samples are shown column-wise and colored by tissues. Metabolic pathways, named from the Metacyc database, are reported on the rows.

Even if a certain level of dispersions was maintained, samples showed an overall tendency towards the segregation between water, gills and hemolymph. A cluster including stomach, digestive glands and foot samples was also obtained. The clustering analysis indicated for seawater a distinguished functional profile, characterized by the enrichment in pathways involved in nitrogen cycle (i.e. L-histidine degradation II and nitrate reduction VI) and in the degradation of the aromatic compound gallate. Although sharing several functionalities with the seawater microbiome, hemolymph was characterized by the over-abundance of pathways involved in sulfur metabolism (i.e. superpathway

937 of sulfolactate degradation), in the regulation of osmolarity (i.e. superpathway of taurine degradation
938 and glycine betaine degradation I) and in the degradation of aromatic compounds (i.e protocatechuate
939 degradation II). Conversely, gills microbiome showed an enrichment in pathways involved in the
940 respiratory electron transport (i.e. quinol and quinone biosynthesis). Notably, the digestive gland and
941 the stomach microbiomes were both characterized by pathways involved in fermentation (i.e. pyruvate
942 fermentation to acetate and lactate II and heterolactic fermentation) and in the degradation of several
943 aromatic compounds (i.e. catechol, nicotinate, salicylate and toluene).

944

945 ## 4.2 Variability of metabolic, protective, antioxidant, and lysosomal gene
946 ## transcriptional profiles and microbiota composition of *Mytilus*
947 ## *galloprovincialis* farmed in the North Adriatic Sea (Italy)

948 Variations of gene transcriptional profiles between sexes or across season are reported in Fig. 7.
949 Results from PERMANOVA analyses demonstrated that the single factors “Season” and “Sex” had a
950 significant effect on the whole dataset ($P < 0.05$). Furthermore, PERMA- NOVA analysis showed a
951 significant interaction ($P < 0.05$) between the factors. The BEST/BioEnV analysis showed the
952 environ- mental variables that best correlated with the overall transcriptional dataset (Table S3).
953 Significantly different expression levels between males and females are observed for mt20, abcb and
954 hex ($P < 0.05$). All gene products showed complex transcriptional patterns across season in both males
955 and females (Fig. 7), with a tendency to increased (amil, lys, mt20, abcb, cat, sod, hex, ctsl, gusb) or
956 decreased (pk, idp) expression from winter to summer. DISTLM analyses performed on separate
957 female and male datasets by considering environmental parameters and gonadal matu- ration level
958 (assessed through VCL/VERL expression profiling) showed that in females’ temperature, salinity,
959 chlorophyll-a, and gonadal maturation explained most of the variation of the observed transcriptional
960 profiles (Fig. 8).

961

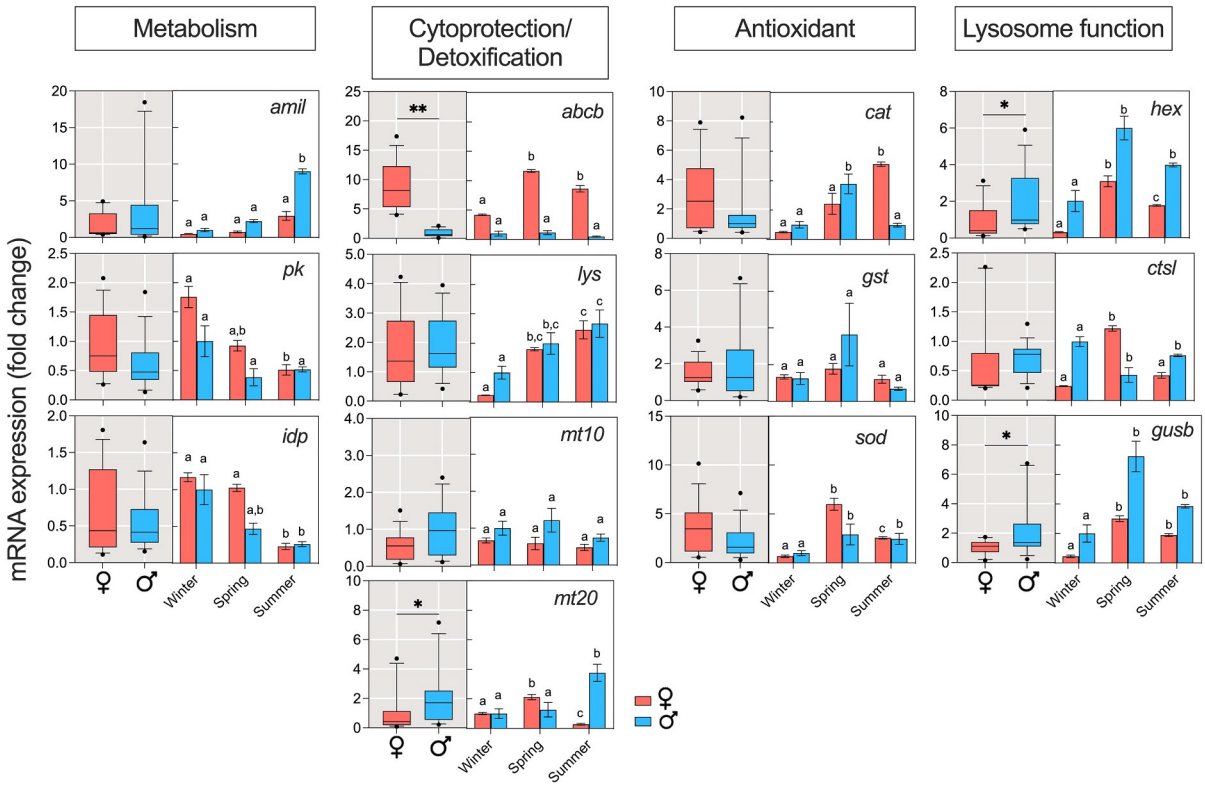

*Fig. 7. Transcriptional profiles of metabolic (amil, pk, idp), cytoprotective/detoxification (lys, mt10, mt20, abcb), antioxidant (cat, gst, sod), and lysosomal (hex, ctsl,gusb) mRNAs in females (♀) and males (♂) farmed Mediterranean mussels from the North Adriatic Sea. For each target transcript box plots (grey area) report overall expression levels in female's vs males (median, upper and lower quartiles; N =21), while bar plots (white area) show transcriptional profiles across the sampling seasons and for the different genders (mean ± sem; N = 7). In box plots: *P < 0.05 male vs female. In bar plots: different letters indicate statistical differences between samples within male or female sample groups (P<0.05). Full transcript names are reported in Table S2. (For interpretation of the references to color in this figure legend, the reader is referred to the web version of this article).*

Among these explaining variables, the BEST/ BioEnV analysis showed that temperature and gonad maturation significantly correlated with transcriptional profiles of females, while salinity, surface oxygen and transparency significantly correlated with transcriptional profiles of males (Fig. 8; Table S3).

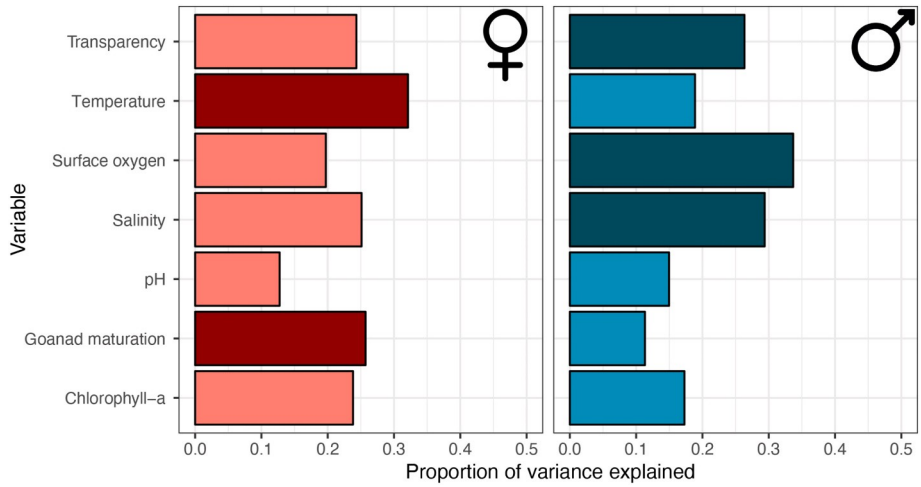

Fig. 8. DISTLM analysis to explore trends of biological parameters with environmental variables in females (♀) and males (♂) sample groups. Results from the test of marginality related to the distance-based redundancy (DISTLM) analysis showing contribution of each environmental variable to the total variance observed in female and male datasets of gene tran- scription profiles. VERL/VCL expression levels (which are proxies of gonadal cycles in females/males). DISTLM used the BEST selection procedure and adjusted R2 selection criteria. Dark red (females) and dark cyan (males) bars indicate the best correlated environmental variables according to the BEST/ BioEnV analysis reported in Table S2. (For interpretation of the references to color in this figure legend, the reader is referred to the web version of this article).

4.2.1 Digestive gland mussels microbiome variation across seasons

The compositional structure of the DG (digestive gland) microbiome from 41 mussels collected across the sampling period was obtained by NGS sequencing of the V3–V4 hypervariable region of the 16S rRNA gene. A total number of 623,000 high quality reads were obtained (mean per sample SD, 15195 ± 11,581) and clustered in 614 ASVs at 97% identity.

To explore overall differences in the DG microbiome composition between samples, an unweighted Unifrac-based PCoA of the correspondent compositional profiles was carried out. According to our findings, mussel samples clustered in 3 groups which correspond to the collection seasons (permutation test with pseudo-F ratios, P-value 0.02) (Fig. 9A).

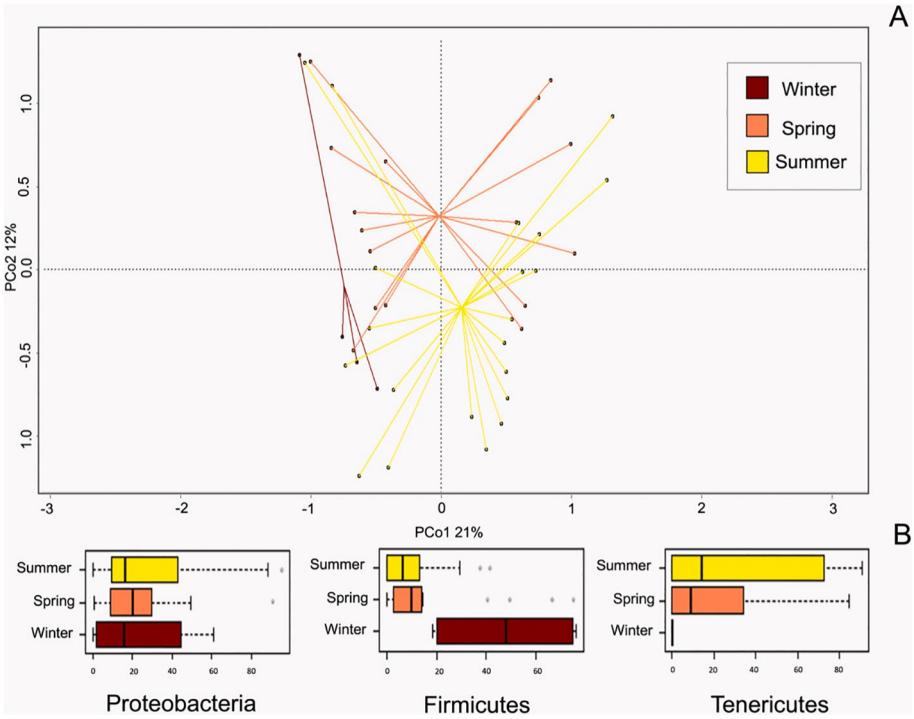

Fig.9. Variation of M. galloprovincialis DG micro- biome according to seasonality. (A) Principal Co- ordinates Analysis (PCoA) based on unweighted UniFrac distances between samples compositional profiles. Samples are significantly separated (permu- tation test with pseudo-F ratios, P-value ≤ 0.02). The percentage of variance in the dataset explained by each axis, first and second principal component (PCo1 and PCo2), is 21% and 12%, respectively. (B) Boxplot showing relative abundance of dominant phyla in winter, spring and summer. The color legend is depicted at the top-right of the plot in panel A. (For interpretation of the references to color in this figure legend, the reader is referred to the web version of this article).

From the compositional point of view, Firmicutes characterized winter samples, while Tenericutes were most abundant in the summer. Conversely, Proteobacteria appeared to be constant throughout the year (Fig. 10B). Besides seasonal variation, Fig. 10A shows a tendency of microbiome composition segregation according to mussel sex, though not statistically significant (permutation test with pseudo-F ratios, P-value 0.12). Particularly, as shown in Fig. 12B, males are most abundant in Cyanobacteria (6%±11.4% in male, 2.1%±7.6% in female), Planctomycetes (5.3% ± 7.7% in male 0.6% ± 1.5% in female) and Chlamydiae (2% ± 4.7% in male, 0.6% ± 1.5% in female), while females show an increase in Firmicutes (16.1%± 22.5% in male, 19.7% ± 26.9% in female),

Bacteroidetes (2.7% ± 3.4% in male, 8.9% ± 16.2% in female) and Actinobacteria (4.7%± 6.6% in male, 5.9%±12.7% in female).

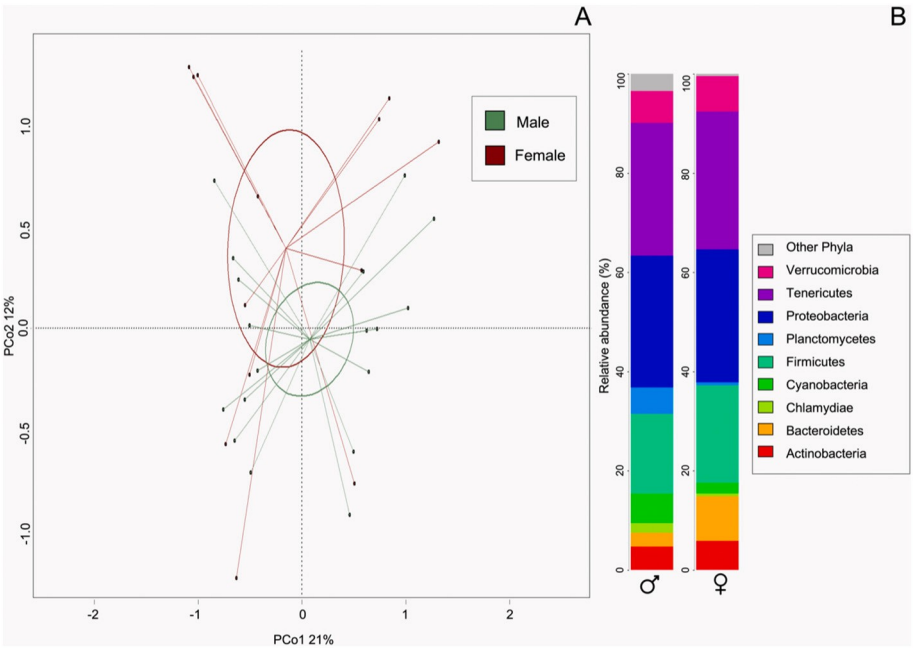

Fig. 10. Variation of M. galloprovincialis DG micro- biome composition according to sex. (A) Principal Coordinates Analysis (PCoA) based on unweighted UniFrac distances between samples compositional profiles. Samples, color coded according to sex, showed a tendency to separate (permutation test with pseudo-F ratios, P-value ≤ 0.2). The percentage of variance in the dataset explained by each axis, first and second principal component (PCo1 and PCo2), is 21% and 12%, respectively. (B) Barplot showing phylum-level mean relative abundance in male (♂) and female (♀) samples. Only phyla with relative abundance >1% in at least 10% of samples are represented.

To detect possible associations between mussel transcriptional profiles and the observed seasonal pattern DG microbiome segregation, we performed an indirect gradient analysis using Kendall correlation test. No significant correlation ($P > 0.05$) was observed between the samples PCoA coordinates and the correspondent expression profiles of the genes analyzed in Fig. 7. Nevertheless, the DSTLM analysis (Fig. 11; Table S4) shows that sample grouping based on transcriptional changes correlate with vectors describing trends of relative abundance of some microbial phyla disclosed in the DG microbiome. In particular, Chlamydiae and Planctomycetes appear correlated with

transcriptional changes between males and females, while Actinobacteria, Bacteroidetes, Firmicutes, and Tenericutes seem correlated with transcriptional changes between winter to spring/summer samples (Fig. 11, Table S4).

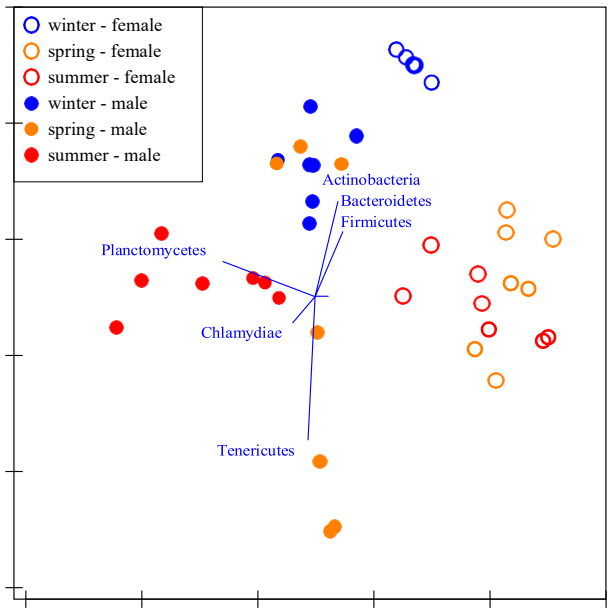

Fig. 11. DISTLM analysis on the gene transcription dataset with superimposed correlation vectors with relative DG microbiome composition. Results from the test of marginality related to the DISTLM analysis is reported in Table S4. DISTLM used the BEST selection procedure and adjusted R2 selection criteria.

4.3 Microbiome characterization of M. galloprovincialis along a spatial and temporal environmental stress gradient.

Mussels were collected from the three locations, namely: Goro, Cattolica, and Senigallia. The farms at Goro, Cattolica, and Senigallia represent from the north to the south coastal part of the western Adriatic Sea. Those farms are generally well-established in the area. Other than the location factor, to stimulate the seasonal effects, sampling was carried out in consecutive three seasons, including autumn, spring, and summer in each location. To explore overall differences in the microbiome composition between samples, a weighted Unifrac-based PCoA of the correspondent compositional profiles was carried out. According to our findings, mussel samples clustered in 3 groups which correspond to the collection sites, with site Goro more separated than Cattolica and Senigallia (permutation test with pseudo-F ratios, P-value 0.001) (Fig. 12A). From the compositional point of view, Planctomycetaceae and Helicaceae families were more abundant in Goro than Cattolica and Senigallia samples, while Lachnospiraceae, Lactobacillaceae and Ruminococcaceae families characterized Cattolica and Senigallia sites (Fig. 12B).

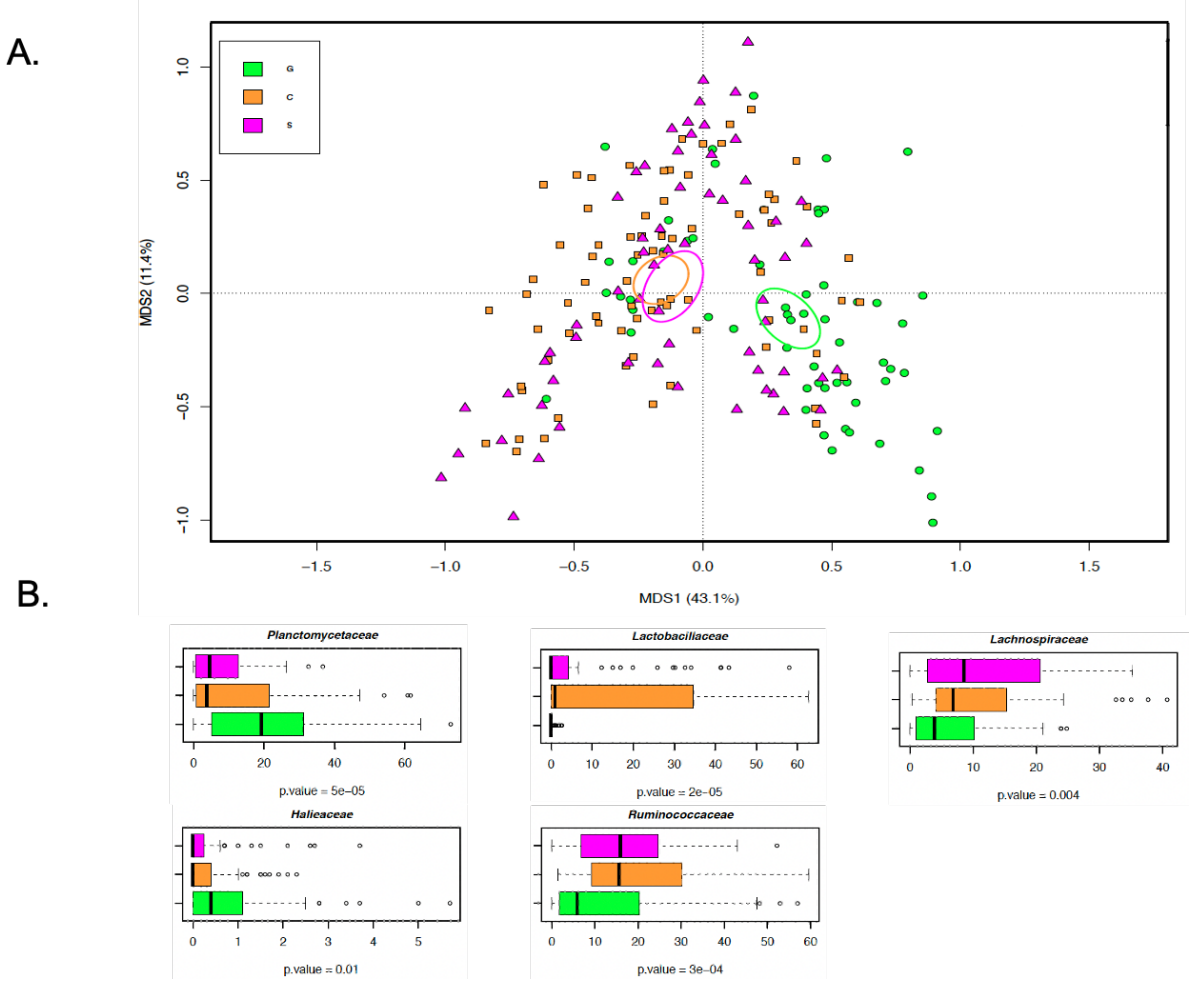

1087

1088 *Fig. 12. Variation of M. galloprovincialis DG microbiome according to sites. (A) Principal Co- ordinates Analysis (PCoA)*
1089 *based on weighted UniFrac distances between samples compositional profiles. Samples are significantly separated*
1090 *(permutation test with pseudo-F ratios, P-value ≤ 0.001). The percentage of variance in the dataset explained by each*
1091 *axis, first and second principal component (PCo1 and PCo2), is 43.1% and 11.4%, respectively. (B) Boxplot showing relative*
1092 *abundance of families in Goro, Cattolica and Senigallia sites. The color legend is depicted at the top-right of the plot in panel A, G=Goro,*
1093 *C=Cattolica, S=Senigallia.*

1094
1095 Besides sites variation, Fig. 13 shows microbiome composition segregation according to seasonal
1096 variation. Mussel samples clustered, in fact, in 3 groups which correspond to the collecting seasons -
1097 Spring, Summer and Autumn (permutation test with pseudo-F ratios, P-value 0.001) (Fig. 13A). From
1098 the compositional point of view, Lachnospiraceae and Planctomycetaceae characterized autumn
1099 season, while Enterobacteriaceae in mussels sampled during summer season. Ruminococcaceae,

Lactobacillaceae and Shringomonadaceae families, instead, remained constant during the whole year. (Fig. 13B).

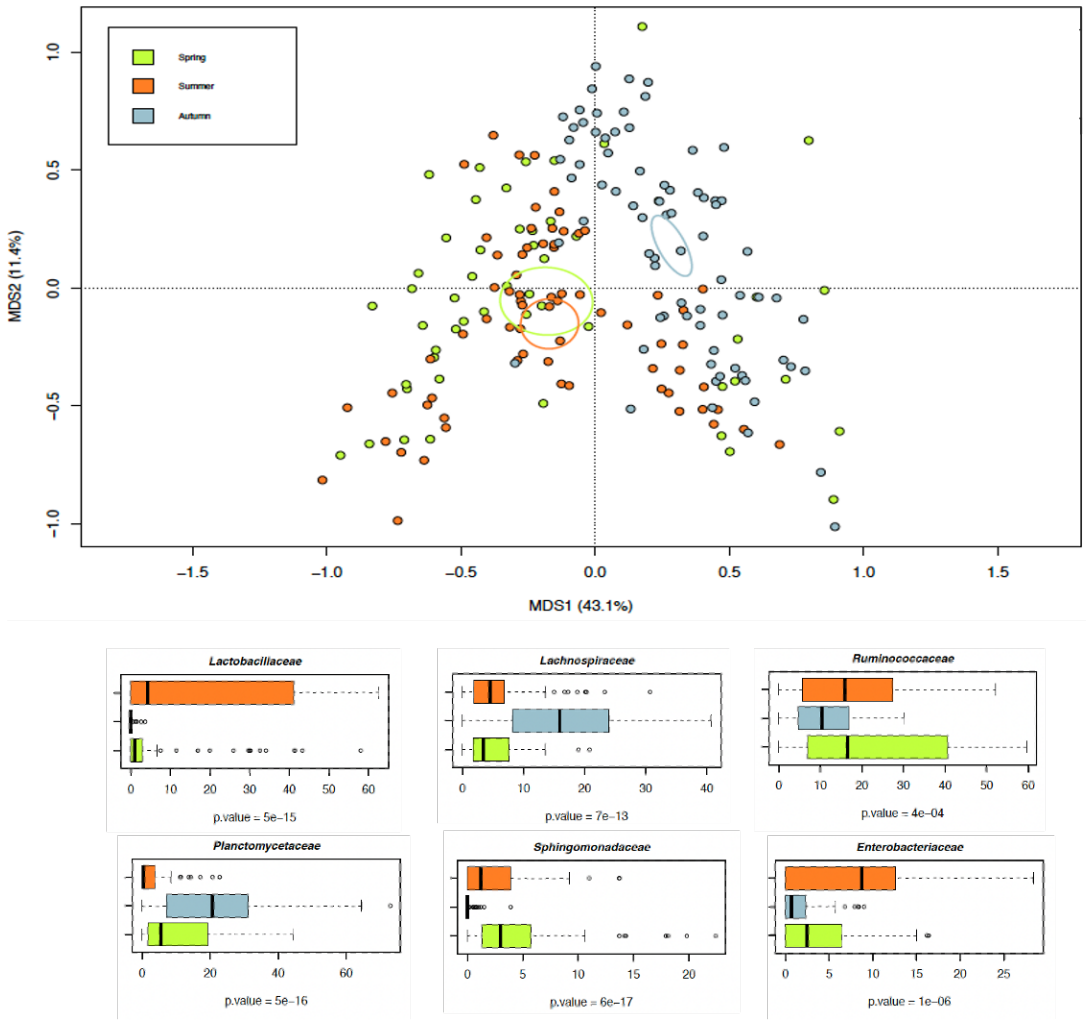

Fig. 13. Variation of M. galloprovincialis DG microbiome according to seasonality. (A) Principal Co- ordinates Analysis (PCoA) based on weighted UniFrac distances between samples compositional profiles. Samples are significantly separated (permutation test with pseudo-F ratios, P-value ≤ 0.001). The percentage of variance in the dataset explained by each axis, first and second principal component (PCo1 and PCo2), is 43.1% and 11.4%, respectively. (B) Boxplot showing relative abundance of families during spring, summer and autumn season. The color legend is depicted at the top-right of the plot in panel A.

With regard to alpha diversity, significant differences were observed in species richness among different seasons for each site. In particular, we found differences in summer and autumn for Cattolica

and Senigallia sites, and for spring and summer for Goro site (PD whole tree, p-value < 0.01) (Fig. 14).

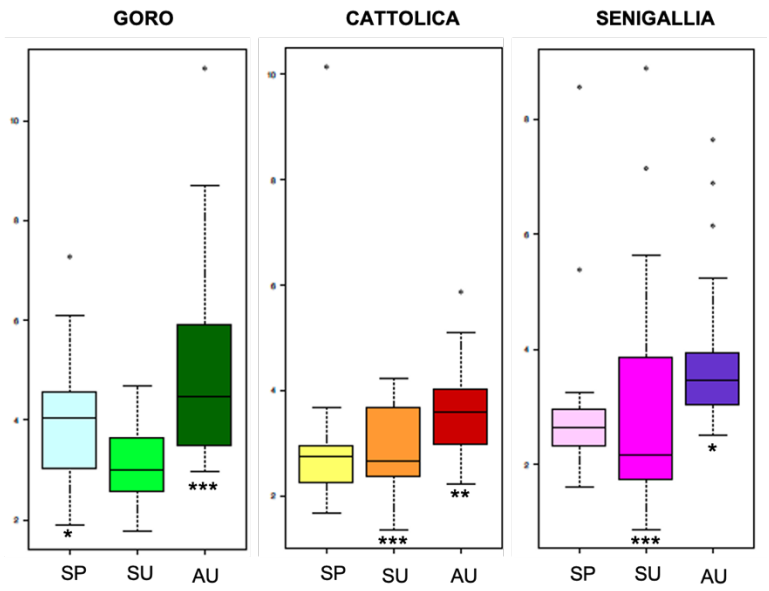

*Fig.14. Box and whiskers plots showing the alpha diversity values, measured as amplicon sequence variants (ASVs) *, P-value ≤.05, Wilcoxon test.*

4.4 *Development and validation of a liquid chromatography – mass spectrometry method for multiresidue analysis in mussel of the Adriatic Sea*

4.4.1 Analytical separation method development

To select the optimal separation conditions, single solutions and mixture of standards underwent a series of iterated analyses, using a conventional experimental design approach. Two different reversed phase separation columns were trialed for the separation of the target bioactive molecules. Between the two columns tested the XBridge C18 showed co-elution of various analytes and unacceptable separative performances, thus the Atlantis T3 column was selected because it provided good chromatographic separation and peak symmetry in a relatively short time. As a second step, different

mobile phase compositions were evaluated at different solvent gradients, according with common solvents and buffer used for fatty matrix analysis. We tested as organic phases pure methanol, pure acetonitrile and mix of them, while as water phases we tested pure water, water with different amount of formic acid and acetic acid from 0.01 to 0.1% (v/v), ammonium acetate buffer at three different pH levels (6-7-8). Mobile phases with low pH levels were not tested because of potential epimerization process of the investigated antibiotics compounds.

In terms of chromatographic resolution, peak shapes, and analysis times, the best compromise was obtained by using a mobile phase composed of 0.01% acetic acid in water and a solution of methanol and acetonitrile 65:35 (v/v) with 0,01% acetic acid.

Finally, we investigated the influence of flow rate, in the range 0.10–0.50 mL/min, and column temperature, in the range 20–60 ◦C. The flow rate was set at 0.15 mL/min, because higher flow rates lead to poorer peak shape and loss of resolution, and a temperature of 20 °C.

Figure 15 shows the chromatograms relative to the different analytes included in the method at medium concentration (10MQL).

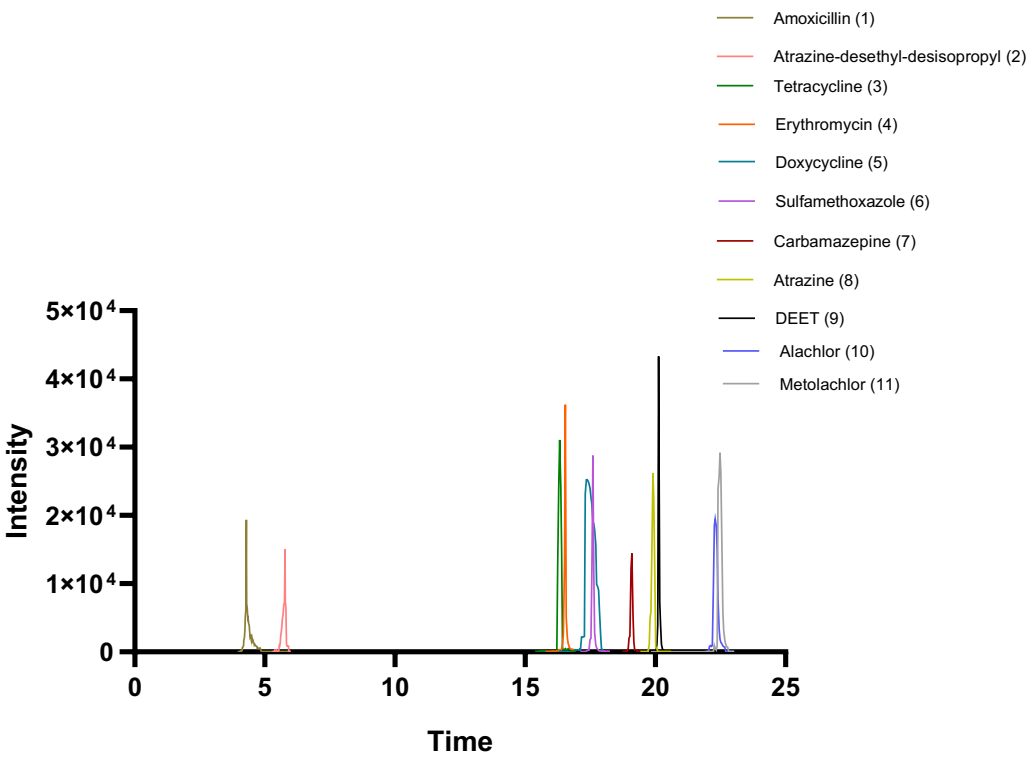

Fig. 15. Total ion current chromatogram reporting the separation of all 11 analytes investigated. [365.69] > [349.03] transition (1), [146.03] > [110.08] transition (2), [444.59] > [427.38] transition (3), [733.84] > [576.35] transition (4), [444.62] > [428.20] transition (5), [253.63] > [155.99] transition (6), [237.12] > [194.05] transition (7), [216.34] > [174.02] transition (8), [192.13] > [119.10] transition (9), [238.32] > [162.13] transition (10), [284.04] > [252.03] transition (11).

The analysis of residues in fatty matrices as mussels is still a challenging issue, because of the intrinsic complexity of the matrix and the relatively low concentration. It is very difficult to purify the analyte of interest avoiding the co-extraction of fatty material, which may hamper proper detection affecting recovery and matrix effect. Furthermore, some of the pesticides we desired to quantify are fat-soluble non-polar compounds (e.g. organochlorine) and tend to concentrate and accumulate in fat. Considered the different chemical physical properties of the compounds analyzed here, and based on several articles reporting similar approaches, firstly we essayed extractions with different pure solvents. Among non-polar solvents we tested hexane, cyclohexane, and dichloromethane. Cyclohexane and hexane showed similar recoveries for carbamazepine, sulfamethoxazole, and erythromycin but cyclohexane showed much lower recoveries for all the other compounds. Between hexane and DCM, we have comparable recoveries for pesticides but better recoveries of pharmaceuticals with DCM; nonetheless DCM shows an increase in matrix effect for most analytes thus we choose hexane. Considering the too low recoveries for some specific analytes (i.e. Sulfamethoxazole, Erythromycin) and taken into account their specific solubility in acetone[1,2], we decided to also test acetone in the extraction mixture. Pure acetone and a mixture of hexane and acetone 50:50 (v/v) were tested. The latter proved to be the best solution providing a significant increase in Sulfamethoxazole recovery and an increase in almost all other compounds. With this extraction we obtained acceptable recoveries and matrix effects only for some of the compound desired, especially pesticides. Recovery and matrix effect values obtained with single solvent and binary mixture extractions are reported in figures 16a

and 17a. Recovery was calculated as percentage of our final method described in section 2.5 (dash line) considered as 100%.

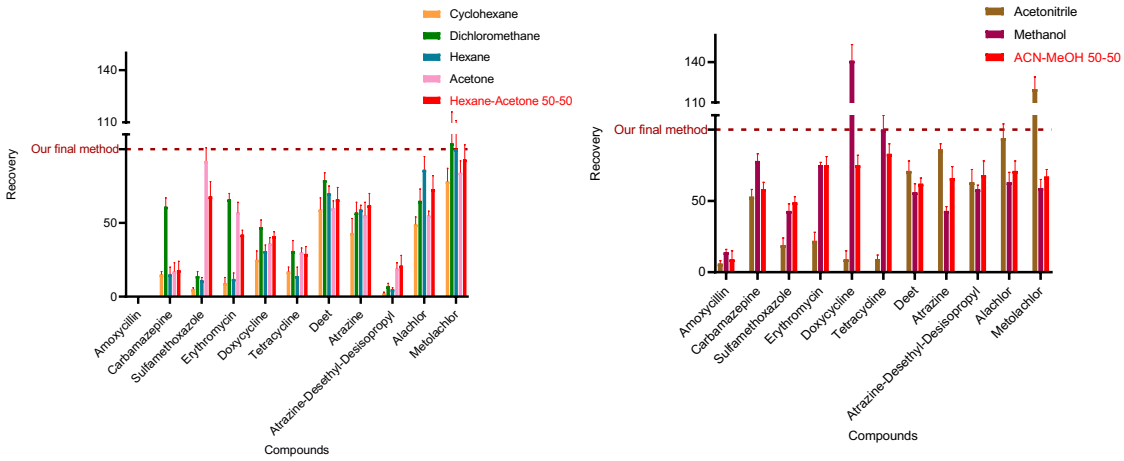

Fig. 16. Recovery and relative standard deviation (RSD) of different extraction solvents: a) non-polar solvents; b) polar solvents. Dash line represents the recovery obtained with our final method (section 2.5) considered as 100% recovery.

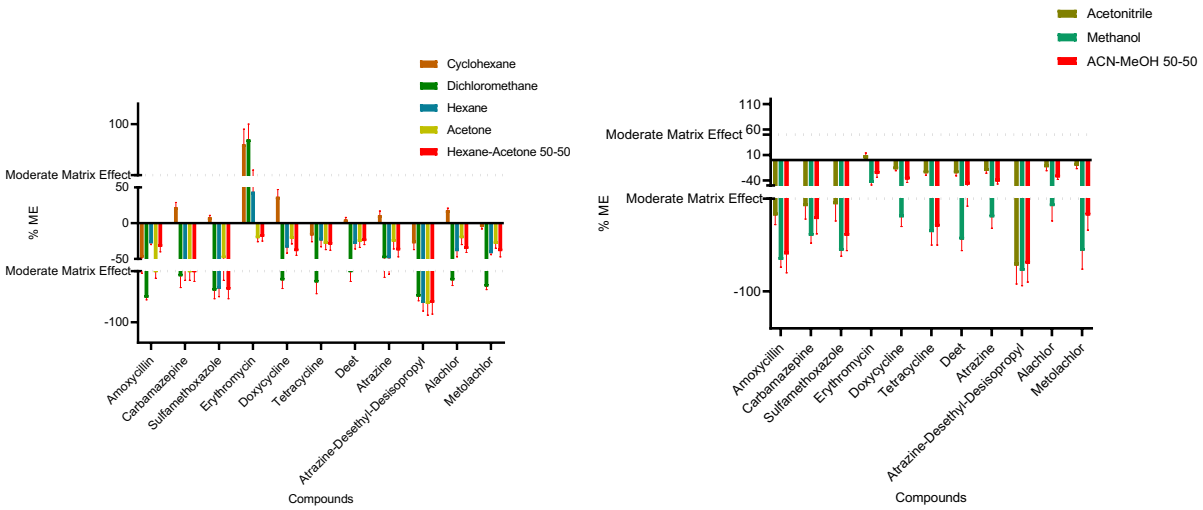

Figure 17. Matrix effect relative standard deviation (RSD) of different extraction solvents: a) non-polar solvents; b) polar solvents.

To improve our results on antibiotics we tested two more solvents with higher polarity: acetonitrile and methanol. Acetonitrile worked well for pesticides, with an acceptable matrix effect, methanol drastically increased recoveries for pharmaceuticals, especially doxycycline and tetracycline, but also

raised matrix effect for most compounds, by extracting more interferences. We found an acceptable compromise between recoveries and matrix effect using a mixture (50:50 v/v) of the two solvents (Figures 16b and 17b). Finally, two separate extractions with two different solvent mixtures (ACN:MeOH) (50:50 v/v) and Hexane: Acetone (50:50 v/v)) on the same freeze-dried sample were carried out.

Recovery and matrix effect of different solvent extraction and of complete extraction method are shown in Table S1-S9.

The use of CHAPS as zwitterionic surfactant was found to be of detrimental importance to analyze the entire oily residue, we proved to contain a non-negligible quantity of analytes. The formation of this residue was reported in literature and it was simply discharged. Since none of the pretreatments described above (SPE and QuEChERS) were satisfactory in avoiding oil formation in the dried sample, an aqueous solution with CHAPS 0.6 % (m/v) instead of FM was used to re-dissolved the oily residue. CHAPS is a mixture of zwitterionic detergents that are particularly well suited for mass spectrometry. The use of a substance with detergent properties is aimed at helping the re-dissolution of analytes trapped in the fatty oily residue. The use of chaps improved recoveries especially for pesticides (i.e. Deet, Atrazine, Atrazine-Desethyl-Desisopropyl, Metolachlor) while we obtained comparable or slightly worse results for pharmaceuticals such as Tetracycline, Doxycycline (figure 5b). Recovery was calculated as percentage of our final method recovery (section 2.5, dashed line) considered as 100%. However, the significant decrease in matrix effects that occurs in almost all cases makes the method using CHAPS the best, among those tested, for the extraction and purification of these compounds in mussel samples (Figure 18). Recoveries and matrix effect at medium concentration can be found in section 3.2.2 and in Table S16 (low to high concentration) in supplementary information.

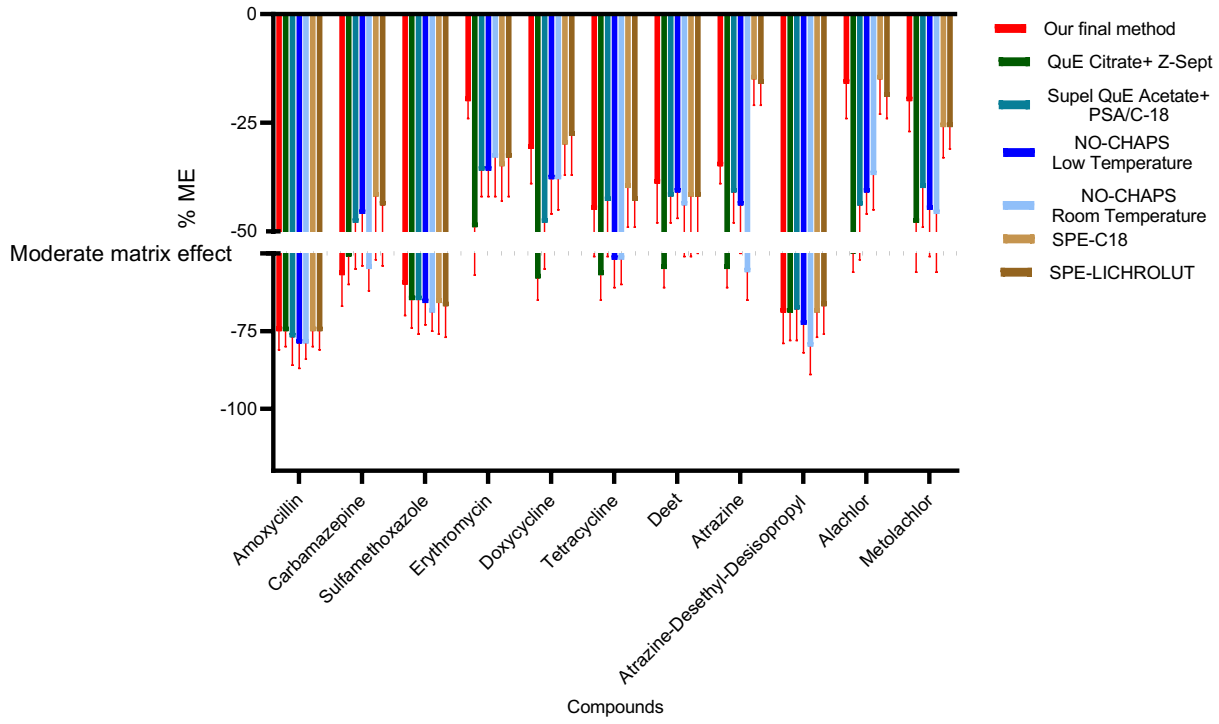

Fig. 18. Matrix effect and relative standard deviation (RSD) of different methods

Calibration curve parameters for all the considered compounds, in the specific concentration range for each analyte, were obtained by plotting the peak area of the spiked sample solution against their theoretical concentration through a linear least-square regression analysis.

Linearity was assessed through six-point calibration curves in matrix-matched curve due to the presence of medium or high matrix effect for most analytes. The calibration curves for analytes the ratio between analytes peak area and IS peak area was used. The resulting calibration curve equations were in the form of $Y = a (\pm \delta a)X + b(\pm \delta b)$. Calibration curve determination coefficients (r^2) were $\geq$ 0.995 for all molecules in the linearity ranges (0.002-500 ng/g). Table S17 reports the regression coefficients and the linearity range for each analyte.

Accuracy was defined as the deviation of the measured mean concentration from the spiked concentration, expressed in percentage, as described by Muñoz et al. whereas precision was expressed as the relative standard deviation of the measured concentration.

Accuracy values ranged between -7 and 12% at three different concentrations levels. RSD values for the intra-day analysis (repeatability) ranged between 1 and 6% while they were between 2 and 6% for the inter-day analysis (reproducibility). This demonstrates the repeatability and reproducibility of the method with an error below 20% and therefore its effectiveness for quantification purposes. Table S18 reports the results obtained.

MDLs and MQLs for all the analytes ranged from 9E-4 ng/g to 10 ng/g and from 3E-3 ng/g to 30 ng/g respectively. Table S19 resumes the results obtained.

Using the optimized method we obtained a significant decrease of MLOD for pharmaceuticals, amoxycillin, sulfamethoxazole and carbamazepine, respect previously reported methods developed by R. Fernandez-Torres et all[3] and by R. Cueva-Mestanza et al.

Higher MQLs than our method was described by A. J. Ramirez et al., for the extraction of pharmaceuticals from fish muscle using LC-MS/MS (i.e sulfamethoxazole, carbamazepine, erythromycin). For the same compound we obtained similar MDLs respect the method developed by D. Alvarez-Muñoz (sulfamethoxazole, erythromycin, carbamazepine) using UHPLC–MS/MS in the same matrix (Mytilus galloprovincialis, Mediterranean mussel) and by W. Li et al. (sulfamethoxazole, erythromycin) using HPLC-MS/MS but both using more time-spending method (PLE and SPE).

A.-Munoz et al. have published a second most recent paper without consider tetracycline and macrolides antibiotics. They have reported comparable results in terms of MDLs for sulfamethoxazole and carbamazepine. On the other hand, their procedure involved the use of ACN that we have investigated for all of our compounds with poor efficiency specifically for penicillin and tetracycline antibiotics in our method.

Interestingly, Martínez Bueno et al. have reported a method for the extraction of two anticonvulsants and their transformation products in marine mussels comparing PLE and Quechers extraction. In this paper they obtained better results with Quechers extraction reporting MLOD for carbamazepine higher than ours.

Compte et al. reported a method for the determination of antibiotics and their metabolite in seafoods. They obtained better result for tetracycline and comparable for sulfamethoxazole.

For pesticides and herbicides, the method developed by A.-Muñoz showed similar MDL compared to ours for atrazine, while sensitivity for metolachlor was improved in our method.

Geng-Ruei Chang et al. reported LOQs higher than our MQLs for herbicide residues in hard clam and oyster using Quechers method in the case of metolachlor and atrazine, and comparable in the case of alachlor.

Matrix effects may severely influence sensitivity, linearity, accuracy and precision of quantitative LC MS/MS determinations, particularly with complex matrices. All compounds included in this method were subjected to ion suppression. Thus, 3 compounds (Erythromycin, Alachlor and Metolachlor) showed no matrix effect (≤20%, because this variation is close to the repeatability values), 4 analytes (Doxycycline, Tetracycline, Deet and Atrazine) presented a medium effect (50–20%) whereas 4 showed a high effect (> 50%) (Amoxycillin, Carbamazepine, Sulfamethoxazole and Atrazine-Desethyl-Desisopropyl). Coextracted matrix components were found to have maximum effect on the analytical response of early-eluting analytes (i.e amoxycillin and atrazine desethyl- desysopropyl).

Our results are comparable with the method used by Alvarez-Muñoz focused on pharmaceuticals for sulfamethoxazole and carbamazepine whereas for erythromycin we have significantly lowered the matrix effect.

Respect the method focused on pesticides, endocrine disruptors and pharmaceuticals we obtained worst results for atrazine, metolachlor, carbamazepine and sulfamethoxazole. As already mentioned, in our method, the presence especially of penicillin and tetracycline antibiotics did not allow the exclusive use of ACN as extraction solvent and the presence of methanol significantly increases matrix effect.

Considering our results, accurate quantitation of analytes in mussels extracts is not feasible using calibration standards prepared in mobile phase. It was necessary to use matrix-matched calibration curves, with addition of isotopically labelled internal standards when available.

Recoveries varied between 32% and 95% with relative standard deviation (RDS) below 10%, which indicates high reproducibility of the extraction. Only four analytes were extracted with less than 40% of efficiency. In these cases, low RDS were observed too.

We obtained higher recovery respect to the method focused on pharmaceuticals developed by A. Muñoz at al. for sulfamethoxazole, carbamazepine and erythromycin. We have obtained lower recovery respect to the second most recently paper of the same research group[Errore. Il segnalibro non è definito.] for atrazine, metolachlor, carbamazepine and sulfamethoxazole even if they didn't consider tetracycline antibiotics.

Comparable results were obtained for tetracycline and sulfamethoxazole with the method developed by Compte et al. They tried to use d-SPE with Quechers during the extraction procedure, but no significant results were obtained with the use of d-SPE, supporting our choice to exclude the use of these chemicals.

M. Bueno et al[Errore. Il segnalibro non è definito.] have reported lower recovery for carbamazepine both for different Quenchers method extraction and for PLE extraction from mussel samples.

Slightly better recoveries were obtained by Fernandez et al. for amoxycillin and sulfamethoxazole even if they didn't consider pesticides.

Considering the published papers so far, a comprehensive analytical method for the main chemicals potentially present in mussels is an analytical challenge. Tetracycline and penicillin antibiotics, pesticides and several other pharmaceuticals with different polarities does not make possible the exclusive use of a single solvent extraction step. On the other hand, it is necessary to find the best compromise between recovery method performance and matrix effect, obtaining the highest sensitivity as described in our method. Table 2 resumes recovery, matrix effect and their respective relative standard deviation (RSD) (n=3) for each analyte at medium concentration (10 MQL).

COMPOUND	RECOVERY	MATRIX EFFECT
Amoxycillin	35% ± 6%	-75% ± 6%
Carbamazepine	72% ± 5%	-57% ± 10%
Sulfamethoxazole	37% ± 8%	-60% ± 10%
Erythromycin	67% ± 3%	-20% ± 4%
Doxycycline	32% ± 5%	-31% ± 8%
Tetracycline	35% ± 7%	-45% ± 6%
Deet	86% ± 9%	-40% ± 9%
Atrazine	58% ± 10%	-35% ± 4%
Atrazine-Desethyl-Desisopropyl	95% ± 10%	-69% ± 10%
Alachlor	51% ± 9%	-16% ± 8%
Metolachlor	46% ± 5%	-20% ± 7%

4.4.2 Analysis in real samples from Adriatic Sea

The method developed was applied for the determination of pharmaceuticals and pesticides in Mediterranean mussel collected form Adriatic Sea. The results obtained after the analysis of these samples are presented in Table S20. Seven out of the 11 contaminants included in the method were determined at concentrations above their respective MDLs.

Two pesticides, atrazine desethyl-desisopropil and alachor, and two pharmaceuticals, amoxicillin and doxycycline hyclate, were under the detection method limit. Among pesticides and herbicides, metholachlor and DEET (N,N-Diethyl-m-toluamide) were founded at concentrations near to the MQL, while the concentration of atrazine was 7 time higher than its MQL. Among pharmaceuticals,

carbamazepine was founded at a concentration near to the MQL, while the concentrations of Sulfomethoxazole, Tetracycline and Erythromycin were much higher than their MQLs.

The results obtained agree with other studies in fish. Bueno et al. reported a carbamazepine concentration ranging from 0.5 -3.5 ng/g (dw) depending on the mussel sampling site.

Even though some antibiotics residues were found in mussels samples, their levels were far away from the Maximum Residue Limits established by the authorities being between 100 and 600 ng/g (ww) for the compounds detected in the analyzed sample.

5. Discussion

In this thesis we investigate the impact of environmental stressors and pollution and how these can alter mussels' physiology and microbiota in terms of adaptive or maladaptive response. To better dissect the possible contribution of the mussel microbiota to the host physiology, we specifically explored its variation at the tissue scale. Interesting, the microbiota of each tissue was characterized by a specific pattern of dominant families, suggesting a peculiar ecological propensity. The digestive gland was then selected as the target tissue for further analysis, because it plays a major role in food digestion, detoxification (Izagirre and Marigómez, 2009) and recognized as the best organ to perceive physiological changes in the natural environment. We then investigate the digestive gland microbiome composition across season in order to find seasonal pattern, together with the physiological response of the animal. We succeeded in find patterns in mussel responsiveness to environmental stressors by showing differential regulation of gene transcripts that may be affected by natural environmental variables and by endogenous factors, like the microbiome composition. Since this study provided baseline information on the seasonal progression of M. galloprovincialis physiological traits in the study area, we performed a broader study integrating regional trends to the seasonal stress gradient. We analyzed, indeed, samples from 3 large farms located across the north western Adriatic Sea in 3 different seasons in order to find patterns of adaptative/maladaptive response to anthropogenic and environmental stress, along a spatial and temporal stress gradient.

Lastly, we validated a method for pollution assessment of aquatic pollution levels together with the bioaccumulation of xenobiotics in organisms inhabiting the specific environment. An optimized and validated method for the determination of pharmaceutical and pesticides could be an important tool to shed some light on the effect of a pollution environment on marine holobionts.

5.1 Tissue-specific composition of M. galloprovincialis microbial ecosystems

We characterized the Mediterranean mussel microbiota, also exploring its structural variation at the tissue scale and the connection with the microbial ecosystem of the surrounding seawater. According to our findings, the mussel microbiota was well differentiated from that of seawater. Indeed, at the phylum level the mussel microbiota was dominated by Proteobacteria, Firmicutes and Bacteroidetes, while that of seawater showed only Proteobacteria and Bacteroidetes as dominant phyla. However, it is at lower phylogenetic levels that the differences between the animal and seawater taxa, the mussel microbiota included well-known animal microbial commensals, such as Ruminococcaceae, Lachnospiraceae and Bacillaceae, and possibly opportunistic ecosystems were more evident. While showing a similar pattern of dominant families, which mainly encompasses microorganisms of marine origin, such the plot in panel A. as Flavobacteriaceae, Alteromonadales and Rhodobacteriaceae, the subdominant fraction of the mussel and seawater ecosystems was remarkably different. Unlike seawater, which was characterized by a vast diversity of marine microorganism such as members of the family Spirochaetaceae. The inferred metagenomics also highlights an overall distinct functional profile between the seawater and the mussel microbiomes. While seawater was characterized by functions involved in sulfur and nitrogen cycling, the mussel ecosystems are enriched in genes involved in carbohydrates oxidation or fermentation, with specific variations depending on the tissue. Taken together, these data may indicate the propensity of mussels to select and retain microorganisms with animal tropism, such as symbiotic microbial partners. A similar behavior was recently reported for the sea cucumber, Holothuria glaberrima (Pagán-Jiménez et al., 2019), in which the presence of Ruminococcaceae and Lachnospiraceae in the gut was suggested to influence the gastrointestinal metabolism of the host, as well demonstrated in terrestrial animals. To better dissect the possible contribution of the mussel microbiota to the host physiology, we explored its variation at the tissue scale. Interestingly, although showing an overall comparable biodiversity, the microbiota of each tissue was characterized by a specific pattern of dominant families, suggesting a peculiar ecological propensity. For instance, being dominated by Ruminococcaceae and Lachnospiraceae, the digestive

gland microbiota was configured as an anaerobic ecosystem enriched in commensal microorganisms capable of fermenting complex polysaccharides to short-chain fatty acids (SCFAs), well matching the general asset of animal gut microbiota (Muegge et al., 2011). Indeed, the digestive gland is the main site for the digestive, metabolic, and detoxification functions of mussels. These physiological activities may contribute to the establishment of suitable conditions to promote anaerobic bacteria capable of producing SCFAs through the fermentation of dietary fibers (Saltzman et al., 2017), such as cellulose and hemicellulose (La Reau et al., 2016), which are commonly found in bivalve food, as dinoflagellate algae (Arapov et al., 2010; Rouillon et al., 2005). Further supporting these considerations, a recent study showed that an α-D-glucan (MP-A) polysaccharide isolated from the mussel Mytilus coruscus affects the gut microbiota composition in Sprague Dawley rats fed with a high-fat diet, promoting SCFA production and alleviating the deleterious effects of the diet (Wu et al., 2019). Similarly, the stomach and foot microbiota were dominated by anaerobic microorganisms with animal tropism, especially Spirochaetaceae and Mycoplasmataceae. These microorganisms are generally considered as opportunistic rather than commensal, at least in mammalian hosts (Hampson and Ahmed, 2009; Waites and Talkington, 2004). However, according to van de Water et al. (2016), Spirochaetes members may act as symbionts in mollusks. Gills and hemolymph microbiota showed a completely different ecological structure compared to the other tissues, being dominated by aerobes of marine origin, such as Alteromonadales and Hahellaceae (gill), and Flavobacteriaceae (hemolymph). These findings well agree with the common role of the tissues as a primary biological barrier between the animal and the external environment, being in direct contact with the surrounding seawater. Therefore, their microbial composition most likely reflects the conditions imposed by the external environment, as observed in previous studies (Brito et al., 2018). On the other hand, gills and hemolymph may also exert an active role in the selection of microbial symbionts composing the microbiota of internal tissues (i.e. digestive gland and stomach), by means of filtering activity (gill), or immune recognition and phagocytosis operated by hemocytes and translocation to other organs/animal districts (hemolymph) (Ikuta et al., 2019; Burgos-Aceves and Faggio, 2017). Inferred

metagenomes at the tissue scale confirmed the hypothesized metabolic propensities of the corresponding microbiota. Indeed, according to our findings, the gills ecosystem was characterized by functions involved in oxidative respiration, while the stomach and, particularly, the digestive gland, were over-abundant in functions related to the fermentation of polysaccharides and the degradation of aromatic compounds. These specificities of mussel microbiota at the tissue scale were robust to inter-individual variability. This suggests that the main determinant of the mussel microbiota variation is the niche-specificity rather than the individual differences. The same behavior was observed for mammals, where the structure of symbiont microbial ecosystems segregates according to the body district (Integrative HMP-iHMP- Research Network Consortium, 2014). Finally, we explored the impact of mussel farming on the microbiota of the surrounding water. Compared to the control seawater (i.e. water collected 3 miles away from the mussel farm), seawater collected close to the farm was enriched in Pseudoalteromonadaceae, Verrucomicrobiaceae and Vibrionaceae, while being depleted in Halieaceae. This data emphasizes the potential of mussel farming to directly affect microbial ecology of seawater by releasing microorganisms that characterize the gill (i.e. Vibrionaceae and Pseudoalteromonadaceae) and hemolymph (i.e. Verrucomicrobiaceae), while retaining Halieaceae in the mussel microbiota. These findings further stress the close contact between gill/hemolymph and the external environment, as well as the function displayed by both tissues as the main route for tissue uptake of waterborne compounds and particulate material (including microorganisms).

5.2 Mussels microbiome variation across seasons

Data reported in this study show the influence of both seasonality and gender bias on transcriptional profiles and microbiota composition of M. galloprovincialis from the Northwestern Adriatic Sea. Season related fluctuations of molecular and biochemical biomarkers in mussels can be expected, as reported by a relevant amount of scientific evidence on this topic (Balbi et al., 2017; Benito et al., 2019; Leinio¨ and Lehtonen, 2005), and suggested to mainly depend on seawater temperature and

salinity variations, which are considered among the main drivers of physiological regulation for mussels and other intertidal marine invertebrates (Lockwood et al., 2015). Indeed, the BEST/BioEnV analysis performed on the whole transcriptional dataset showed that temperature and salinity are the best correlated environmental variables with the observed biological outcomes, together with pH and chlorophyll-a variations. This finding suggests a more complex interaction with the environmental conditions provided by the sampling area in the Northwestern Adriatic Sea, which are characterized by a large river runoff from the Italian border and by highly variable meteorological conditions (Alvisi and Cozzi, 2016). DG microbiome composition also followed a seasonal pattern, with Firmicutes and Tenericutes characterizing winter and summer samples, respectively. The overall seasonal pattern of gene transcription shows a general increasing expression from winter to summer, except for transcripts encoding metabolic enzymes, that show both increasing (amyl) and decreasing (pk, idp) expressions across season. Amylase is a key enzyme in carbohydrate metabolism; pyruvate kinases and isocitrate de- hydrogenases are engaged in channeling glycolytic substrates toward aerobic metabolic pathways (Canesi et al., 1999; Liu et al., 2017). On the whole, the relative expression patterns of these gene products suggest a lower aerobic capacity of the mussels in summer, or, alternatively, an enhanced occurrence of substrates for anaerobic metabolism. Interestingly, the DISTLM analysis show the (significant) correlation between gender and season sample groupings based on the overall mussel gene transcriptional profiles and vectors describing trends of relative abundance of some microbial phyla disclosed in the DG microbiome that may be related to the host metabolic layout. At low (winter) temperatures, the mussel DG microbiome enriches fiber fermenting anaerobes belonging to Firmicutes, which generally populate digestive tract of terrestrial and marine animals (Musella et al., 2020; Rausch et al., 2019), and can take advantage of the oxidative propensity of the host overall metabolic layout. Conversely, with a raised temperature (summer), the DG microbiome becomes characterized by Tenericutes, a microbiome taxon that includes non-peptogenic parasites living in close association (and dependence) with host cells (Lee et al., 2018), which do not suffer the host shift toward an anaerobic metabolic layout. Further investigations integrating transcriptomic, proteomic,

and metabolomic profiles could probably disclose the crosstalk interactions occurring between host physiology and microbiome composition (Balbi et al., 2021; Ferna´ndez Robledo et al., 2019; Utermann et al., 2018). At any rate, measured values of condition factor, an indicator of the physiological state and growth of mussels (Andral et al., 2004), and LMS, a well-consolidated general stress biomarker, are within the range representing stressed but compensating organisms, likely indicating that the overall host transcriptional and microbiome composition is suitable to support such a physiological condition of the animals. Results of this study further demonstrate sex related expression of some gene transcripts and of DG microbiome. Generally speaking, females and males differ for their expression profiles across seasons. Both DISTLM and BEST/BioEnV analyses indicated that transcriptional profiles of males seem related only to environmental variables, mainly to salinity, surface oxygen, and transparency, whereas in female's seawater surface temperature and gonad maturation are the best correlated factors and explained most of the variance of the transcriptional dataset. Furthermore, while males show almost constant LMS levels values across season, females show a significant reduction of NRRT values (i.e. decreased LMS) from winter to summer, which indicate an increase of stress levels. Besides environmental conditions, LMS is known be affected by endogenous factors as reproduction and dietary budget (Moore, 2004; Múgica et al., 2015). Taken together, results of this study agree with previous findings assessing that season-related differences in biomarker responses of mussels between females and males may reflect the progression of the reproductive cycle (Blanco-Rayo´n et al., 2020). From the DG microbiome side, males resulted enriched in environmental aerobes from the water column, such as Cyanobacteria and Planctomycetes, supporting a closer connection with the surrounding environment. Being characterized by a higher abundance of Firmicutes, Bacteroidetes and Actinobacterial, females showed DG microbiome enriched in host-associated taxa with a clear functional propensity to- ward carbohydrate fermentation. Some gene products displayed significantly different overall expression levels between sexes. The most remarkable difference is observed for the abcb transcript encoding the mussel P-glycoprotein (P- gp), whose expression is significantly higher in females than in males. P-gp is a member of the

ATP-binding cassette (ABC) membrane trans- porters. ABC transporters are ATP-dependent active transporters pumping out from cells both endogenous chemicals and xenobiotics, thus preventing their accumulation and toxic effects (Bard, 2000). These proteins are generally considered to build up a first-tier defense against chemical toxicities. Besides this, their role in mammalian oocyte maturation has been postulated (Bloise et al., 2016). It is worth noting that well detectable levels of abcb mRNA were observed in unfertilized (after spawning) and fertilized mussel oocytes (Franzellitti et al., 2017), suggesting a similar function in mussels. The maternal origin is not impairing the induction of cytoprotective mechanisms, altering animal capacities to cope with environmental stressors (Bedulina et al., 2020; Meistertzheim et al., 2009). Together with LMS results, which indicate the season related onset of stress conditions for females but not for males, this observed differential expression and season regulation of cytoprotective mechanisms corroborates previous investigations showing sex related differences in pollutant bioaccumulation and in biological responses to pollutants (Blanco-Rayo´n et al., 2020; Schmidt et al., 2013a).

5.3 Microbiome characterization of M. galloprovincialis along a spatial and temporal environmental stress gradient.

We managed to characterize the mussel microbiota along a longitudinal spatial and temporal gradient from the Northwestern Adriatic Sea. Digestive gland microbiome composition also followed a seasonal pattern, as previously described in Wathsala et al., 2021. In particular, Enterobacteriaceae family were significantly more abundant in summer than in autumn and spring, consistent with the literature (Salgueiro et al., 2021); probably in relation to the Adriatic Sea increased coastal pollution possibly linked to the tourism season (Kvesić et al., 2022), together with the highly variable meteorological conditions (Alvisi and Cozzi, 2016). For what concerns regional trends, according to our findings, Mediterranean mussels' microbiome from Goro well differentiate from the other two sampling site of Cattolica and Senigallia, being characterized by a specific relative abundance families' pattern. Planctomycetaceae and Helicaceae families were, indeed, more abundant in Goro

than Cattolica and Senigallia samples,while Lachnospiraceae, Lactobacillaceae and Ruminococcaceae families characterized Cattolica and Senigallia sites. Interesting, families found to be enriched in the Mediterranean mussels' digestive gland sampled in Goro, like Planctomycetaceae, are commonly found in freshwater mussels (Lawson at al., 2022; Higgins et al., 2022), suggesting a direct influence of the Po river proximity. Indeed, is well known that Po river runoff greatly impact the Northwestern Adriatic Sea. Conversely, Firmicutes represent large components of microbial communities in soils (Roesch et al., 2007; Youssef and Elshahed, 2009), the members of which have also been reported as feces-associated bacteria in coastal waters (Basili et al., 2020). Their enrichment in the digestive gland of mussels from Cattolica and Senigallia, may indicate a higher anthropic pollution (i.e. a higher presence of tourism). Further investigations integrating transcriptomic, proteomic, and metabolomic profiles could probably disclose the crosstalk interactions occurring between host physiology and microbiome composition (Balbi et al., 2021; Ferna´ndez Robledo et al., 2019; Utermann et al., 2018).

6. Conclusions

Our study provides the first integrative description of the mussel microbiota variation in the north-western Adriatic Sea. According to our findings, mussels possess a characteristic microbiota, well differentiated from the seawater microecosystem, with robust compositional variations at the organ level. We then investigated seasons related mussel responsiveness to environmental stressors highlighting the differential regulation of gene transcripts that may underpin such physiological responses may be affected by natural environmental variables and by endogenous factors like microbiome composition. Indeed, putative physiological variations occur with compositional changes in microbiome of digestive gland, the organ in which digestive and detoxification processes allow animal to tolerate and accumulate xenobiotics of natural and anthropogenic origin (Faggio et al., 2018). We then manage to assess microbiome region trends across the north Adriatic, with each sampling site well differentiated from the others. These results may provide baseline information for future studies approaches of seasonal and region trends of microbiota profiles and physiological responses in terms of metabolism. Widespread contamination by different classes of chemicals have been largely documented in the Northwestern Adriatic Sea, including metals, polyaromatic hydrocarbon (PAHs), pesticides, therefore we developed a method that can be applied for the determination of pharmaceuticals and pesticides in Mediterranean mussel collected form Adriatic Sea. This analytical method is a powerful tool for the analytical detection of the major pollutants in aquatic fauna, specifically for high fat complex matrixes like mussels. We aim to use this method in future studies to explore the connection between the health and productivity of farmed mussels and the environmental quality.

Supplement 1

Tissue-scale microbiota of the Mediterranean mussel (*Mytilus galloprovincialis*) and its relationship with the environment

Margherita Musella, Rasika Wathsala, Teresa Tavella, Simone Rampelli, Monica Barone, Giorgia Palladino, Elena Biagi, Patrizia Brigidi, Silvia Turroni, Silvia Franzellitti *, Marco Candela*

*Corresponding Authors: silvia.franzellitti@unibo.it; marco.candela@unibo.it **Supplementary Figure S1.**

The sampling site of seawater located in North Adriatic Sea coast. Blue cross, seawater collected close to the mussel farm. Red circle, seawater collected 3 miles away from the mussel farm. Samples were collected at a depth of 3 m.

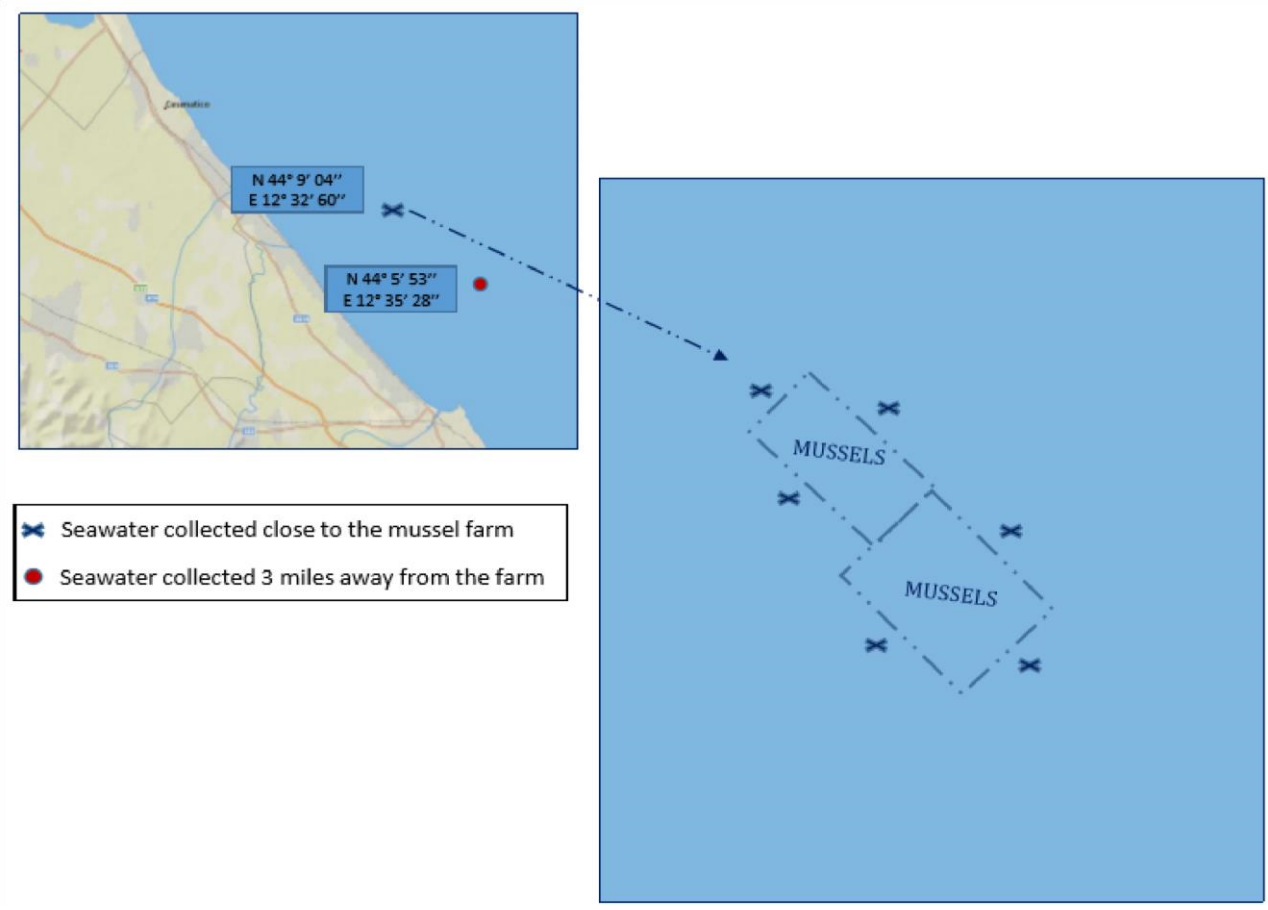

Supplementary Figure S2.

Family-level relative abundance profiles of bacterial communities in the seawater surrounding the mussel farm (FSW) and in seawater taken 3 miles from the farm (CSW). (A). Family-level relative abundance profiles of FSW and CSW. Only families with a relative abundance of

≥1.5% in at least 10% of samples (B). Scatter plots showing the relative abundance values of the main families differently represented between FSW and CSW. The black bar in the graphs indicates the median.

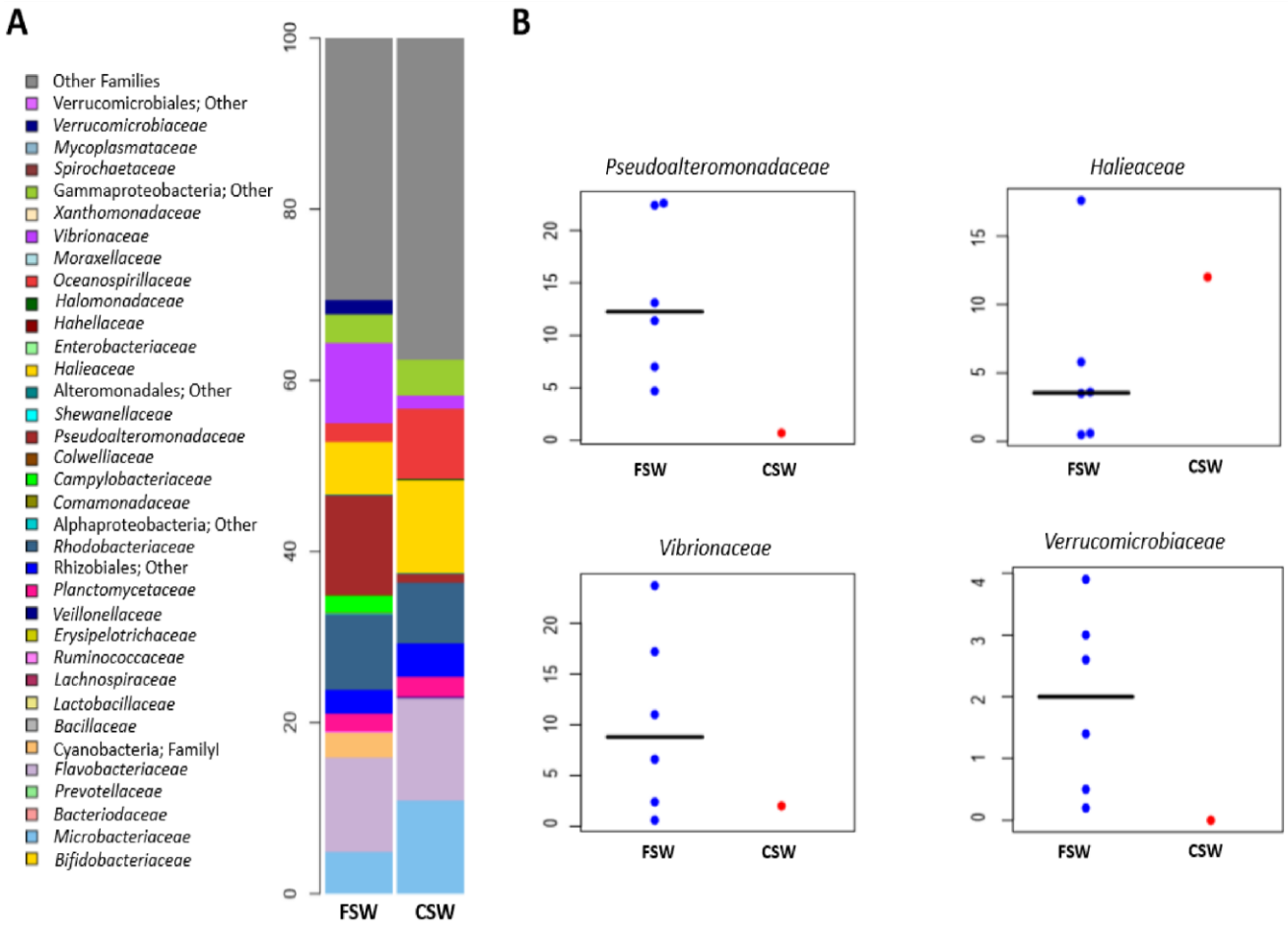

Table S1. Description of the samples. For each tissue type, number of samples, quantity analyzed, and method of extraction are reported. All samples were collected on April 3, 2019.

tissue	samples number	amount analyzed	extraction method
DIGESTIVE GLAND	25	20-30 mg	DNeasy PowerSoil kit
GILL	25	20-30 mg	DNeasy PowerSoil kit
FOOT	25	20-30 mg	DNeasy PowerSoil kit

STOMACH	21	20-30 mg	DNeasy PowerSoil kit
HEMOLYMPH	18	200 µl	DNeasy PowerSoil kit
WATER	7	2 l	DNeasy PowerWater kit

Table S2. Results of adonis statistics applied to the ordination analysis of figure 2 (A).

organs	**R_2**	**P-value**
Digestive gland vs Foot	0.01	0.03
Digestive gland vs Gill	0.01	0.003
Digestive gland vs Hemolymph	0.02	0.002
Digestive gland vs Stomach	0.02	0.002
Foot vs Gill	0.02	0.002
Foot vs Hemolymph	0.02	0.002
Foot vs Stomach	0.02	0.002
Gill vs Hemolymph	0.01	0.006
Gill vs Stomach	0.01	0.03
Stomach vs Hemolymph	0.02	0.002

Table S3. Relative abundance values of the most represented families in *M. galloprovincialis* organs and seawater.

family	**r. a. in digestive gland (%)**	**r. a. in foot (%)**	**r. a. in gill (%)**	**r. a. in stomach (%)**	**r. a. in hemolymph (%)**	**r. a. in seawater (%)**
Bifidobacteriaceae	1.04	2.92	0.09	1.17	0.46	0.00
Microbacteriaceae	0.32	0.13	0.07	1.02	1.02	4.88
Bacteroidaceae	2.06	2.38	0.17	1.34	1.34	0.00

Prevotellaceae	1.69	1.86	0.03	0.83	0.83	0.00
Flavobacteriaceae	7.69	6.93	4.27	19.64	19.64	11.01
Cyanobacteria; FamilyI	0.88	0.04	0.09	1.33	1.33	3.02
Bacillaceae	4.14	0.79	0.68	8.38	8.38	0.00
Lactobacillaceae	1.24	2.11	0.12	0.01	0.01	0.00
Lachnospiraceae	10.42	4.74	1.26	1.70	1.70	0.00
Ruminococcaceae	13.97	5.34	1.55	1.00	1.00	0.03
Erysipelotrichaceae	1.34	0.74	0.43	0.04	0.04	0.00
Veillonellaceae	1.37	0.60	0.11	0.29	0.29	0.00
Planctomycetaceae	3.81	2.67	0.40	0.34	0.34	2.12
Rhizobiales;Other	0.50	0.23	0.21	0.38	0.38	2.70
Rhodobacteraceae	2.89	1.86	1.38	9.43	9.43	8.80
Alphaproteobacteria;Other	1.72	0.14	0.81	0.36	0.36	0.21
Comamonadaceae	2.34	1.56	0.20	0.29	0.29	0.00
Campylobacteraceae	0.07	0.47	1.66	0.80	0.80	2.01
Colwelliaceae	0.34	0.95	0.99	0.88	0.88	0.17
Pseudoalteromonadaceae	0.59	3.27	3.49	0.13	0.13	11.66
Shewanellaceae	0.89	0.77	0.64	0.04	0.04	0.00
Alteromonadales;Other	0.16	0.55	43.43	0.81	0.81	0.01
Halieaceae	1.42	0.16	0.41	4.34	4.34	6.14
Enterobacteriaceae	1.58	0.90	0.41	0.08	0.08	0.00
Hahellaceae	0.08	0.86	11.53	0.84	0.84	0.00
Halomonadaceae	2.18	2.24	0.09	1.49	1.49	0.00
Oceanospirillaceae	0.07	0.51	1.08	0.60	0.60	2.25
Moraxellaceae	1.95	0.97	0.27	0.32	0.32	0.00
Vibrionaceae	2.93	2.18	4.95	1.52	1.52	9.34
Xanthomonadaceae	1.76	1.33	0.22	0.44	0.44	0.00
Gammaproteobacteria;Other	0.36	0.52	1.76	1.17	1.17	3.37
Spirochaetaceae	0.09	22.53	0.26	0.73	0.73	0.00
Mycoplasmataceae	0.39	0.73	0.18	0.07	0.07	0.00
Verrucomicrobiaceae	2.79	2.01	0.96	9.21	9.21	1.63
Verrucomicrobiales;Other	0.70	0.25	0.27	0.79	0.79	0.01
Other Families	24.24	23.73	15.56	28.94	28.94	30.60

1577

1578

Table S4. Over-abundance metagenomic inferred pathways.

pathways	pathways	pathways
1,4-dihydroxy-2-naphthoate biosynthesis I 1,4-dihydroxy-6-naphthoate biosynthesis I superpathwayof menaquinol-10 biosynthesis superpathwayof menaquinol-6 biosynthesis I superpathwayof demethylmenaquinol-6 biosynthesis I superpathwayof demethylmenaquinol-9 biosynthesis superpathwayof menaquinol-9 biosynthesis acetylene degradation Bifidobacteriumshunt heterolacticfermentation hexitolfermentation to lactate, formate, ethanol and acetate superpathwayof Clostridium acetobutylicumacidogenicfermentation pyruvate fermentation to acetate and lactate II pyruvate fermentation to acetone pyruvate fermentation to butanoate allantoindegradation to glyoxylateIII creatinine degradation I androstenedione degradation aromatic biogenic amine degradation (bacteria) aromatic compounds degradation via β-ketoadipate 4-hydroxyphenylacetate degradation catechol degradation III (ortho-cleavage pathway) catechol degradation to βketoadipate biotin biosynthesis II cob(II)yrinatea,c-diamidebiosynthesis I (early cobalt insertion) cob(II)yrinatea,c-diamidebiosynthesis II (late cobalt incorporation) adenosylcobalaminbiosynthesis II (late cobalt incorporation) chondroitin sulfate degradation I (bacterial) lactose and galactose degradation I mannandegradation superpathwayof fucoseand rhamnosedegradation 1,4-dihydroxy-2-naphthoate biosynthesis I 1,4-dihydroxy-6-naphthoate biosynthesis I superpathwayof menaquinol-10 biosynthesis superpathwayof menaquinol-6 biosynthesis I	superpathwayof UDP -N-acetylglucosamine-derived Oblocks biosy nthesis 2 -methylcitrate cycle I glutaryl-CoA degradation coenzyme M biosynthesis I enterobacterialcommon antigen biosynthesis enterobactinbiosynthesis ethylmalonyl-CoA pathway formaldehyde assimilation II (RuMP Cycle) formaldehyde oxidation I fuco se degradation gallate degradation I gallate degradation II methylgallate degradation protocatechuate degradation II (ortho -cleavage pathway) nicotinate degradation I superpathway of salicylate degradation toluene degradation IV (aerobic) (via catechol) glycine betaine degradation I methyl ketone biosynthesis glycolysis V (Pyrococcus) isoprene biosynthesis II (engineered) L -arginine degradation II (AST pathway) L -glutamate and L-glutamine biosynthesis L -glutamate degradation V (via hydroxyglutarate) L -histidine degradation II superpathway of L-arginine and L-ornithine degradation superpathway of L-arginine, putrescine, and 4aminobutanoate degradation superpathway of L -tryptophan biosynthesis L-lysine biosynthesis II L -rhamnose degradation I 4-deoxy-L-threo-hex-4-enopyranuronate degradation ketogluconate metabolism superpathwayof hexitoldegradation (bacteria) methanogenesisfrom acetate methylphosphonatedegradation I	superpathway of glycol metabolism and degradation mevalonate pathway I mono-trans, poly-cis decaprenyl phosphate biosynthesis mycolyl-arabinogalactan-peptidoglycan complex biosynthesis mycothiol biosynthesis peptidoglycan biosynthesis IV (Enterococcus faecium) peptidoglycan biosynthesis V (β-lactam resistance) teichoic acid (poly-glycerol) biosynthesis NAD salvage pathway II nitrate reduction VI (assimilatory) octane oxidation palmitate biosynthesis II (bacteria and plants) polymyxin resistance reductive acetyl coenzyme A pathway S-methyl-5-thio-α-D-ribose 1-phosphate degradation sitosterol degradation to androstenedione starch biosynthesis superpathway of (Kdo)2-lipid A biosynthesis superpathway of (R,R)-butanediol biosynthesis superpathway of 2,3-butanediol biosynthesis superpathway of geranylgeranyldiphosphate biosynthesis I (via mevalonate) superpathway of methylglyoxal degradation superpathway of ornithine degradation superpathway of sulfolactate degradation superpathway of sulfur oxidation (Acidianus ambivalens) superpathway of taurine degradation thiazolebiosynthesis II (Bacillus)

Supplement 2

Variability of metabolic, protective, and antioxidant gene transcriptional profiles and microbiota composition of Mediterranean mussels (*Mytilus galloprovincialis*) farmed in the North Adriatic Sea (Italy)

Table S1. Primers sequences and qPCR performances

Acronym	Transcript name	Primers (5'-3')	Amplicon size (bp)	Amplification efficiency (%)	Accession number	References
ABCB	***genes (assessed in glands)***					
	P-glycoprotein	CACCATAGCCGAGAACATCC CTCCACGCTCTCCAACTAG	139	112	EF057747	**(Franzellitti and Fabbri, 2013)**
Amyl	a-Amylase	CCTCGGGGTAGCTGGTTTTA TCCAAAGTTACGGGCTCCTT	232	90.7	EU336958	**(Paul-Pont et al., 2016)**
pk	Pyruvate kinase	AGACTTGGAGCTGCCTTCAG GGAATGCACAGAGGGTTCAT	228	102.33	Locus22823a	**(Paul-Pont et al., 2016)**
idp	Isocitrate dehydrogenase (NADP) cytoplasmic	GGAGGTACTGTATTTCGTGAGGC TGATCTCCATAAGCATGACGTCC	104	99.25	Locus2855a	**(Paul-Pont et al., 2016)**
lys	Lysozyme	ATGTGGAATCTGAAGGACTTGT CCAGTATCCAATGGTGTTAGGG	368	124	AF334665	**(Balbi et al., 2017a))**
mt10	10 kDa metallothionein	GGGCGCCGACTGTAAATGTTC- CACGTTGAAGGYCCTGTACACC	346	91	AY566247	**(Dondero et al., 2005)**
mt20	20 kDa metallothionein	TGTGAAAGTGGCTGCGGA GTACAGCCACATCCACACGC	430	92	AY566248	**(Dondero et al., 2005)**
cat	catalase	CGACCAGAGACAACCCACC GCAGTAGTATGCCTGTCCATCC	131	96	AY743716	**(Canesi et al., 2007)**
GST-π	glutathione s-transferase	TCCAGTTAGAGGCCGAGCTGA CTGCACCAGTTGGAAACCGTC	129	100	AF527010	**(Hoarau et al., 2006)**

sod	superoxide dismutase	AGCCAATGCAGAGGGAAAAGCAG A	177 129	97	FM177867	**(Koutso** 92
ctsl	Cathepsin L	CCACAAGCCAGACGACCCCC CCGAGGCTTCATACCCATATAC				AY618311 **(Capolu po et al., 2018)**
hex	Hexosaminidase	CGACAGCGGACATCAAATCT GATACTCCAGGACACACTCAATC CTGGTCCATAGCTACCATCAAATA	97	101	EU339934	**(Capolupo et al., 2018)**
gusb	ß-Glucuronidase	GCGGTCATTATCTGGTCTGTAG CCGGTCTTGTTGGGTCTAAAT	112	120	EU339935	**(Capolupo et al., 2018)**
Sex-specific genes (assessed in mantle/gonads)						
VCL	vitelline coat lysin	AGAGCTGTTTTGGCCACAGT TTGCGTTTGACATGGTTGAT	250	100	FM995162	**(Anantharaman and Craft, 2012)**
VERL	vitelline envelope receptor for lysin	CCGAAGGAAATGGAACTGAAA CCCTGCAATCGTATGGAATC	350	100	FM995161	**(Anantharaman and Craft, 2012)**
Reference genes (assessed both in digestive glands and mantle/gonads)						
18S	*18S rRNA*	TCGATGGTACGTGATATGCC CGTTTCTCATGCTCCCTCTC	90	95	L33451	**(Dondero et al., 2005)**
28S	*28S rRNA*	AGCCACTGCTTGCAGTTCTC ACTCGCGCACATGTTAGACTC	142	94	DQ158078	**(Ciocan et al., 2011)**
ACT	*Actin*	GTGTGATGTCATATCCGTAAGGA GCTTGGAGCAAGTGCTGTGA	120	114	AF157491	**(Banni et al., 2011)**
TUB	*Tubulin*	TTGCAACCATCAAGACCAAG TGCAGACGGCTCTCTGT	135	102	HM537081	**(Cubero-Leon et al., 2012)**
EF1	*Elongation factor-1α*	CGTTTTGCTGTCCGAGACATG CCACGCCTCACATCATTTCTTG	135	99	AB162021	**(Ciocan et al., 2011)**
HEL	*Helicase*	GCACTCATCAGAAGAAGGTGGC GCTCTCACTTGTGAAGGGTGAC	129	132	DQ158075	**(Cubero-Leon et al., 2012)**

1595

giannaki et al., 2014)

Table S2. Results of the BEST/BioEnv analysis

	Best correlated environmental variables	Rho	Level of significance
Whole dataset	• Temperature • Salinity • pH • Chloropyll-a • Gonad maturation level	0.538	0.1 %
Females	• Gonad maturation level • Temperature	0.742	0.1%
Males	• Salinity • Surface oxygen • Transparency	0.846	0.1%

Supplementary 3

Development and validation of a liquid chromatography – mass spectrometry method for multiresidue analysis in mussel of the Adriatic Sea

N. Interino[1], R Comito[1], E Porru[2], P. Simoni[2], S. Franzellitti[4], M. Musella[5], R. Gotti[5], A. Roda[1,6], M. Candela[5], J. Fiori[1]

[1]Department of Chemistry "G. Ciamician", Alma Mater Studiorum- Università di Bologna, Via Selmi 2, 40126 Bologna
[2]Department of Medical and Surgical Sciences, Alma Mater Studiorum, University of Bologna, Bologna, 40138, Italy
[4]Animal and Environmental Physiology Laboratory, Department of Biological, Geological and Environmental Sciences (BiGeA), Alma Mater Studiorum- Università di Bologna, Via S. Alberto 163, 48123 Ravenna, Italy
[5]Department of Pharmacy and Biotechnology (FaBiT), Alma Mater Studiorum- Università di Bologna, Via Belmeloro 6, 40126 Bologna, Italy
[6]INBB, National Institute of Biostructure and Biosystems, Viale delle Medaglie d'Oro, Rome, Italy

Table S1. Recovery, Matrix effect (%) and their respective relative standard deviation (n=3) with Cyclohexane extraction.

COMPOUND	RECOVERY	MATRIX EFFECT
Amoxycillin	0±0%	-48%±4%
Carbamazepine	11±2%	22%±7%
Sulfamethoxazole	2±1%	8%±3%
Erythromycin	6±4%	80%±15%
Doxycycline	8±6%	37%±10%
Tetracycline	6±3%	-17%±9%
Deet	51±8%	5%±3%
Atrazine	25±10%	11%±6%
Atrazine-Desethyl-Desisopropyl	2±1%	-28%±9%
Alachlor	25±5%	18%±3%
Metolachlor	36±9%	-5%±3%

Table S2. Recovery, Matrix effect (%) and their respective relative standard deviation (n=3) with Dichloromethane extraction.

COMPOUND	RECOVERY	MATRIX EFFECT
Amoxycillin	0±0%	-76%±2%
Carbamazepine	44±6%	-55%±11%
Sulfamethoxazole	5±3%	-69%±8%
Erythromycin	44±4%	85%±15%
Doxycycline	15±5%	-59%±8%
Tetracycline	11±7%	-61%±11%
Deet	68±5%	-51%±9%
Atrazine	33±7%	-49%±7%
Atrazine-Desethyl-Desisopropyl	7±2%	-75%±4%
Alachlor	33±8%	-59%±5%
Metolachlor	48±12%	-65%±3%

Table S3. Recovery, Matrix effect (%) and their respective relative standard deviation (n=3) with Hexane extraction.

COMPOUND	RECOVERY	MATRIX EFFECT
Amoxycillin	0±0%	-28%±2%
Carbamazepine	11±5%	-50%±9%
Sulfamethoxazole	4±2%	-67%±8%
Erythromycin	8±4%	44%±11%
Doxycycline	10±4%	-34%±8%
Tetracycline	5±6%	-24%±9%
Deet	60±5%	-29%±7%
Atrazine	34±3%	-49%±4%
Atrazine-Desethyl-Desisopropyl	5±1%	-81%±8%
Alachlor	44±9%	-39%±8%
Metolachlor	46±11%	-42%±2%

Table S4. Recovery, Matrix effect (%) and their respective relative standard deviation (n=3) with Acetone extraction.

COMPOUND	RECOVERY	MATRIX EFFECT
Amoxycillin	0±0%	-51%±6%
Carbamazepine	12±6%	-51%±8%
Sulfamethoxazole	34±9%	-49%±10%
Erythromycin	38±7%	-21%±5%
Doxycycline	10±4%	-22%±7%
Tetracycline	9±3%	-29%±8%
Deet	52±5%	-26%±8%
Atrazine	32±9%	-26%±10%
Atrazine-Desethyl-Desisopropyl	18±4%	-82%±11%
Alachlor	17±3%	-21%±9%
Metolachlor	39±8%	-29%±6%

Table S5. Recovery, Matrix effect (%) and their respective relative standard deviation (n=3) with Hexane-Acetone (50-50 v/v) extraction.

COMPOUND	RECOVERY	MATRIX EFFECT
Amoxycillin	0±0%	-33%±7%
Carbamazepine	13±6%	-51%±9%
Sulfamethoxazole	25±10%	-68%±9%
Erythromycin	28±3%	-19%±6%
Doxycycline	13±3%	-39%±6%
Tetracycline	10±5%	-30%±8%
Deet	57±8%	-25%±5%
Atrazine	36±8%	-38%±9%
Atrazine-Desethyl-Desisopropyl	20±7%	-81%±11%
Alachlor	37±9%	-36%±5%
Metolachlor	43±10%	-39%±8%

Table S6. Recovery, Matrix effect (%) and their respective relative standard deviation (n=3) with Acetonitrile extraction.

COMPOUND	RECOVERY	MATRIX EFFECT
Amoxycillin	2±4%	-59%±5%
Carbamazepine	38±5%	-54%±7%
Sulfamethoxazole	7±5%	-53%±9%
Erythromycin	15±6%	10%±4%
Doxycycline	3±6%	-18%±3%
Tetracycline	3±3%	-26%±4%
Deet	61±7%	-26%±5%
Atrazine	50±4%	-21%±5%
Atrazine-Desethyl-Desisopropyl	60±9%	-86%±10%
Alachlor	48±10%	-14%±7%
Metolachlor	55±9%	-11%±6%

Table S7. Recovery, Matrix effect (%) and their respective relative standard deviation (n=3) with Methanol extraction.

COMPOUND	RECOVERY	MATRIX EFFECT
Amoxycillin	5±2%	-83%±4%
Carbamazepine	56±5%	-70%±4%
Sulfamethoxazole	16±5%	-78%±3%
Erythromycin	50±2%	-45%±4%
Doxycycline	45±12%	-60%±5%
Tetracycline	35±10%	-68%±7%
Deet	48±6%	-72%±6%
Atrazine	25±3%	-60%±6%
Atrazine-Desethyl-Desisopropyl	55±3%	-89%±8%
Alachlor	32±7%	-54%±8%
Metolachlor	27±6%	-78%±10%

Table S8. Recovery, Matrix effect (%) and their respective relative standard deviation (n=3) with Acetonitrile-Methanol (50-50 v/v) extraction.

COMPOUND	RECOVERY	MATRIX EFFECT
Amoxycillin	3±2%	-80%±10%
Carbamazepine	42±5%	-61%±8%
Sulfamethoxazole	18±4%	-70%±8%
Erythromycin	50±6%	-27%±7%
Doxycycline	24±7%	-38%±6%
Tetracycline	29±7%	-65%±10%
Deet	53±4%	-48%±6%
Atrazine	38±8%	-42%±5%
Atrazine-Desethyl-Desisopropyl	65±10%	-85%±10%
Alachlor	36±7%	-34%±4%
Metolachlor	31±5%	-59%±8%

Table S9. Recovery, Matrix effect (%) and their respective relative standard deviation (n=3) with two separate extractions with different solvents (ACN: MeOH) (50:50 v/v) and Hexane: Acetone (50:50 v/v) at room temperature.

COMPOUND	RECOVERY	MATRIX EFFECT
Amoxycillin	2±4%	-79%±5%
Carbamazepine	52±9%	-55%±7%
Sulfamethoxazole	35±9%	-69%±6%
Erythromycin	64±10%	-33%±9%
Doxycycline	24±8%	-38%±7%
Tetracycline	27±7%	-52%±8%
Deet	48±8%	-44%±7%
Atrazine	32±9%	-56%±9%
Atrazine-Desethyl-Desisopropyl	63±6%	-80%±9%
Alachlor	36±8%	-37%±8%
Metolachlor	35±5%	-46%±10%

Table S10. Relative recovery and standard deviation (n=3) of mixed standards solution after t= 8h of storage at three different storage temperature respect the measured analyte concentration at baseline (t = 0).

COMPOUND	STORAGE TEMPERATURE		
	_-20°C	_-4°C	ROOM TEMPERATURE
Amoxycillin	85% ± 12%	85% ±12%	72%± 25%
Carbamazepine	91% ±10%	90% ±8%	87%±16%
Sulfamethoxazole	90% ±8%	89% ±12%	87%±6%
Erythromycin	89% ±8%	85% ±9%	69%±9%
Doxycycline	86% ±6%	82% ±10%	58%±6%
Tetracycline	85% ±7%	84% ±10%	68% ±4%
Deet	91% ±12%	89% ±12%	85% ±11%
Atrazine	96% ±10%	92% ±10%	87% ±8%
Atrazine-Desethyl-Desisopropyl	92% ±11%	90% ±9%	87% ±28%
Alachlor	98% ±6%	97% ±17%	89%±4%
Metolachlor	95% ±7%	92% ±9%	88%±8%

Table S11. Recovery, Matrix effect (%) and their respective relative standard deviation (n=3) with two separate extractions with different solvents, ACN: MeOH, (50:50 v/v) and Hexane: Acetone (50:50 v/v) at low temperature.

COMPOUND	RECOVERY	MATRIX EFFECT
Amoxycillin	37%±10%	-79±8%
Carbamazepine	55%±7%	-46±8%
Sulfamethoxazole	37%±9%	-66±7%
Erythromycin	67%±8%	-36±6%
Doxycycline	27%±10%	-38±8%
Tetracycline	36%±6%	-52±9%
Deet	65%±8%	-41±6%
Atrazine	35%±7%	-44±6%
Atrazine-Desethyl-Desisopropyl	73%±8%	-73±9%
Alachlor	48%±10%	-41±5%
Metolachlor	30%±10%	-45±6%

Table S12. Recovery, Matrix effect (%) and their respective relative standard deviation (n=3) including SPE with LiChrolut EN column

COMPOUND	RECOVERY	MATRIX EFFECT
Amoxycillin	3±3%	-75±6%
Carbamazepine	34±3%	-44±10%
Sulfamethoxazole	22±7%	-67±10%
Erythromycin	23±4%	-33±9%
Doxycycline	34±9%	-28±9%
Tetracycline	37±8%	-43±6%
Deet	32±4%	-42±8%
Atrazine	25±7%	-16±5%
Atrazine-Desethyl-Desisopropyl	44±5%	-67±9%
Alachlor	16±7%	-19±5%
Metolachlor	18±6%	-26±5%

Table S13. Recovery, Matrix effect (%) and their respective relative standard deviation (n=3) including SPE with Silicycle C18 column

COMPOUND	RECOVERY	MATRIX EFFECT
Amoxycillin	3±5%	-75±5%
Carbamazepine	33±6%	-42±10%
Sulfamethoxazole	20±8%	-66±10%
Erythromycin	21±5%	-35±8%
Doxycycline	33±3%	-30±7%
Tetracycline	36±3%	-40±9%
Deet	51±8%	-42±9%
Atrazine	33±8%	-15±6%
Atrazine-Desethyl-Desisopropyl	47±9%	-69±8%
Alachlor	24±9%	-15±8%
Metolachlor	22±5%	-26±7%

Table S14. Recovery, Matrix effect (%) and their respective relative standard deviation (n=3) with Quechers and dispersive solid phase extraction (dSPE) mixtures (QuE Citrate (EN) + Supel QuE Z-Sep+ Extraction tubes).

COMPOUND	RECOVERY	MATRIX EFFECT
Amoxycillin	39±8%	-75±5%
Carbamazepine	66±6%	-51±9%
Sulfamethoxazole	37±8%	-65±9%
Erythromycin	78±10%	-49±8%
Doxycycline	31±10%	-58±7%
Tetracycline	36±6%	-57±8%
Deet	74±10%	-55±6%
Atrazine	46±8%	-55±6%
Atrazine-Desethyl-Desisopropyl	80±8%	-69±9%
Alachlor	61±12%	-50±6%
Metolachlor	34±6%	-48±8%

Table S15. Recovery, Matrix effect (%) and their respective relative standard deviation (n=3) with Quechers and dispersive solid phase extraction (dSPE) mixtures (Supel QuE Acetate (AC) + Supel QuE PSA/C18 extraction Tube).

COMPOUND	RECOVERY	MATRIX EFFECT
Amoxycillin	4±3%	-77±9%
Carbamazepine	73±10%	-48±7%
Sulfamethoxazole	45±8%	-65±11%
Erythromycin	60±6%	-36±6%
Doxycycline	37±5%	-48±7%
Tetracycline	39±7%	-43±8%
Deet	56±8%	-42±6%
Atrazine	53±9%	-41±7%
Atrazine-Desethyl-Desisopropyl	27±6%	-68±10%
Alachlor	37±7%	-44±8%
Metolachlor	40±8%	-40±9%

Table S16. Recovery, Matrix effect (%) and their respective relative standard deviation (n=3) the final extraction procedure (with CHAPS) at three different concentrations (low to high).

	Low Concentration (MQL)		Medium Concentration (10 MQL)		High Concentration (100 MQL)	
COMPOUND	RECOVERY	MATRIX EFFECT	RECOVERY	MATRIX EFFECT	RECOVERY	MATRIX EFFECT
Amoxycillin	39% ± 7%	-75% ± 3%	35% ± 6%	-75% ± 6%	33% ±8%	-75% ± 5%
Carbamazepine	66% ± 7%	-56% ± 9%	72% ± 5%	-57% ± 10%	78% ±6 %	-62% ± 8%
Sulfamethoxazole	39% ± 5%	-59% ± 10%	37% ± 8%	-60% ± 10%	31% ±7%	-64% ±7 %
Erythromycin	55% ± 8%	-24% ± 4%	67% ± 3%	-20% ± 4%	72% ±9%	-19% ± 6%
Doxycycline	39% ± 5%	-33% ± 9%	32% ± 5%	-31% ± 8%	25% ± 6%	-31% ±8%
Tetracycline	44% ± 4%	-42% ± 5%	35% ± 7%	-45% ± 6%	29% ± 9%	-47% ± 4%
Deet	71% ± 9%	-41% ± 6%	86% ± 9%	-40% ± 9%	81% ±8 %	-39% ± 8%
Atrazine	43% ± 9%	-38% ± 9%	58% ± 10%	-35% ± 4%	51% ± 8%	-34% ± 7%
Atrazine-Desethyl-Desisopropyl	73% ± 10%	-70% ± 8%	95% ± 10%	-69% ± 10%	84% ±9 %	-68% ± 9%
Alachlor	69% ± 8%	-15% ±6 %	51% ± 9%	-16% ± 8%	41% ±6 %	-19% ± 7%
Metolachlor	58% ±6%	-18% ± 5%	46% ± 5%	-20% ± 7%	40% ±6 %	-22% ±7 %

Table S17. Linearity (regression coefficient) obtained from matrix-matched calibration curves made in mussels extract and the range concentration.

Compound	Range concentration (ng/mL)	r^2
Amoxycillin	15-500	0.998
Carbamazepine	0.5-100	0.995
Sulfamethoxazole	0.5-100	0.995
Erythromycin	0.5-100	0.999
Doxycycline	15-500	0.995
Tetracycline	0.5-100	0.997
Deet	0.002-10	0.995
Atrazine	2-500	0.996
Atrazine-Desethyl-Desisopropyl	2-500	0.999
Alachlor	15-500	0.995
Metolachlor	0.05-50	0.998

Table S18. Accuracy and precision of the whole method calculated intra-day and inter-day from three repeated injections of a sample spiked at three concentration level and extracted.

	Intraday measurement (n = 3)						Interday measurement (n = 9)					
	QC_{low}		QC_{med}		QC_{high}		QC_{low}		QC_{med}		QC_{high}	
	Accuracy%	RSD %	Accuracy%	RSD %	Accuracy%	RSD %	Accuracy%	RSD %	Accuracy%	RSD %	Accuracy%	RSD %
Amoxycillin	5	6	4	2	4	1	5	2	6	3	4	3
Carbamazepine	8	6	9	2	6	2	7	3	7	3	8	3
Sulfamethoxazole	6	2	7	3	5	3	7	3	6	4	8	3
Erythromycin	8	4	7	2	5	3	6	2	5	2	4	3
Doxycycline	7	3	11	2	5	3	8	2	9	3	4	2
Tetracycline	-6	4	-4	3	4	2	4	2	5	3	-7	2
Deet	11	3	11	3	7	3	11	3	10	4	9	4
Atrazine	6	2	4	3	6	2	5	2	4	4	5	2
Atrazine-Desethyl-Desisopropyl	8	3	7	3	10	2	9	3	6	3	7	2
Alachlor	6	5	9	4	8	4	5	6	9	4	7	5
Metolachlor	5	2	4	2	5	3	7	3	4	2	6	3

Table S19. Limit of detection (LOD) and limit of quantification (LOQ) of the method for each single analyte determined in mobile phase. Method detection limits (MDL) and Method quantification limits (MQL) determined in spiked samples before the extraction (n=3).

COMPOUND	MDL (ng/g)	MQL (ng/g)
Amoxycillin	5	15
Carbamazepine	0.2	0.6
Sulfamethoxazole	0.1	0.3
Erythromycin	0.2	0.5
Doxycycline	5	15
Tetracycline	0.1	0.4
Deet	9E-4	3E-3
Atrazine	0.7	3
Atrazine-Desethyl-Desisopropyl	2	7
Alachlor	10	30
Metolachlor	6E-3	0.02

Table S20. Analysis in real mussels samples from Adriatic Sea. Concentration (ng/g) and standard deviation (SD)

COMPOUND	Concentration (ng/g)
Amoxycillin	< MDL
Carbamazepine	2±4
Sulfamethoxazole	43±19
Erythromycin	9 ±7
Doxycycline	< MDL
Tetracycline	35±16
Deet	6E-3±3E-3
Atrazine	21±18
Atrazine-Desethyl-Desisopropyl	< MDL
Alachlor	< MDL
Metolachlor	7E-2±1E-2

References

Alvisi, F., Cozzi, S., 2016. Seasonal dynamics and long-term trend of hypoxia in the coastal zone of Emilia Romagna (NW Adriatic Sea, Italy). Sci. Total Environ. 541, 1448–1462. https://doi.org/10.1016/j.scitotenv.2015.10.011

Anantharaman, S., Craft, J.A., 2012. Annual Variation in the Levels of Transcripts of Sex-Specific Genes in the Mantle of the Common Mussel, Mytilus edulis. PLoS One 7. https://doi.org/10.1371/journal.pone.0050861

Anderson, M., Gorley, R., Clarke, K., 2008. PERMANOVA+ for PRIMER: Guide to Software and Statistical Methods.

Arapov, J., Bali, D.E., Peharda, M., Gladan, N., 2010. Bivalve feeding — how and what they eat? Croat. J. Fish. 68, 105–116.

Azizi, G., Layachi, M., Akodad, M., Yáñez-Ruiz, D.R., Martín-García, A.I., Baghour, M., Mesfioui, A., Skalli, A., Moumen, A., 2018. Seasonal variations of heavy metals content in mussels (Mytilus galloprovincialis) from Cala Iris offshore (Northern Morocco). Mar. Pollut. Bull. 137, 688–694. https://doi.org/10.1016/j.marpolbul.2018.06.052

Balbi, T., Fabbri, R., Montagna, M., Camisassi, G., Canesi, L., 2017. Seasonal variability of different biomarkers in mussels (Mytilus galloprovincialis) farmed at different sites of the Gulf of La Spezia, Ligurian sea, Italy. Mar. Pollut. Bull. 116, 348–356. https://doi.org/10.1016/j.marpolbul.2017.01.035

Balbi, T., Franzellitti, S., Fabbri, R., Montagna, M., Fabbri, E., Canesi, L., 2016. Impact of bisphenol A (BPA) on early embryo development in the marine mussel Mytilus galloprovincialis: effects on gene transcription. Environ. Pollut. 218, 996–1004. https://doi.org/10.1016/j.envpol.2016.08.050

Banni, M., Negri, A., Mignone, F., Boussetta, H., Viarengo, A., Dondero, F., 2011. Gene expression rhythms in the mussel Mytilus galloprovincialis (Lam.) across an annual cycle. PLoS One 6, e18904. https://doi.org/10.1371/journal.pone.0018904

Barbera, P., Kozlov, A.M., Czech, L., Morel, B., Darriba, D., Flouri, T., Stamatakis, A., 2019. EPA-ng: Massively Parallel Evolutionary Placement of Genetic Sequences. Syst. Biol. 68(2). 365–369. https://doi.org/10.1093/sysbio/syy054.

Bard, S.M., 2000. Multixenobiotic resistance as a cellular defense mechanism in aquatic organisms. Aquat. Toxicol. https://doi.org/10.1016/S0166-445X(00)00088-6

Barone, M., Turroni, S., Rampelli, S., Soverini, M., D'Amico, F., Biagi, E., et al., 2019. Gut microbiome response to a modern Paleolithic diet in a Western lifestyle context. PloS one. 14, 8 e0220619. https://doi.org/10.1371/journal.pone.0220619

Baker-Austin, C., Oliver, J.D., Alam, M., Ali, A., Waldor, M.K., Qadri, F., et al., 2018. Vibrio spp. infections. Nat. Rev. Dis. Primers 4, 8. https://doi.org/10.1038/s41572-018-0010-y.

Bedulina, D., Drozdova, P., Gurkov, A., von Bergen, M., Stadler, P.F., Luckenbach, T., Timofeyev, M., Kalkhof, S., 2020. Proteomics reveals sex-specific heat shock response of Baikal amphipod Eulimnogammarus cyaneus. Sci. Total Environ. 143008. https://doi.org/10.1016/j.scitotenv.2020.143008

Benito, D., Ahvo, A., Nuutinen, J., Bilbao, D., Saenz, J., Etxebarria, N., Lekube, X., Izagirre, U., Lehtonen, K.K., Marigómez, I., Zaldibar, B., Soto, M., 2019. Influence of season-depending ecological variables on biomarker baseline levels in mussels (Mytilus trossulus) from two Baltic Sea subregions. Sci. Total Environ. 689, 1087–1103. https://doi.org/10.1016/j.scitotenv.2019.06.412

Blalock, B.J., Robinson, W.E., Poynton, H.C., 2020. Assessing legacy and endocrine disrupting pollutants in Boston Harbor with transcriptomic biomarkers. Aquat. Toxicol. 220, 105397. https://doi.org/10.1016/j.aquatox.2019.105397

Blanco-Rayón, E., Ivanina, A. V., Sokolova, I.M., Marigómez, I., Izagirre, U., 2020. Sex and sex-related differences in gamete development progression impinge on biomarker responsiveness in sentinel mussels. Sci. Total Environ. 740, 140178. https://doi.org/10.1016/j.scitotenv.2020.140178

Bloise, E., Ortiga-Carvalho, T.M., Reis, F.M., Lye, S.J., Gibb, W., Matthews, S.G., 2016. ATP-binding cassette transporters in reproduction: A new frontier. Hum. Reprod. Update 22, 164–181. https://doi.org/10.1093/humupd/dmv049

Bolyen, E., Rideout, J. R., Dillon, M. R. et al., 2019. Reproducible, interactive, scalable and extensible microbiome data science using QIIME 2. Nat. Biotechnol. 37, 852–857 https://doi.org/10.1038/s41587-019-0209-9.

Brigolin, D., Porporato, E.M.D., Prioli, G., Pastres, R., 2017. Making space for shellfish farming along the adriatic coast. ICES J. Mar. Sci. 74, 1540–1551. https://doi.org/10.1093/icesjms/fsx018.

Brito, T.L., Campos, A.B., Bastiaan von Meijenfeldt, F.A., Daniel, J.P., Ribeiro, G.B., Silva, G.G.Z., et al., 2018. The gill-associated microbiome is the main source of wood plant polysaccharide hydrolases and secondary metabolite gene clusters in the mangrove shipworm Neoteredo reynei. PLoS One 13, e0200437. https://doi.org/10.1371/journal.pone.0200437.

Buratti, S., Franzellitti, S., Poletti, R., Ceredi, A., Montanari, G., Capuzzo, A., et al., 2013. Bioaccumulation of algal toxins and changes in physiological parameters in Mediterranean mussels from the North Adriatic Sea (Italy). Environ. Toxicol. 28, 451–470.

Burgos-Aceves, M.A., Faggio, C., 2017. An approach to the study of the immunity functions of bivalve haemocytes: Physiology and molecular aspects. Fish Shellfish Immunol. 16 67. 513-517. https://doi.org/10.1016/j.fsi.2017.06.042.

Callahan, B.J., McMurdie, P.J., Rosen, M.J., Han, A.W., Johnson, A.J., Holmes, S.P., 2016. DADA2: High-resolution sample inference from Illumina amplicon data. Nat. Methods 13, 581–583. https://doi.org/10.1038/nmeth.3869.

Canesi, L., Ciacci, C., Betti, M., Malatesta, M., Gazzanelli, G., Gallo, G., 1999. Growth Factors Stimulate the Activity of Key Glycolytic Enzymes in Isolated Digestive Gland Cells from Mussels (Mytilus galloprovincialis Lam.) through Tyrosine Kinase Mediated Signal Transduction. Gen. Comp. Endocrinol. 116, 241–248. https://doi.org/10.1006/gcen.1999.7366

Capolupo, M., Franzellitti, S., Kiwan, A., Valbonesi, P., Dinelli, E., Pignotti, E., et al., 2017. A comprehensive evaluation of the environmental quality of a coastal lagoon (Ravenna, Italy): Integrating chemical and physiological analyses in mussels as a biomonitoring strategy. Sci. Total Environ. 598, 146–159.

Cappello, S., Volta, A., Santisi, S., Genovese, L., Maricchiolo, G., 2015. Study of bacterial communities in mussel Mytilus galloprovincialis (Bivalvia: Mytilidae) by a combination of 16S crDNA and 16S rDNA sequencing. JSM Microbiol. 3, 1016.

Carella, F., Aceto, S., Mangoni, O., Mollica, M.P., Cavaliere, G., Trinchese, G., et al., 2018. Assessment of the health status of mussels Mytilus galloprovincialis along the Campania coastal areas: a multidisciplinary approach. Front. Physiol. 9, 683. https://doi.org/10.3389/fphys.2018.00683.

Caricato, R., Lionetto, M.G., Schettino, T., 2010. Seasonal variation of biomarkers in Mytilus galloprovincialis sampled inside and outside Mar Piccolo of taranto (Italy). Chem. Ecol. 26, 143–153. https://doi.org/10.1080/02757541003627639.

Caspi, R., Billington, R., Fulcher, CA., Keseler, I.M., Kothari A., Krummenacker M., Latendresse M., Midford P.E., Ong Q., Ong W.K., Paley S., Subhraveti P., Karp P.D., 2018. The MetaCyc database of metabolic pathways and enzymes. Nucleic Acids Res. 46:D633–D639. https://doi.org/10.1093/nar/gkx935.

Combi, T., Pintado-Herrera, M.G., Lara-Martin, P.A., Miserocchi, S., Langone, L., Guerra, R., 2016. Distribution and fate of legacy and emerging contaminants along the Adriatic Sea: A comparative study. Environ. Pollut. 218, 1055–1064. https://doi.org/10.1016/j.envpol.2016.08.057

Counihan, K.L., Bowen, L., Ballachey, B., Coletti, H., Hollmen, T., Pister, B., Wilson, T.L., 2019. Physiological and gene transcription assays to assess responses of mussels to environmental changes. PeerJ 2019, 1–33. https://doi.org/10.7717/peerj.7800

Czech, L., Stamatakis, A., 2019. Scalable methods for analyzing and visualizing phylogenetic placement of metagenomic samples. PLoS One, 14 (5) e0217050. https://doi.org/10.1371/journal.pone.0217050.

Daczkowska-Kozon, E.G., Dabworski, W., Bernardczyk-Drag, A., Szymczak, B., 2010. Safety aspects of seafood. Environmental effects on seafood availability, safety, and quality. Florida (USA): CRC Press; p. 129.

Desriac, F., Le Chevalier, P., Brillet, B., Leguerinel, I., Thuillier, B., Paillard, C., et al., 2014. Exploring the hologenome concept in marine bivalvia: haemolymph microbiota as a pertinent source of probiotics for aquaculture. FEMS Microbiol. Lett. 350, 107–116. https://doi.org/10.1111/1574-6968.12308.

Elia, A.C., Burioli, E., Magara, G., Pastorino, P., Caldaroni, B., Menconi, V., Dörr, A.J.M., Colombero, G., Abete, M.C., Prearo, M., 2020. Oxidative stress ecology on Pacific oyster Crassostrea gigas from lagoon and offshore Italian sites. Sci. Total Environ. 739, 139886. https://doi.org/10.1016/j.scitotenv.2020.139886

Erol, N., Delibaş, S.B., Özkoç, S., Ergüden, C., Aksoy, Ü.C., 2016. Investigation of parasitic and viral pathogens in mussels (Mytilus galloprovincialis) in the Gulf of Izmir, Turkey. Saudi Med. J. 37, 703–706. https://doi.org/10.15537/Smj.2016.6.15034.

Evans, T.G., Hofmann, G.E., 2012. Defining the limits of physiological plasticity: how gene expression can assess and predict the consequences of ocean change. Philos. Trans. R. Soc. B Biol. Sci. 367, 1733–1745. https://doi.org/10.1098/rstb.2012.0019

Faggio C., Tsarpali V., Dailianis S., 2018. Mussel digestive gland as a model for assessing xenobiotics: an overview. Science of the Total Environmental 613: 220-229. https://doi.org/10.1016/j.scitotenv.2018.04.264.Franzellitti, S., Striano T., Valbonesi P., Fabbri E., 2016. Insights into the regulation of the MXR response in haemocytes of the Mediterranean mussel (Mytilus galloprovincialis). Fish Shellfish Immunol. 58, 349–358.

Figueras, A., Moreira, R., Sendra, M., Novoa, B., 2019. Genomics and immunity of the Mediterranean mussel Mytilus galloprovincialis in a changing environment. Fish Shellfish Immunol. 90, 440–445. https://doi.org/10.1016/j.fsi.2019.04.064

Franzellitti, S., Balbi, T., Montagna, M., Fabbri, R., Valbonesi, P., Fabbri, E., Canesi, L., 2019. Phenotypical and molecular changes induced by carbamazepine and propranolol on larval stages of Mytilus galloprovincialis. Chemosphere 234, 962–970. https://doi.org/10.1016/j.chemosphere.2019.06.045

Franzellitti, S., Buratti, S., Donnini, F., Fabbri, E., 2010. Exposure of mussels to a polluted environment: insights into the stress syndrome development. Comp. Biochem. Physiol. Part C 152, 24–33. https://doi.org/10.1016/j.cbpc.2010.02.010

Franzellitti, S., Prada, F., Viarengo, A., Fabbri, E., 2020. Evaluating bivalve cytoprotective responses and their regulatory pathways in a climate change scenario. Sci. Total Environ. 720, 137733. https://doi.org/10.1016/j.scitotenv.2020.137733

Franzellitti, S., Striano, T., Pretolani, F., Fabbri, E., 2017. Investigating appearance and regulation of the MXR phenotype in early embryo stages of the Mediterranean mussel (Mytilus galloprovincialis). Comp. Biochem. Physiol. Part - C Toxicol. Pharmacol. 199, 1–10. https://doi.org/10.1016/j.cbpc.2016.11.004

Frapiccini, E., Annibaldi, A., Betti, M., Polidori, P., Truzzi, C., Marini, M., 2018. Polycyclic aromatic hydrocarbon (PAH) accumulation in different common sole (Solea solea) tissues from

the North Adriatic Sea peculiar impacted area. Mar. Pollut. Bull. 137, 61–68. https://doi.org/10.1016/j.marpolbul.2018.10.002

Frapiccini, E., Panfili, M., Guicciardi, S., Santojanni, A., Marini, M., Truzzi, C., Annibaldi, A., 2020. Effects of biological factors and seasonality on the level of polycyclic aromatic hydrocarbons in red mullet (Mullus barbatus). Environ. Pollut. 258, 113742. https://doi.org/10.1016/j.envpol.2019.113742

Fraser, M., Fortier, M., Roumier, P.H., Parent, L., Brousseau, P., Fournier, M., Surette, C., Vaillancourt, C., 2016. Sex determination in blue mussels: Which method to choose? Mar. Environ. Res. 120, 78–85. https://doi.org/10.1016/j.marenvres.2016.07.008

Freitas R., Silvestro S., Coppola F., Meucci V., Battaglia F., Intorre L., Soares A.M.V.M., Pretti C., Faggio C., 2019. Biochemical and physiological responses induced in Mytilus galloprovincialis after a chronic exposure to Salicylic Acid. Aquatic toxicology. https://doi.org/10.1016/j.aquatox.2019.105258.

Gagné, F., Auclair, J., Turcotte, P., Gagnon, C., Peyrot, C., Wilkinson, K., 2019. The influence of surface waters on the bioavailability and toxicity of zinc oxide nanoparticles in freshwater mussels. Comp. Biochem. Physiol. C Toxicol. Pharmacol. 219, 1-11. https://doi.org/10.1016/j.cbpc.2019.01.005.

Gavin M. Douglas, Vincent J. Maffei, Jesse Zaneveld, Svetlana N. Yurgel, James R. Brown, Christopher M. Taylor, Curtis Huttenhower, Morgan G. I. Langille., 2019. bioRxiv 672295 [Preprint]. https://doi.org/10.1101/672295.

Glasl, B., Herndl, G.J., Frade, P.R., 2016. The microbiome of coral surface mucus has a key role in mediating holobiont health and survival upon disturbance. ISME J. 10, 2280–2292. https://doi.org/10.1038/ismej.2016.9.

Gracey, A.Y., 2007. Interpreting physiological responses to environmental change through gene expression profiling. J. Exp. Biol. https://doi.org/10.1242/jeb.004333

Grbin, D., Sabolić, I., Klobučar, G., Dennis, S.R., Šrut, M., Bakarić, R., Baković, V., Brkanac, S.R., Nosil, P., Štambuk, A., 2019. Biomarker response of Mediterranean mussels Mytilus galloprovincialis regarding environmental conditions, pollution impact and seasonal effects. Sci. Total Environ. 694, 1–10. https://doi.org/10.1016/j.scitotenv.2019.07.276

Grenier, C., Román, R., Duarte, C., Navarro, J.M., Rodriguez-Navarro, A.B., Ramajo, L., 2020. The combined effects of salinity and pH on shell biomineralization of the edible mussel Mytilus chilensis. Environ. Pollut. 263, 114555. https://doi.org/10.1016/j.envpol.2020.114555

Hamdoun, A., Epel, D., 2007. Embryo stability and vulnerability in an always changing world. Proc. Natl. Acad. Sci. U. S. A. 104, 1745–50. https://doi.org/10.1073/pnas.0610108104

Hampson, D. J., Ahmed, N. 2009. Spirochaetes as intestinal pathogens: lessons from a Brachyspira genome. Gut Pathog. 1, 1-10. https://doi.org/10.1186/1757-4749-1-10.

Hines, A., Yeung, W.H., Craft, J., Brown, M., Kennedy, J., Bignell, J., Stentiford, G.D., Viant, M.R., 2007. Comparison of histological, genetic, metabolomics, and lipid-based methods for sex determination in marine mussels. Anal. Biochem. 369, 175–186. https://doi.org/10.1016/j.ab.2007.06.008

Higgins E, Parr TB, Vaughn CC. Mussels and Local Conditions Interact to Influence Microbial Communities in Mussel Beds. Front Microbiol. 2022 Jan 13;12:790554. doi: 10.3389/fmicb.2021.790554. PMID: 35095802; PMCID: PMC8793333.

Hu, Z., Chen, X., Chang, J., Yu, J., Tong, Q., Li, S., et al., 2018. Compositional and predicted functional analysis of the gut microbiota of Radix auricularia (Linnaeus) via high-throughput Illumina sequencing. PeerJ 6, e5537. https://doi.org/10.7717/peerj.5537.

Islam, M.S., Tanaka, M., 2004. Impacts of pollution on coastal and marine ecosystems including coastal and marine fisheries and approach for management: A review and synthesis. Mar. Pollut. Bull. 48, 624–649. https://doi.org/10.1016/j.marpolbul.2003.12.004

Ikeda-Ohtsubo, W., Brugman, S., Warden, C.H., Rebel, J.M.J., Folkerts, G., Pieterse, C.M.J., 2018. How can we define “optimal microbiota?”: a comparative review of structure and functions of microbiota of animals, fish, and plants in agriculture. Front. Nutr. 5, 90. https://doi.org/10.3389/fnut.2018.00090.

Ikuta, T., Tame, A., Saito, M., Aoki, Y., Nagai, Y., Sugimura, M., et al., 2019. Identification of cells expressing two peptidoglycan recognition proteins in the gill of the vent mussel, Bathymodiolus septemdierum. Fish Shellfish Immunol. 93, 815–822. https://doi.org/10.1016/j.fsi.2019.08.022.

Integrative HMP (iHMP) Research Network Consortium, 2014. The Integrative Human Microbiome Project: dynamic analysis of microbiome-host omics profiles during periods of human health and disease. Cell Host Microbe 16, 276–289. https://doi.org/10.1016/j.chom.2014.08.014.

Ivanković, D., Pavičić, J., Erk, M., Filipović-Marijić, V., Raspor, B., 2005. Evaluation of the Mytilus galloprovincialis Lam. digestive gland metallothionein as a biomarker in a long-term field study: Seasonal and spatial variability. Mar. Pollut. Bull. 50, 1303–1313. https://doi.org/10.1016/j.marpolbul.2005.04.039

Izagirre, U., Marigomez, I., 2009. Lysosomal enlargement and lysosomal membrane destabilisation in mussel digestive cells measured by an integrative index. Environ. Pollut. 157, 1544-1553. https://doi.org/10.1016/j.envpol.2009.01.011.

Kamada, N., Seo, S.U., Chen, G.Y., Nunez, G., 2013. Role of the gut microbiota in immunity and inflammatory disease. Nat. Rev. Immunol. 13, 321–335. https://doi.org/10.1038/nri3430.

Lacroix, C., Duvieilbourg, E., Guillou, N., Guyomarch, J., Bassoulet, C., Moraga, D., Chapalain, G., Auffret, M., 2017. Seasonal monitoring of blue mussel (Mytilus spp.) populations in a harbor area: A focus on responses to environmental factors and chronic contamination. Mar. Environ. Res. 129, 24–35. https://doi.org/10.1016/j.marenvres.2017.04.008

La Reau, A.J., Meier-Kolthoff, J.P., Suen, G., 2016. Sequence-based analysis of the genus Ruminococcus resolves its phylogeny and reveals strong host association. Microb. Genom. 2, e000099. https://doi.org/10.1099/mgen.0.000099.

Landrigan, P.J., Stegeman, J.J., Fleming, L.E., Allemand, D., Anderson, D.M., Backer, L.C., Brucker-Davis, F., Chevalier, N., Corra, L., Czerucka, D., Bottein, M.-Y.D., Demeneix, B., Depledge, M., Deheyn, D.D., Dorman, C.J., Fénichel, P., Fisher, S., Gaill, F., Galgani, F., Gaze, W.H., Giuliano, L., Grandjean, P., Hahn, M.E., Hamdoun, A., Hess, P., Judson, B., Laborde, A., McGlade, J., Mu, J., Mustapha, A., Neira, M., Noble, R.T., Pedrotti, M.L., Reddy, C., Rocklöv, J., Scharler, U.M., Shanmugam, H., Taghian, G., Van de Water, J.A.J.M., Vezzulli, L., Weihe, P., Zeka, A., Raps, H., Rampal, P., 2020. Human Health and Ocean Pollution. Ann. Glob. Heal. 86, 151. https://doi.org/10.5334/aogh.2831

Lawson, Lauren A., Atkinson, Carla L., and Jackson, Colin R. The gut bacterial microbiome of the Threeridge mussel, Amblema plicata , varies between rivers but shows a consistent core community. Retrieved from https://par.nsf.gov/biblio/10344702. Freshwater Biology 67.7 Web. doi:10.1111/fwb.13905.

Lee, M.D., Kling, J.D., Araya, R., Ceh, J., 2018. Jellyfish life stages shape associated microbial communities, while a core microbiome is maintained across all. Front. Microbiol. 9, 1534. https://doi.org/10.3389/fmicb.2018.01534

Leiniö, S., Lehtonen, K.K., 2005. Seasonal variability in biomarkers in the bivalves Mytilus edulis and Macoma balthica from the northern Baltic Sea. Comp. Biochem. Physiol. - C Toxicol. Pharmacol. 140, 408–421. https://doi.org/10.1016/j.cca.2005.04.005

Li, Y.F., Xu, J.K., Chen, Y.W., Ding, W.Y., Shao, A.Q., Liang, X., et al., 2019. Characterization of gut microbiome in the mussel Mytilus galloprovincialis in response to thermal stress. Front. Physiol. 10, 1086. https://doi.org/10.3389/fphys.2019.01086.

Lindsay, E.C., Metcalfe, N.B., Llewellyn, M.S., 2020. The potential role of the gut microbiota in shaping host energetics and metabolic rate. J. Anim. Ecol. 89, 2415–2426. https://doi.org/10.1111/1365-2656.13327

Liu, C., Lin, D., Dong, Y., Xue, Q., Yao, H., Lin, Z., 2017. Association of α-amylase gene with growth traits in the razor clam Sinonovacula constricta. Invertebr. Surviv. J. 14, 494–504. https://doi.org/10.25431/1824-307x/isj.v14i1.494-504

Le Roux, F., Wegner, K. M., Baker-Austin, C., Vezzulli, L., Osorio, C. R., Amaro, C., et al., 2015. The emergence of Vibrio pathogens in Europe: ecology, evolution, and pathogenesis. Front. Microbiol. 6, 830. https://doi.org/10.3389/fmicb.2015.00830.

Lockwood, B.L., Connor, K.M., Gracey, A.Y., 2015. The environmentally tuned transcriptomes of Mytilus mussels. J. Exp. Biol. 218, 1822–1833. https://doi.org/10.1242/jeb.118190

Lokmer, A., Kuenzel, S., Baines, J.F., Wegner, K.M., 2016. The role of tissue-specific microbiota in initial establishment success of Pacific oysters. Environ. Microbiol. 18, 970-987. https://doi.org/10.1111/1462-2920.13163.

Louca, S., Doebeli, M., 2018. Efficient comparative phylogenetics on large trees. Bioinformatics. 34, 6. 1053–1055. https://doi.org/10.1093/bioinformatics/btx701

Love, M.I., Huber, W., Anders, S., 2014. Moderated estimation of fold change and dispersion for RNA-seq data with DESeq2. Genome Biol. 15:550. https://doi.org/10.1186/s13059-014-0550-8.

Marini, M., Jones, B.H., Campanelli, A., Grilli, F., Lee, C.M., 2008. Seasonal variability and Po River plume influence on biochemical properties along western Adriatic coast. J. Geophys. Res. Oceans 113, C05S90. https://doi.org/10.1029/2007JC004370.

Masella, A.P., Bartram, A.K., Truszkowski, J.M., Brown, D.G., Neufeld, J.D., 2012. PANDAseq: paired-end assembler for illumina sequences. BMC Bioinformatics 13, 31. https://doi.org/10.1186/1471-2105-13-31.

Meisterhans, G., Raymond, N., Girault, E., Lambert, C., Bourrasseau, L., de Montaudouin, X., et al., 2016. Structure of Manila clam (Ruditapes philippinarum) microbiota at the organ scale in contrasting sets of individuals. Microb. Ecol. 71, 194–206. https://doi.org/10.1007/s00248-015-0662-z.

Meistertzheim, A.-L., Lejart, M., Le Goïc, N., Thébault, M.-T., 2009. Sex-, gametogenesis, and tidal height-related differences in levels of HSP70 and metallothioneins in the Pacific oyster Crassostrea gigas. Comp. Biochem. Physiol. Part A Mol. Integr. Physiol. 152, 234–239. https://doi.org/10.1016/j.cbpa.2008.10.004

Mezzelani, M., Fattorini, D., Gorbi, S., Nigro, M., Regoli, F., 2020. Human pharmaceuticals in marine mussels: Evidence of sneaky environmental hazard along Italian coasts. Mar. Environ. Res. 162, 105137. https://doi.org/10.1016/j.marenvres.2020.105137

Minarelli, F., Raggi, M., Galioto, F., Viaggi, D., 2018. SUFISA Mussels Report An Extended Summary 1–8.

Moschino, V., Del Negro, P., De Vittor, C., Da Ros, L., 2016. Biomonitoring of a polluted coastal area (Bay of Muggia, Northern Adriatic Sea): A five-year study using transplanted mussels. Ecotoxicol. Environ. Saf. 128, 1-10. https://doi.org/10.1016/j.ecoenv.2016.02.006.

Muegge, B.D., Kuczynski, J., Knights, D., Clemente, J.C., González, A., Fontana, L., et al., 2011. Diet drives convergence in gut microbiome functions across mammalian phylogeny and within humans. Science 332, 970–974. https://doi.org/10.1126/science.1198719.

Neori, A., Chopin, T., Troell, M., Buschmann, A.H., Kraemer, G.P., Halling, C., et al., 2004. Integrated aquaculture: rationale, evolution and state of the art emphasizing seaweed biofiltration in modern mariculture. Aquaculture 231, 361–391. https://doi.org/10.1016/j.aquaculture.2003.11.015.

O'Brien, P.A., Webster, N.S., Miller, D.J., Bourne, D.G., 2019. Host-microbe coevolution: applying evidence from model systems to complex marine invertebrate holobionts. MBio 10. pii: e02241-18. https://doi.org/10.1128/mBio.02241-18.

Pagán-Jiménez, M., Ruiz-Calderón, J.F., Dominguez-Bello, M.G., García-Arrarás, J.E., 2019. Characterization of the intestinal microbiota of the sea cucumber Holothuria glaberrima. Plos one. 14, e0208011. https://doi.org/10.1371/journal.pone.0208011.

Pagano, M., Capillo, G., Sanfilippo, M., Palato, S., Trischitta, F., Manganaro, A., Faggio, C., 2016. Evaluation of Functionality and Biological Responses of Mytilus galloprovincialis after Exposure to Quaternium-15 (Methenamine 3-Chloroallylochloride). Molecules. 26 21(2). pii: E144. https://doi.org/10.3390/molecules21020144.

Pagano, M., Porcino, C., Briglia, M., Fiorino, E., Vazzana, M., Silvestro, S., Faggio, C., 2017. The influence of exposure of cadmium chloride and zinc chloride on haemolymph and digestive gland cells from Mytilus galloprovincialis. Int. J. Environ. Res. 11(2): 207-216. https://doi.org/10.1007/s41742-017-0020-8.

Pathirana, E., McPherson, A., Whittington, R., Hick, P., 2019. The role of tissue type, sampling and nucleic acid purification methodology on the inferred composition of Pacific oyster (Crassostrea gigas) microbiome. J. Appl. Microbiol. 127, 429-444. https://doi.org/10.1111/jam.14326. Pita, L., Rix, L., Slaby, B.M., Franke, A., Hentschel, U., 2018. The sponge holobiont in a changing ocean: from microbes to ecosystems. Microbiome 6, 46. https://doi.org/10.1186/s40168-018-0428-1.

Pickard J.M., Zeng M.Y., Caruso R., Núñez G. Gut microbiota: Role in pathogen colonization, immune responses, and inflammatory disease. Immunol Rev. 2017 Sep;279(1):70-89. doi: 10.1111/imr.12567.

Quast, C., Pruesse, E., Yilmaz, P., Gerken, J., Schweer, T., Yarza, P., et al., 2013. The SILVA ribosomal RNA gene database project: improved data processing and web-based tools. Nucleic Acids Res. 41, D590–D596. https://doi.org/10.1093/nar/gks1219.

Rausch, P., Rühlemann, M., Hermes, B.M., Doms, S., Dagan, T., Dierking, K., et al., 2019. Comparative analysis of amplicon and metagenomic sequencing methods reveals key features in the evolution of animal metaorganisms. Microbiome 7, 133. https://doi.org/10.1186/s40168-019-0743-1.

Richards, G.P., Mcleod, C., Le Guyader, S.F., 2010. Processing strategies to inactivate enteric viruses in shellfish. Food Environ. Virol. 2, 183–193. https://doi.org/10.1007/s12560-010-9045-2.

Rognes, T., Flouri, T., Nichols, B., Quince, C., Mahé, F., 2016. VSEARCH: a versatile open source tool for metagenomics. PeerJ 4, e2584. https://doi.org/10.7717/peerj.2584.

Roméo, M., Hoarau, P., Garello, G., Gnassia-Barelli, M., Girard, J.P., 2003. Mussel transplantation and biomarkers as useful tools for assessing water quality in the NW Mediterranean. Environ. Pollut. 122, 369–378. https://doi.org/10.1016/S0269-7491(02)00303-2

Rossi, F., Palombella, S., Pirrone, C., Mancini, G., Bernardini, G., Gornati, R., 2016. Evaluation of tissue morphology and gene expression as biomarkers of pollution in mussel Mytilus galloprovincialis caging experiment. Aquat. Toxicol. 181, 57–66. https://doi.org/10.1016/j.aquatox.2016.10.018

Rouillon, G., Rivas, J.G., Ochoa, N., Navarro, E., 2005. Phytoplancton composition of the stomach contents of the mussel Mytilus edulis L. from two populations: comparison with its food supply. J. Shellfish Res. 24, 5–14. https://doi.org/10.2983/0730-8000(2005)24[5:PCOTSC]2.0.CO;2.

Schmidt, W., Power, E., Quinn, B., 2013a. Seasonal variations of biomarker responses in the marine blue mussel (Mytilus spp.). Mar. Pollut. Bull. 74, 50–55. https://doi.org/10.1016/j.marpolbul.2013.07.033

Schmidt, W., Rainville, L.C., Mceneff, G., Sheehan, D., Quinn, B., 2013b. A proteomic evaluation of the effects of the pharmaceuticals diclofenac and gemfibrozil on marine mussels (Mytilus spp.): Evidence for chronic sublethal effects on stress-response proteins. Drug Test. Anal. 6, 210–219. https://doi.org/10.1002/dta.1463

Schmittgen, T.D., Livak, K.J., 2008. Analyzing real-time PCR data by the comparative CT method. Nat. Protoc. 3, 1101–1108. https://doi.org/10.1038/nprot.2008.73

Salgueiro V, Reis L, Ferreira E, Botelho MJ, Manageiro V, Caniça M. Assessing the Bacterial Community Composition of Bivalve Mollusks Collected in Aquaculture Farms and Respective Susceptibility to Antibiotics. Antibiotics (Basel). 2021 Sep 20;10(9):1135. doi: 10.3390/antibiotics10091135. PMID: 34572717; PMCID: PMC8468174.

Saltzman, E.T., Thomsen, M., Hall, S., Vitetta, L., 2017. Perna canaliculus and the intestinal microbiome. Mar. Drugs 15, pii: E207. https://doi.org/10.3390/md15070207.

Sforzini, S., Oliveri, C., Orrù, A., Chessa, G., Pacchioni, B., Millino, C., Jha, A.N., Viarengo, A., Banni, M., 2018. Application of a new targeted low density microarray and conventional biomarkers to evaluate the health status of marine mussels: A field study in Sardinian coast, Italy. Sci. Total Environ. 628–629. https://doi.org/10.1016/j.scitotenv.2018.01.293

Sheehan, D., Power, A., 1999. Effects of seasonality on xenobiotic and antioxidant defence mechanisms of bivalve molluscs. Comp. Biochem. Physiol. - C Pharmacol. Toxicol. Endocrinol. 123, 193–199. https://doi.org/10.1016/S0742-8413(99)00033-X

Shen, H., Kibria, G., Wu, R.S.S., Morrison, P., Nugegoda, D., 2020. Spatial and temporal variations of trace metal body burdens of live mussels Mytilus galloprovincialis and field validation of the Artificial Mussels in Australian inshore marine environment. Chemosphere 248, 126004. https://doi.org/10.1016/j.chemosphere.2020.126004

Simon, J.C., Marchesi, J.R., Mougel, C., Selosse, M.A., 2019. Host-microbiota interactions: from holobiont theory to analysis. Microbiome 7, 5. https://doi.org/10.1186/s40168-019-0619-4.

Turroni, S., Rampelli, S., Biagi, E. Consolandi, C., Severgnini, M., Peano, C., Quercia, S., Soverini, M., Carbonero, F. G., Bianconi, G., Rettberg, P., Canganella, F., Brigidi P., Candela,

M., 2017. Temporal dynamics of the gut microbiota in people sharing a confined environment, a 520-day ground-based space simulation, MARS500. Microbiome 5 39. https://doi.org/10.1186/s40168-017-0256-8.

van de Water, J. A., Melkonian, R., Junca, H., Voolstra, C. R., Reynaud, S., Allemand, D., Ferrier-Pagès, 2016. Spirochaetes dominate the microbial community associated with the red coral Corallium rubrum on a broad geographic scale. Sci Rep. 6 27277. https://doi.org/10.1038/srep27277.

Vanwonterghem, I., Webster, N.S., 2020. Coral Reef Microorganisms in a Changing Climate. iScience 23, 100972. https://doi.org/10.1016/j.isci.2020.100972

Vernocchi, P., Maffei, M., Lanciotti, R., Suzzi, G., Gardini, F., 2007. Characterization of Mediterranean mussels (Mytilus galloprovincialis) harvested in Adriatic Sea (Italy). Food Control 18, 1575–1583. https://doi.org/10.1016/j.foodcont.2006.12.009

Vezzulli, L., Stagnaro, L., Grande, C., Tassistro, G., Canesi, L., Pruzzo, C., 2018. Comparative 16SrDNA gene-based microbiota profiles of the Pacific oyster (Crassostrea gigas) and the Mediterranean mussel (Mytilus galloprovincialis) from a shellfish farm (Ligurian Sea, Italy). Microb. Ecol. 75, 495-504. https://doi.org/10.1007/s00248-017-1051-6.

Viarengo, A., Lowe, D., Bolognesi, C., Fabbri, E., Koehler, A., 2007. The use of biomarkers in biomonitoring: a 2-tier approach assessing the level of pollutant-induced stress syndrome in

sentinel organisms. Comp. Biochem. Physiol. C Toxicol. Pharmacol. 146, 281–300. https://doi.org/10.1016/j.cbpc.2007.04.011.

Waites, K. B. and Talkington D. F., 2004. Mycoplasma pneumoniae and its role as a human pathogen. Clin. Microbiol. Rev. 17. 4 697–728. https://doi.org/10.1128/CMR.17.4.697-728.2004.

Wu, J., Shao, H., Zhang, J., Ying, Y., Cheng, Y., Zhao, D., et al., 2019. Mussel polysaccharide α-D-glucan (MP-A) protects against non-alcoholic fatty liver disease via maintaining the homeostasis of gut microbiota and regulating related gut-liver axis signaling pathways. Int. J. Biol. Macromol. 130, 68-78. https://doi.org/10.1016/j.ijbiomac.2019.02.097.

Ye, Y., Doak, T.G., 2009. A parsimony approach to biological pathway reconstruction/inference for genomes and metagenomes. PLoS Comput. Biol., 5 (8), e1000465. https://doi.org/10.1371/journal.pcbi.1000465.